Facies Architecture and Stratigraphy of the Paleogene Huntingdon Formation at Abbotsford, British Columbia

By

Brett Hollis Tallentire Gilley

B.Sc., Simon Fraser University, 1999

A THESIS SUBMITTED IN PARTIAL FULFILLMENT OF THE

REQUIREMENTS FOR THE DEGREE OF MASTER OF SCIENCE

In the

DEPARTMENT OF EARTH SCIENCES

© Brett Hollis Tallentire Gilley, 2003

SIMON FRASER UNIVERSITY

December, 2003

APPROVAL

Name: **Brett Hollis Tallentire Gilley**

Degree: Master of Science

Title of Thesis: Facies Architecture and Stratigraphy of the Paleogene Huntingdon Formation at Abbotsford, British Columbia

Examining Committee:

           Chair: **Dr. Glyn Williams-Jones**
                              Assistant Professor

                              Dr. Peter Mustard
                              Senior Supervisor
                              Associate Professor

                              Dr. James MacEachern
                              Supervisory Committee Member
                              Associate Professor

                              Dr. Michael Wilson
                              External Examiner
                              Douglas College, Dept. of Geology & Anthropology

Date Approved: Dec 4, 2003

                              BM

PARTIAL COPYRIGHT LICENCE

I hereby grant to Simon Fraser University the right to lend my thesis, project or extended essay (the title of which is shown below) to users of the Simon Fraser University Library, and to make partial or single copies only for such users or in response to a request from the library of any other university, or other educational institution, on its own behalf or for one of its users. I further agree that permission for multiple copying of this work for scholarly purposes may be granted by me or the Dean of Graduate Studies. It is understood that copying or publication of this work for financial gain shall not be allowed without my written permission.

Title of Thesis/Project/Extended Essay:

Facies Architecture and Stratigraphy of the Paleogene Huntingdon Formation at Abbotsford, British Columbia

Author:
(Signature)

Brett Hollis Tallentire Gilley
(Name)

Dec 11 2003
(Date)

Abstract

The Paleogene Huntingdon Formation is a succession of alluvial mudstone, sandstone, and pebble conglomerate preserved in southwest British Columbia, Canada. The study area includes the proposed type section of the Huntingdon Formation and is located in and near Abbotsford, British Columbia, Canada.

The Huntingdon Formation is correlative with, and continuous in the subsurface to, the Chuckanut Formation in northwest Washington State. The Huntingdon and Chuckanut formations were deposited in the Chuckanut basin during late Paleocene, Eocene, and possibly Oligocene time. The Chuckanut basin probably formed as a complex hybrid basin, reflecting the transpressive nature of the plate margin setting in this part of the Cordillera during Paleogene time.

In general sedimentary strata of the Huntingdon Formation dip gently towards the south and minor faults and multiple fracture sets are present. At Sumas Mountain (Canada) the remnant outcrops areas of the Huntingdon Formation are separated by a horst consisting of an unnamed igneous body. The orientation of brittle structures in a fault domain close to the horst suggests the related faulting did not occur until the middle Miocene.

Fluvial architectural element analysis and facies analysis of the type area indicates that this formation developed as a coarse, sand-dominated, terrestrial fluvial system, with an active floodplain. The range of features suggests proximal to distal transition from alluvial to braided to transitional sand-dominated meandering river systems. Paleocurrent analysis of the Huntingdon Formation indicates that it was sourced to the east. Sandstone and pebble conglomerate clasts are dominated by chert types, typical of first-order basin provenance from nearby Cascade oceanic terranes to the east.

It would be a poor thing to be a mineral in a universe without geologists, and geologists are made of minerals. A geologist is a mineral's way of knowing about minerals.

-With apologies to George Wald

Acknowledgements

Table of Contents

List of Figures

Chapter 1 - Introduction

Purpose

This thesis has several interrelated goals. The first is a review of literature relevant to the Huntingdon Formation. The second is to lay groundwork for the formal definition of this formation. The third goal is to report data collected on the tectonic history of the northern Chuckanut Basin. Finally, a detailed sedimentary analysis of the area is made. The study uses architectural element analysis to make interpretations about the sedimentary environment in which the Huntingdon Formation was deposited.

Scope of Work

The main products of this thesis include:

- A 1:20,000 scale geological base map of southwest Sumas Mountain (Canada) and area, using an orthophoto as a base map.

- Several digital photomosaics of pit exposures and correspondent figures of architecture elements.

- A composite stratigraphic section of the Sumas Mountain (Canada) outcrops, to serve as type and reference sections for the Huntingdon Formation.

- Structural analysis of the region

- Interpretation of the depositional environments for the Huntingdon Formation in its type area.

Physiographic Setting and Study Area

The Huntingdon and Chuckanut formations exist within the present-day Georgia Basin, a northwest-oriented structural and topographic depression in southwestern British Columbia and northwestern Washington State (Figure 1, Figure 2, and Figure 3). The basin includes the Strait of Georgia, eastern Vancouver Island, the modern Fraser River Delta, the mainland of northwest Washington State, and their associated watersheds. Sedimentary rock preserved within the area of the

modern Georgia Basin includes the Cretaceous Nanaimo Group (deposited in the Nanaimo Basin), and the Tertiary Chuckanut and Huntingdon Formations (deposited in the Chuckanut Basin, described below). The Georgia Basin also encompasses various Quaternary-aged sediments of diverse origin.

This study concerns the strata of the Paleogene Chuckanut and Huntingdon formations, both deposited in a paleo-basin which is herein referred to as the Chuckanut Basin. The sedimentological aspects of this study focus on the type section of the Huntingdon Formation as defined here, and exposed at Sumas Mountain in Abbotsford British Columbia (Figure BP - A, back pocket).

Previous work in the Chuckanut Basin

The Paleogene Huntingdon and Chuckanut formations (Figure 2 and Figure 3) make up much of the bedrock under Greater Vancouver and northwestern Washington State. The Huntingdon Formation (in Canada) and the Chuckanut Formation (in the USA) extend to between 2.5 and 3 km depth (Figure 3). These formations are correlative rocks separated by the so-called "Border Fault," an anthropomorphic feature, visible only in the minds of geologists using different formation names for similar rocks on opposite sides of the Canada/US border (Mustard and Rouse, 1994). For the purposes of this study, Huntingdon Formation refers to Tertiary bedrock in the Greater Vancouver area and Chuckanut Formation refers to the fully correlative sedimentary rocks south of the Canada/US border (a discussion of formation names and correlations appears below). The paleobasin into which these formations were deposited is herein referred to as the "Chuckanut Basin."

The Huntingdon and Chuckanut formations are interpreted to reflect alluvial sediments with minor paludal deposits and coal beds. Paludal deposits and coal beds increase in abundance towards the southern end of the Chuckanut Basin. There are no marine sediments present in either formation. A broad range of geological dates have been suggested for the Chuckanut Formation, ranging from Late Cretaceous to Early Oligocene. Recent studies have refined this range. The formations
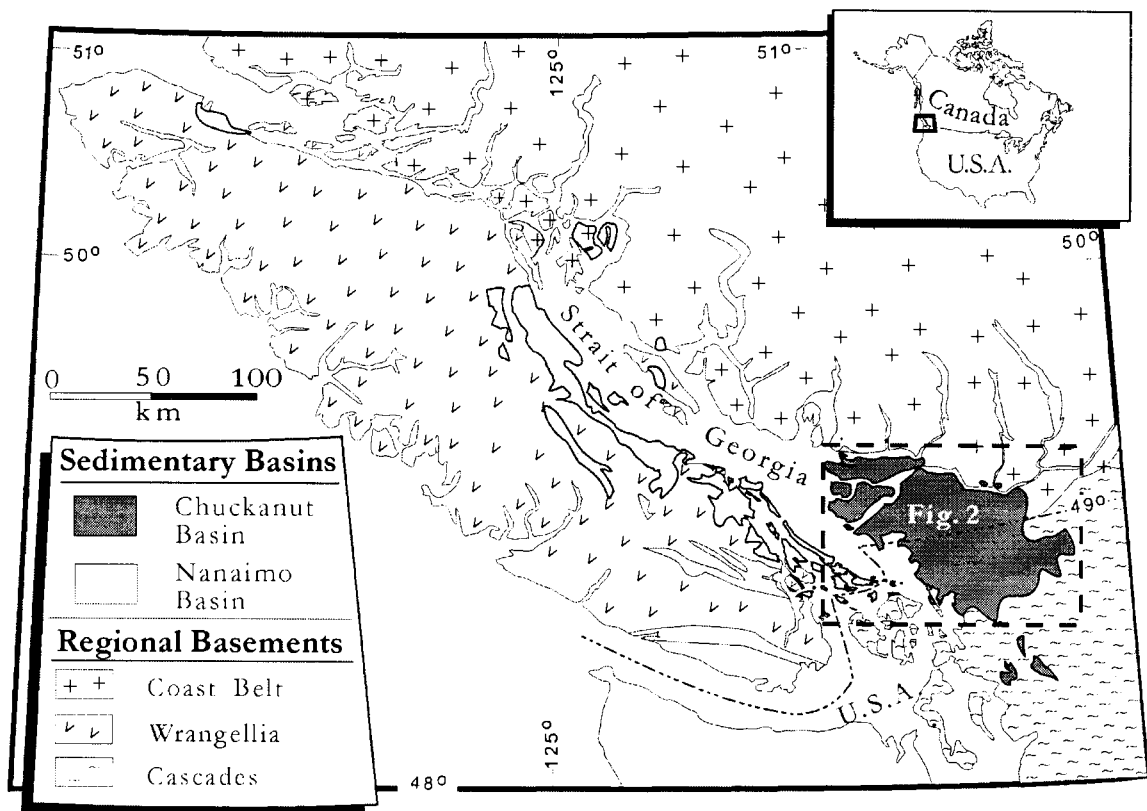
Figure 1 - Site Location map.
The Chuckanut Basin includes Tertiary bedrock in southwestern British Columbia and northwestern Washington State. Modified from Mustard and Rouse (1994) used by permission.

3
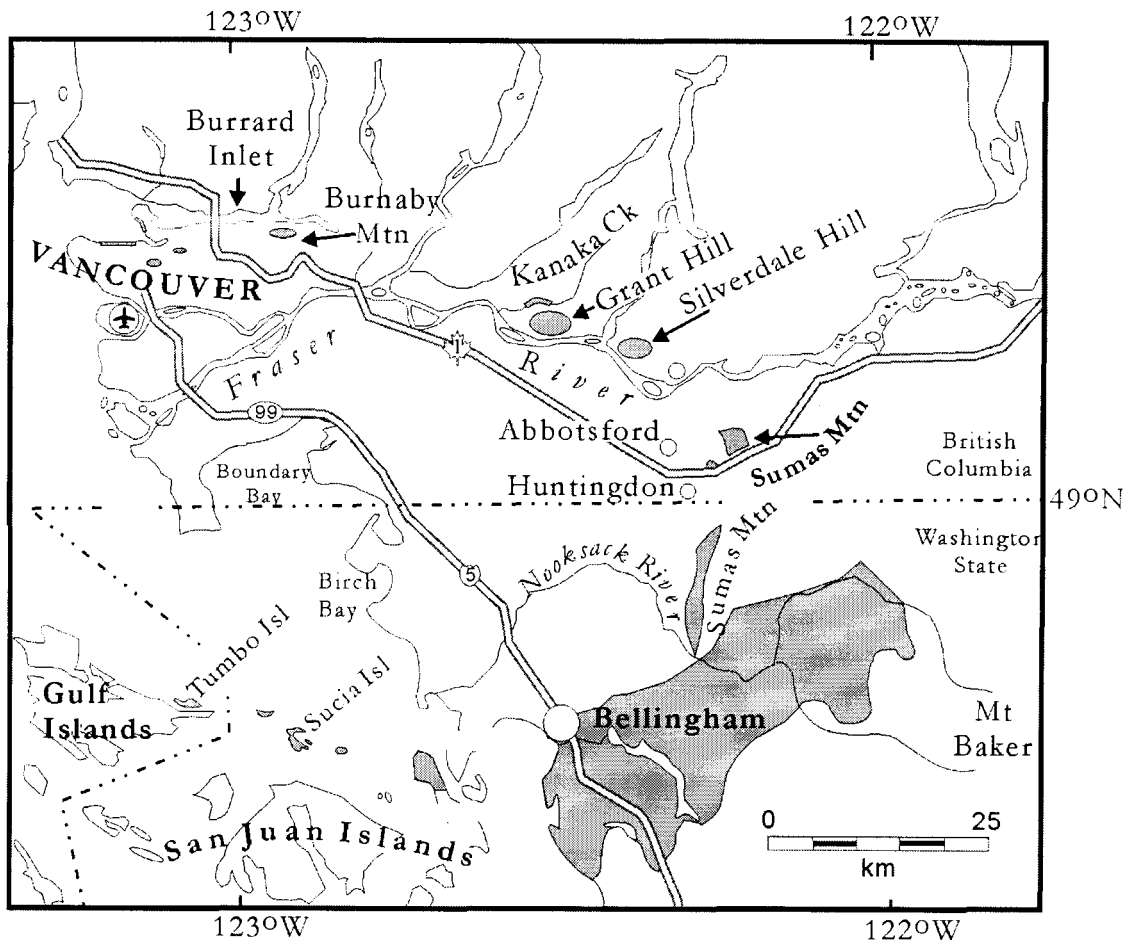
Tertiary Outcrop Areas

Figure 2 - Tertiary outcrop area.

Tertiary aged outcrop in southwestern British Columbia and northwestern Washington State (inset from Figure 1). Modified from Mustard and Rouse (1994) used by permission.
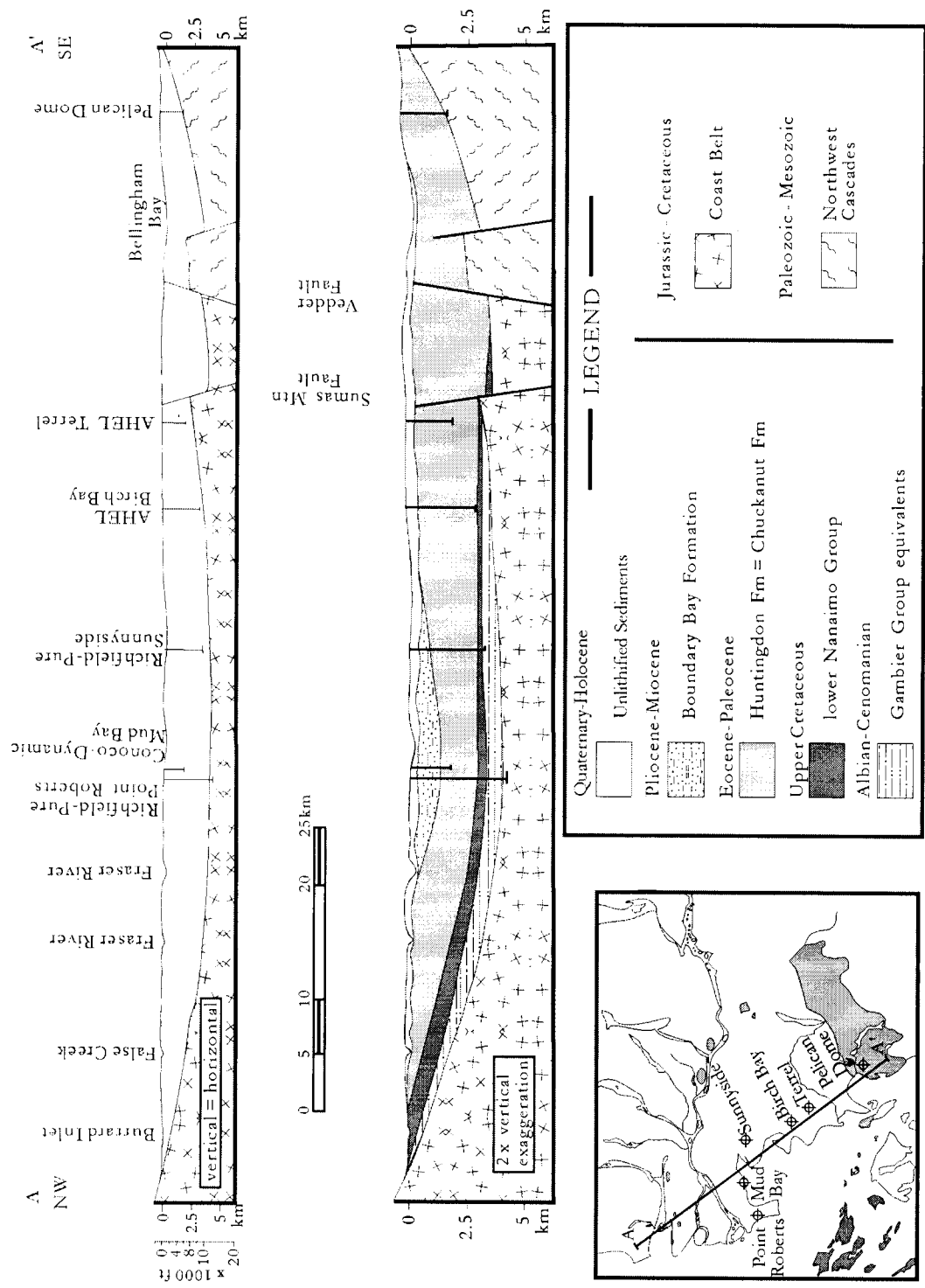
Figure 3 - Cross Section through the Chuckanut basin.
Modified from Mustard and Rouse (1994) used by permission.

5

have been dated using palynology and apatite fission track age-dating, indicating deposition between late Paleocene and early Oligocene time (Mustoe, 1997, Mustard and Rouse, 1994, Johnson, 1984). In general, paleocurrent measurements indicate flow directions towards the south and west (this study and Mustard and Rouse, 1994). However, at the western edge of the preserved basin (on Tumbo Island and the Sucia Island chain) paleocurrents indicate a complex series of flow directions including south, east and northeast (Mustard, 1992). As no marine sediments are present, the basin appears to have been closed on at least three sides (north, west and east), and, because paludal sediments increase towards the south, the basin is interpreted to have drained towards the south (Mustard and Rouse, 1992).

There is much confusion in the previous literature concerning use of the terms "Huntingdon Formation," "Chuckanut Formation," "Burrard Formation," and "Kitsilano Formation" (discussed by Mustard in Rouse, 1994; see also Figure 4). Daly (1912) first proposed the name Huntingdon Formation, and defined its type area as Sumas Mountain (Canada) as part of his geologic traverse of the Canada/US border. The areal extent of the Huntingdon Formation was expanded by Mustard and Rouse (1994) to include all Late Paleocene and Eocene stratigraphy in the Lower Mainland (Greater Vancouver). Correlative rocks in Washington State are known as the Chuckanut Formation, as originally defined by McClellan in 1927 (cited in Griggs, 1966). Burwash (1918) refers to the rocks of the Chuckanut Basin as the "Puget Series". In Vancouver, partially correlative strata were previously termed the Burrard and Kitsilano Formations (Bustin, 1990). However, the Burrard Formation also includes a Cretaceous-aged lower member (Lions Gate Member of Rouse et al., 1975). Mustard and Rouse (1994) redefined the former Lions Gate Member to be part of the Late Cretaceous Nanaimo Group (undifferentiated), and the upper Burrard and Kitsilano formations as the Kitsilano Member of the Huntingdon Formation.

Miller and Misch (1963) correlated another Tertiary sandstone unit, reportedly lying stratigraphically above the Chuckanut Formation, with the

Huntingdon Formation. This unit is located on Sumas Mountain (US), a mountain which unfortunately carries the same name as Sumas Mountain (Canada). A single palynological date, from the stratigraphically lowest part of Miller and Misch's Huntingdon Formation, indicates a late Eocene or early Oligocene age for this unit (Mustard and Rouse, 1994). For this reason Mustard and Rouse suggest that these rocks are correlative to the upper part of the Chuckanut Formation (Padden Member) and thus only correlate to the uppermost part of the true Huntingdon Formation, as defined in its type area at Sumas Mountain (Canada).

A variety of projects have been completed in the Chuckanut Basin. Few have focused specifically on the Huntingdon Formation as its extent/importance was not recognised until recently. In 1912, Daly described the sedimentary bedrock on Sumas Mountain (Canada), using the term Huntingdon Formation. Burwash (1918) completed a PhD thesis on the Tertiary bedrock in the Vancouver Area. Kerr (1942) completed a Master's thesis describing the Tertiary sediments of Sumas Mountain (Canada). Both Burwash and Kerr described short stratigraphic sections from parts of the proposed type area at Sumas Mountain (Canada). As discussed above, Mustard and Rouse completed two studies related specifically to the Huntingdon Formation, (1992 and 1994) which cleared up much confusion about the Tertiary sedimentary bedrock and its regional stratigraphic relationships. As the Chuckanut and Huntingdon formations are equivalent, studies of the Chuckanut Formation are also important to this study.

Shedd first used the name Chuckanut in 1903 to describe a sandstone unit located on Chuckanut Drive, near Bellingham, in Washington State; McClellan first used the term Chuckanut Formation in 1927; and Glover described the type section of the Chuckanut Formation in 1935 (all cited in Griggs, 1966). There were several other smaller or overlapping studies done before Griggs published on the palynology of the Chuckanut Formation in 1966.

Since the 1970s, many projects studying the Chuckanut Formation have been completed. Johnson has published several articles and field trips on this formation
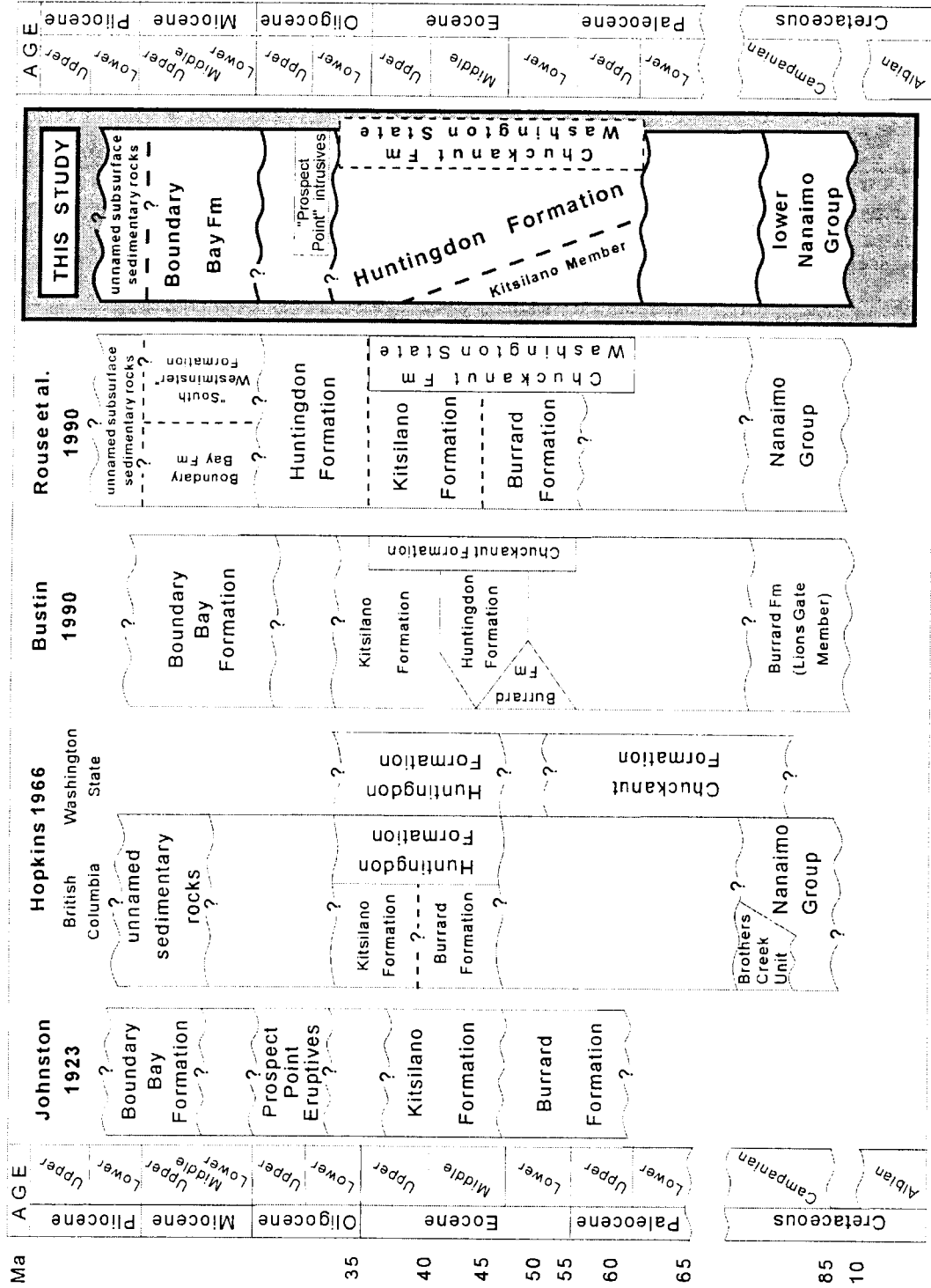
Figure 4 - Formation names in southwestern British Columbia and northwestern Washington State. Modified from Mustard and Rouse (1994) used by permission.

(e.g. Johnson, 1984, 1985). Mustoe has dated various fossils, and attempted paleogeographic reconstructions of the formation; indicating that the formation was deposited in a subtropical environment (Mustoe 1995). Cheney has developed thought-provoking ideas about the tectonic evolution of Eocene basins in the region (e.g. Cheney, 2000). Finally, Haugerud (1998) has presented some preliminary reports on the formation, indicating the thickness was much less than originally presented due to unrecognised thrust faults.

Fossils and Paleoenvironment

Sir J.W. Dawson identified a variety of plant species in the Vancouver area (1895 cited in Burwash 1918). Flora identified are ferns, palms, sedges, cotton-woods, willows, oaks, figs, and redwoods. Burwash (1918) interpreted this to represent a climate much warmer than today. These fossils appear to be generally from the Huntingdon Formation, although plants described from "Stanley Park" may include Upper Cretaceous Nanaimo Group flora.

Mustoe (1997) has published an excellent review of fossils found in the Chuckanut Formation. There is a dearth of animal fossils in the Chuckanut Basin; the most notable rare specimens include a turtle carapace, some unidentified bone fragments of a larger animal, and footprints of a "Heron-like" wading bird. Some locations yield freshwater bivalve specimens, and fossilized insect wings have also been found. Plant fossils are most common (e.g. Figure 27) and almost every site yields new taxa. The paleoenvironmental conditions are interpreted to have been similar to subtropical low elevation rainforests.

Economic potential of the Chuckanut Basin

Hydrocarbons

The Huntingdon and Chuckanut formations are of some economic interest because of their potential for containing hydrocarbons. Several studies have focused on the hydrocarbon potential of the Chuckanut Basin, including a major Geological Survey of Canada initiative (Monger, 1990); a study commissioned by the Province
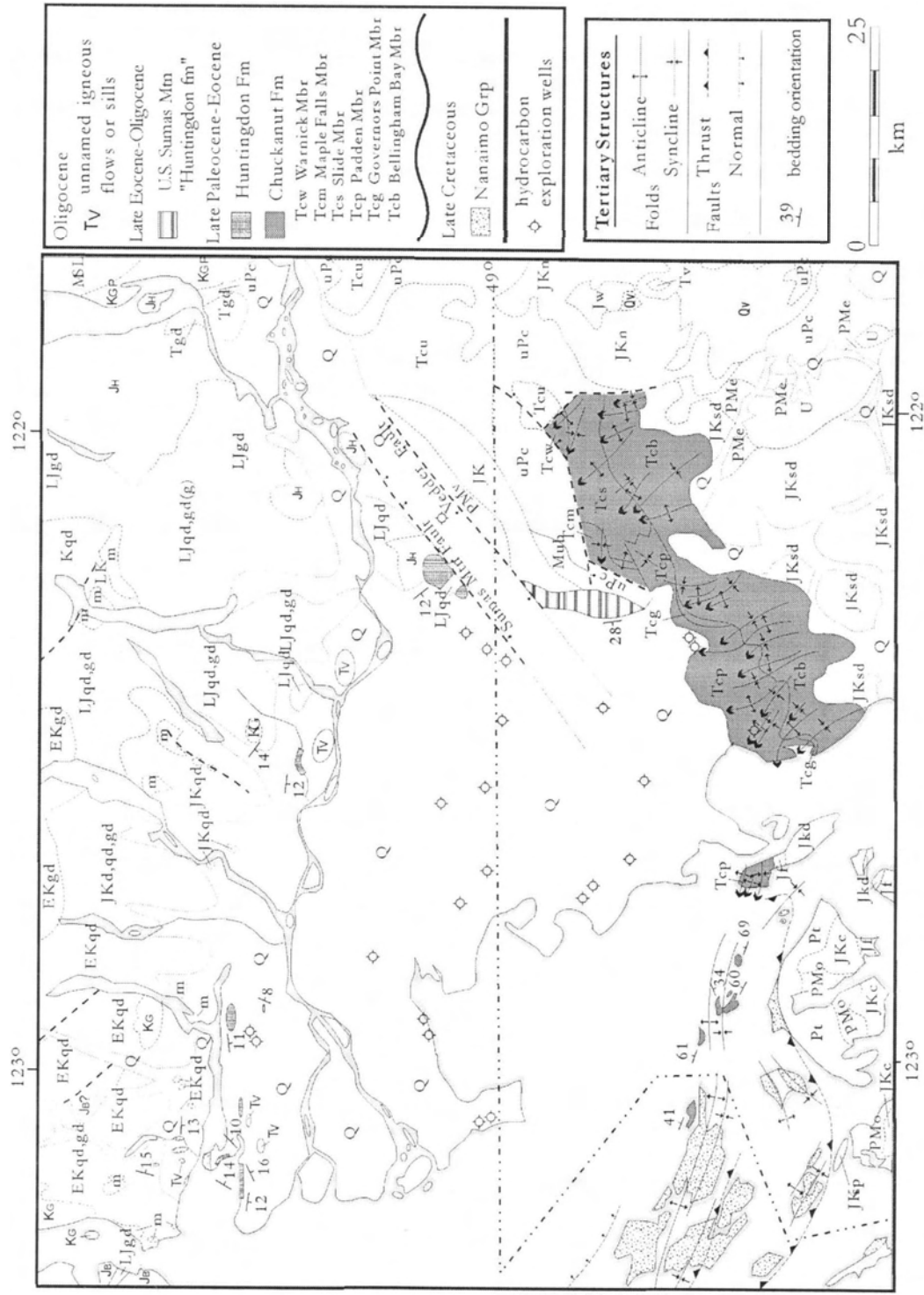
Figure 5 - Petroleum exploration wells in southwestern British Columbia and northwestern Washington State. Modified from Mustard and Rouse (1994) used by permission. See also figure 3 cross section for select well locations.

of British Columbia (Anderson, 1991); and several reviews of research and drilling programs (Bustin, 1990 and Hurst, 1992), among others. More than 20 exploration wells have been drilled in the area (Figure 5), although the findings do not yet demonstrate extensive hydrocarbon preservation.

The sandstones of the Huntingdon Formation, in general, have good potential as a reservoir rock (Anderson, 1991), but the area appears moderate to poor in terms of the extent and maturity of source rocks (Bustin, 1990). Gas dissolved in solution has been found in several wells in the basin (Bustin, 1990; Hurst, 1992) and there is a potential for economic accumulation (Hurst, 1992). Unfortunately, potential structural traps appear to have been perforated by faulting, making large pools unlikely, although there is some chance that numerous ideally restricted gas pools exist in the smaller fault-controlled blocks (Hurst, 1992). If the Mist field in Oregon is used as an example of a similar basin, there may be several pools of less than 2.2×10^8 m^3 (Hurst, 1992).

Coal in the Chuckanut Formation

Coal seams in the Chuckanut Formation are up to 2.5 metres thick (Griggs, 1966). First mined in 1853, the extensive coal beds in the Chuckanut Formation became an important economic resource (Lasmanis, 1991). During the period of 1900-1918 four million tons of coal was produced annually in the region (Lasmanis, 1991). There are currently no active coal mines in the basin.

Aggregate mining in the Huntingdon Formation

The Huntingdon Formation at Sumas Mountain contains clay beds having economic value. It is not clear exactly when the mine began operation, but clay was mined as early as 1907 (Report of the Ministry of Mines for British Columbia 1908, cited by Kerr 1942). Today, the claystones continue to be mined for industrial clay uses by Clayburn Industries Ltd. and are one of the few economic clay deposits in western North America. The pits on Sumas Mountain are also mined by Lafarge Cement. The sandstone, siltstone, and conglomerate of the Huntingdon Formation are crushed to be used as aggregate in local cement production. The pits these
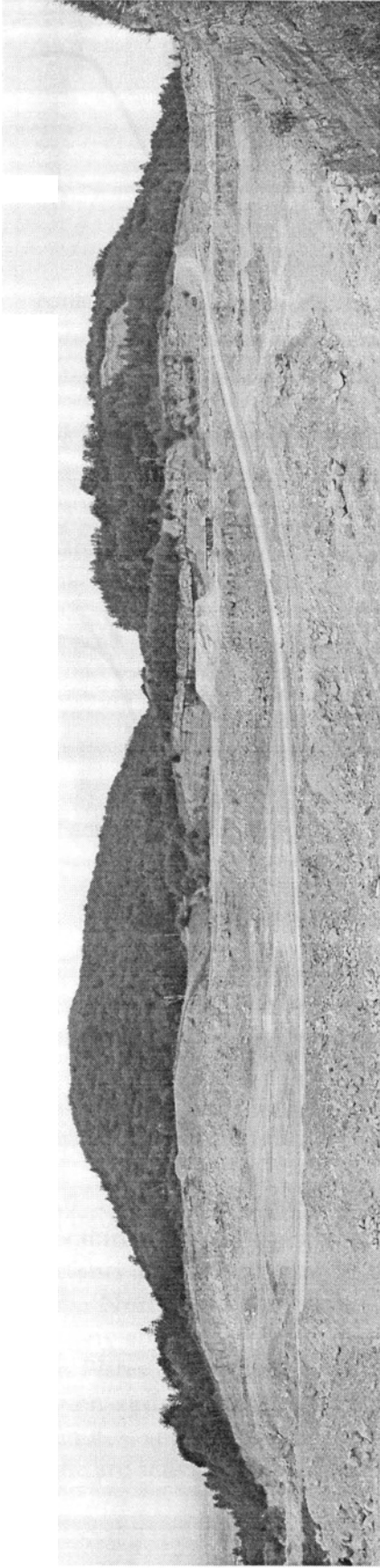
Figure 6 - Quarry at Sumas Mountain (Canada).
Continuous exposure of the Huntingdon Formation in pits such as this greatly facilitated study of the area.
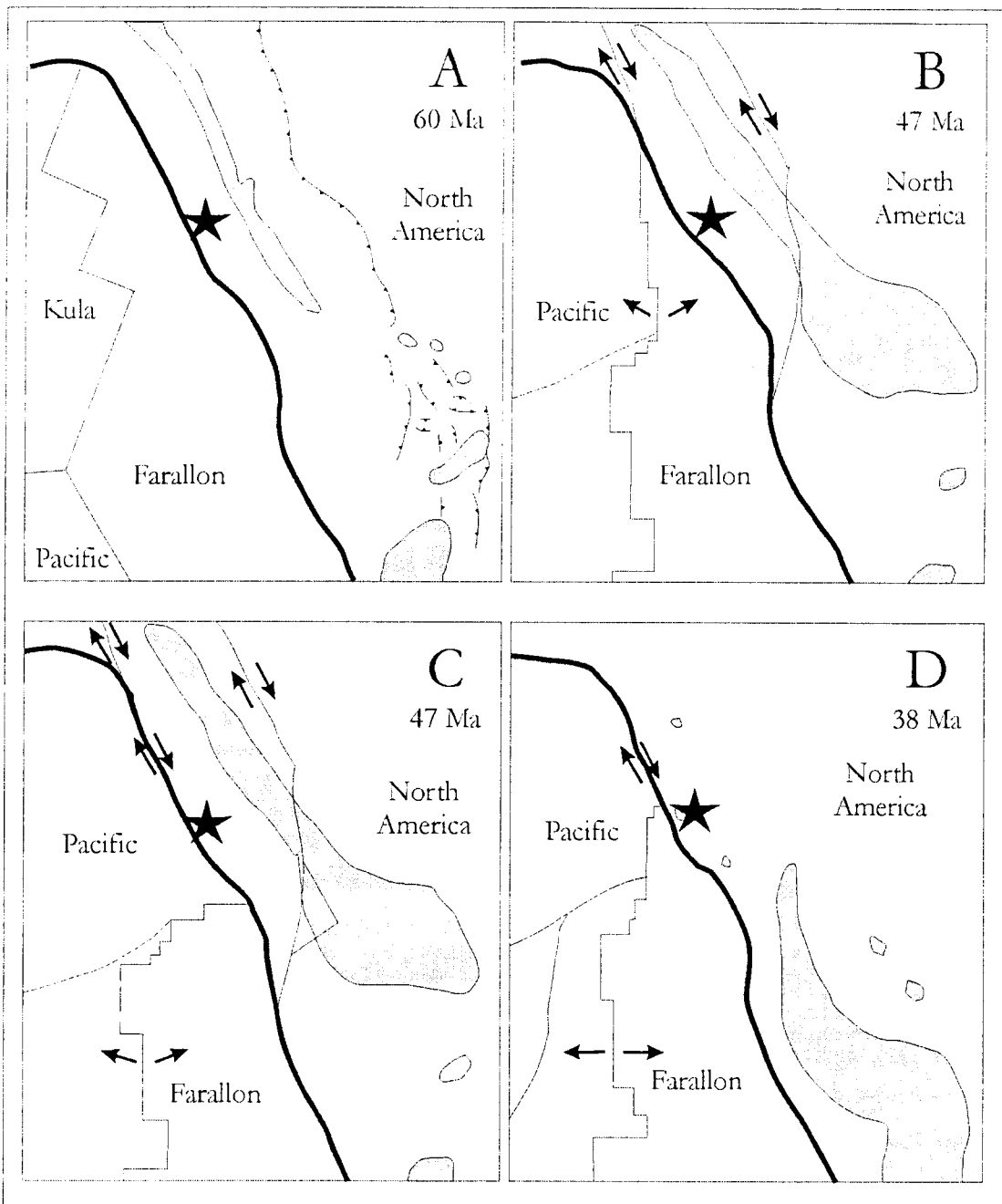
Figure 7 - Generalized tectonic plate configurations of the western margin of North America during the Paleogene Epoch.
A represents an interpretation of the configuration 60 Ma as the Farallon plate subducted under the North American plate. **B** and **C** represent two different interpretations of plate orientations about 47 Mya, in both cases oblique or transform motion of the Pacific or Farallon Plates causes transform motion on the continent. **D** represents a return to normal subduction and the initiation of the Cascade magmatic arc during the Oligocene Period. Star denotes approximate location of the Chucknut Basin, light grey areas represent magmatic arc activity (adapted from Ewing 1980 and Engebretson et al. 1985).

13

sediments are taken from were an invaluable resource for this study, as the exposures within the pits are far superior to those on other parts of the mountain (Figure 6).

Tectonic Setting

Tectonic Regime During the Paleogene Epoch

During the Paleogene Epoch, the western margin of North America in the vicinity of what is now southern British Columbia and north-western Washington State, experienced three major phases of tectonic evolution (Ewing, 1980; Heller et al., 1987) (Figure 7). Only the first two phases contributed significantly to the evolution of the Chuckanut Basin, with the final phase occurring during the Oligocene Epoch as sedimentation in the Basin diminished.

In the Paleocene Epoch and prior to the middle of the Eocene Epoch, tectonic forces in the region were largely compressive (Heller et al. 1987). The most westerly terranes, including the Crescent and Pacific Rim Terranes (of Vancouver Island and the Olympic Peninsula), were accreting to the North American continent. Development of a minor magmatic arc occurred inboard of the Chuckanut Basin. The Cretaceous Nanaimo Group was uplifted, folded, and eroded mostly during middle Eocence time, probably about 45 million years ago (England and Bustin 1998, Mackie, 2002). Evidence for a possible early Paleocene uplift event is suggested by the presence of sedimentary clasts sourced from the Nanaimo Group recognized in the late Paleocene Huntingdon Formation on Sucia Island by Mustard and Rouse (1992). Synsedimentary folds in the lower part of the Chuckanut Formation also occurred in the mid-Tertiary (Haugerud, 1998). The cessation of this folding and uplift coincides with the final docking of the Crescent and Pacific Rim Terranes at around 40-45 Mya (England and Bustin 1998) and the initiation of a new tectonic regime.

By mid-Eocene time what has been interpreted as a distal volcanic arc had developed (Dostal et al., 2001) causing extension in the forearc region (Heller et al., 1987). During much of Eocene time, dextral transcurrent motion occurred on the

continent, likely caused by strain partitioning of oblique (northward) subduction of the Pacific (or Kula) and Farallon plates. This oblique motion was accommodated by major strike-slip faults such as those in the Fraser/Straight Creek Fault System (active after 47 Ma and before 35 Ma; Monger and Journeay, 1994). Several strike-slip basins occurred along these faults, in what is now the United States of America (Tyee, Chumstick, Chikumchuk and Swauk Basins, among others), as well as in Canada (Princeton, Hat Creek, Coldwater, and Tulameen Basins, among others). These non-marine basins are largely graben or wrench-type, pull-apart basins (Heller et al; 1987) They are relatively small and in proximity and relationship to one or more bounding strike-slip faults or half grabens. Basin fills are typically alluvial sediments interbedded with volcanic flows. The rapid deposition in these successions is characteristic of strike-slip basins.

The final tectonic regime was a return to direct subduction of the Juan de Fuca oceanic plate system, a plate boundary compressive regime, and the full development of the Cascade Arc during early Oligocene time (Ewing, 1980; Heller et al., 1987). This third regime coincides with the cessation of sedimentation in the Chuckanut Basin. Models of the basin's tectonic evolution are discussed in Chapter 2.

An alternative hypothesis for the arrangements of the north eastern Pacific tectonic plates during early Paleocene time was presented by Haeussler et al. (2003). In this arrangement, there was an additional plate called the Resurrection Plate east of the Kula Plate and north of the Farallon Plate. In this hypothesis, the Resurrection Plate was subducting eastward under the North American Plate and was separated from the Kula and Farallon Plates by spreading ridges. The subduction of the Resurrection Plate would have been complete by 47 Ma, after which the previously described dextral motion of the Kula or Pacific plate relative to North America would have begun (Haeussler et al., 2003).

Chapter 2 - Geologic and Tectonic Setting

Introduction

Data collected during the field season link the development of the Huntingdon Formation to the tectonic development of the western margin of North America, reinforcing work completed in the region.

General Stratigraphy of the Huntingdon Formation

Depending on the location, the Huntingdon Formation rests either nonconformably on igneous basement (at Sumas Mountain Canada) or disconformably on the lower part of the Cretaceous Nanaimo Group (in Vancouver) (Mustard and Rouse 1994). The Huntingdon Formation is disconformably overlain by the Miocene Boundary Bay Formation (marine silts and sands) (Mustard and Rouse, 1994) (Figure 2 and Figure 3). The Huntingdon Formation is interpreted to be 1.5 to 3 km thick in the subsurface (Figure 3; Mustard and Rouse, 1994; Haugerud, 1998). At Sumas Mountain (Canada) the type section consists of approximately 350 metres of section (Figure 18; Appendix D). Outcrops of the Huntingdon Formation consist of interbedded sandstone, mudstone, and conglomerate and are interpreted to represent fluvial deposition (see Chapters 3 and 4).

General Structure of the Chuckanut Basin

The current margins of the Chuckanut Basin are tectonically controlled, making it a structural basin and not a sedimentary basin. In the north, the uplift of the Coast Plutonic Complex has limited the extent of the basin. In the south, the basin has been extensively folded along a north-north-westerly trend. (Johnson, 1984). In general, bedding in the north dips to the south and bedding in the south dips towards the north (Figure 2, Figure 3 and Figure 5). The basin thus forms a large asymmetrical syncline.

During the Paleogene, the Chuckanut Basin must have covered a larger area. The now missing northern extension of the Huntingdon has been truncated by the

uplift of the Coast Mountains during the last 10 million years (Journeay and van Ulden, 1998).

The southern edge of the Coast Mountains, just north of the city of Vancouver, marks the southern extent of the Coast plutonic uplift. This uplift may have included the northern edge of the Cuckanut Basin. Outcrops in this area form Burnaby Mountain, Grant Hill, Silverdale Hill, and Kitsilano Beach. At these elevated locations the bedding planes of the Huntingdon tend to dip shallowly towards the south. In contrast, bedding planes of the Huntingdon formation encountered towards the centre of the basin and tend to be essentially flat-lying, including at the proposed type section locality (Figure BP - A, Figure 3, Figure 5 and Figure 15).

The working hypothesis of this study is that the uplift of the Coast Plutonic Complex led to erosion of an unknown extent of the Huntingdon Formation while at the same time gently folding material to the south of the Coast Mountains. This uplift formed the northern half of the asymmetrical syncline of the Chuckanut Basin (Figure 3).

Geology and Structure of the Huntingdon Formation at Sumas Mountain (Canada)

At Sumas Mountain (Canada) the Huntingdon Formation and an unnamed igneous body are exposed on the southwest third of mountain, (BP - A) herein referred to as Lower Sumas Mountain (Canada). The eastern contact of the Huntingdon Formation is an apparently noncomformable contact of igneous rock (Kerr, 1942) (cross section on BP - A). This rock body was exposed in the floodplain when the Huntingdon Formation was laid down, and presumably the paludal and economic claystone deposits in the lower part of the stratigraphy (Figure 18 or Appendix D) were enhanced by the sheltering position and weathering of this igneous body (Kerr, 1942). Immediately west of the nonconformity are the aggregate pits of Clayburn Industries and Sumas Shale Limited. These pits expose large areas of sandstone, mudstone, and conglomerate.

Near McKee Peak, the highest point on Lower Sumas Mountain (Canada), resistant conglomerate and sandstone are exposed as cliffs (BP - A, back pocket, Figure 8, and Figure 23). It was these cliffs which originally drew the attention of Daly (1912). Outcrops in this region are generally resistant beds of sandstone or conglomerate underlain by a small exposure of recessively eroded blocky mudstone.

Towards the west, the mudstones, sandstones, and conglomerates of the Huntingdon Formation on Sumas Mountain are separated by a horst of the unnamed igneous rock. This horst is defined by two normal faults on the east (Figure BP - A, back pocket). The sense of motion on these faults is defined by drag folds in the sedimentary rocks. Bedding in the Huntingdon Formation tends to be flat-lying or shallowly dipping (in general to the south), except in a domain near these two faults, where sedimentary beds dip between 40 and 60 degrees towards the northeast (Figure 15). The locations of both normal faults are defined by the formation of recessively eroded valleys (or saddles) in Sumas Mountain (Figure BP - A, back pocket and Figure 8). The western fault is also defined by a lithologic change (sandstone to igneous) and increasing fracture density in the igneous rock. The eastern fault trace is entirely within the Huntingdon Formation. It is interpreted to lie beneath a linear series of ponds and streams in the topographically lowest part of the valley. Existence of the eastern fault is supported by the relatively low topography of the valley, with both sides of the fault made up of the relatively recessive Huntingdon Formation.

The western side of the horst is defined by a deeply eroded valley (Figure BP - A and Figure 8). Lithologies at the base of this valley are obscured by Quaternary deposits (generally till), although to the east cliffs of the unnamed igneous formation occur, and to the west outcrops of the Huntingdon Formation can be found. The contact is interpreted as a fault because of the deeply eroded linear valley, as well as an increase in density and decrease in fracture spacing in outcrops close to the interpreted contact.

At the western edge of Sumas Mountain, the elevation of the bedrock surface
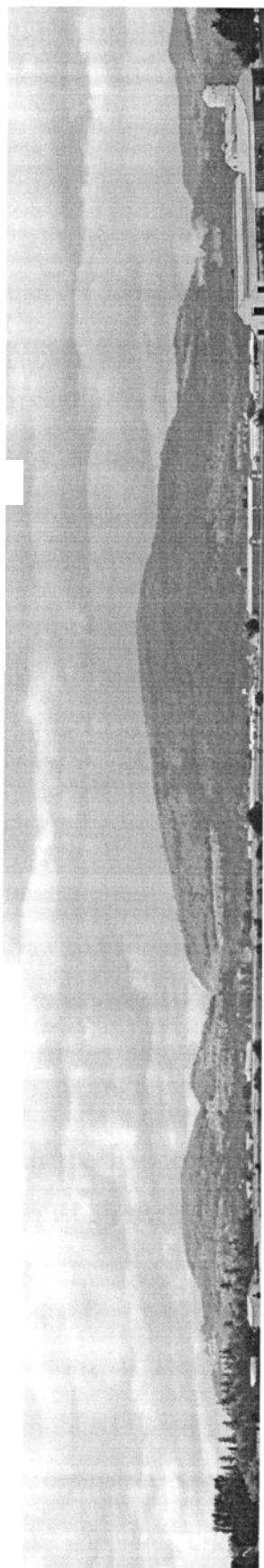
Figure 8 - Sumas Mountain (Canada) facing north from Sumas Prairie.

of the Huntingdon Formation drops steeply and is covered by Quaternary sediments (Figure BP - A). Outcrops on the western side of the mountain are sparse, and generally consist of sandstone and with some conglomerate. Quaternary sediments cover most of the western part of the study area.

South of Sumas Mountain is Sumas Prairie, a flat lying region between Sumas and Vedder Mountains. The prairie is commonly interpreted as a graben; this structure is discussed below. Until the early 20th Century, Sumas Prairie was the site of Sumas Lake, which was drained to create more farmland in the region.

Brittle Structures at Sumas Mountain (Canada)

Brittle deformation structures at Sumas Mountain (Canada) include fractures and faults. Poles to fracture planes presented in this section are plotted on a lower hemisphere equal area Schmidt stereonet projection with a density count of poles to planes. Measurements are uncorrected except for a subset of fractures in the Huntingdon Formation defined to be within a fault domain (discussed below).

All poles to fracture planes show a strong trend to the north-northeast and a slightly weaker trend west-northwest or northwest (Figure 9). Rotation of fracture measurements in the fault domain serves to slightly strengthen these trends, as shown in Figure 9 - C and D and discussed below. These two trends correspond to regional trends discussed by Journeay and van Ulden (1998), and Journeay and Morrison (1999) for the inter-arc setting in the Neogene Period.

The age relationship between the two fracture trends is difficult to unravel with the data collected in this study. The trends were possibly caused by margin-normal shortening during a compressive tectonic phase, by dextral motion due to strain partitioning on the continent, or as a more likely scenario, a combination of both.

By late Eocene time, the accretion of Crescent and Pacific Rim terranes was completed (cited in England and Bustin, 1998). This coincided with a return to an orthogonal stress regime, although further north, in the back arc region, this same event reactivated old features into dextral motion (Journeay and van Ulden, 1998).

A - All poles to fracture Planes measured at Sumas Mountain
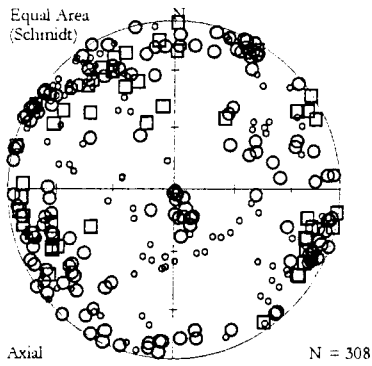
B - Density count of poles to fracture Planes
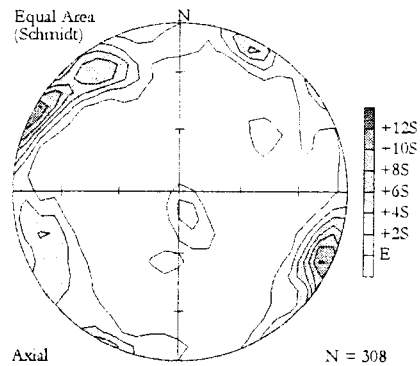
C - All poles to Fracture Planes Measured at Sumas Mountain; Poles within Fault Domain corrected by bedding (308/44)
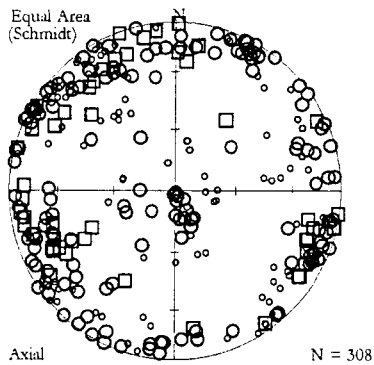
D - Density count of all poles to Fracture Planes Poles within Fault Domain corrected by bedding (308/44)
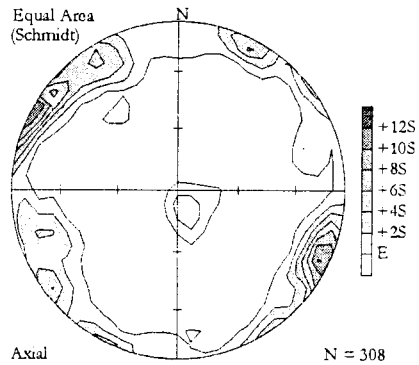
Figure 9 - Fracture planes measured at Sumas Mountain (Canada).
Large circles are extensional fractures, large squares are shear fractures, and small circles are unknown.

All fractures measured in the Huntingdon Formation also show the two regional trends (northeast and northwest) identified by Journeay and Morrison (1999) (Figure 10). Fractures in the unnamed igneous rock depict a very strong northeast trend. This northeast trend is interpreted as the older trend mentioned by Journey and van Ulden (1998) from early Paleogene time. The relative lack of the northwest trend in the igneous rock could be a result of greater rock competence compared to the relatively incompetent sedimentary rocks of the Huntingdon Formation. If the rocks of the Huntingdon Formation are less competent, brittle fractures caused by stress may be more common in the Huntingdon Formation versus the unnamed but highly competent igneous rock. The second major trend (northwest) is then interpreted to have occurred during the middle Eocene, coinciding with Journey and van Ulden's (1998) later brittle fracturing events.

Known extensional fractures in the study area (Figure 11) once again display the two strong (orthogonal) regional trends. This trend occurs in the Huntingdon Formation, but is not as apparent in the unnamed igneous body. However the majority of known extensional features are from the Huntingdon Formation and relatively few extensional fractures were identified in the igneous rocks, making them insufficient for defining these subtle trends.

Known shear fractures at Sumas Mountain display two trends: north-northeast and north-northwest (Figure 12). This may be a result of measurements near faults, as these values are suggestive of rideil shears related to the northwesterly trending horst faults. They are also suggestive of northwest directed compression. A compilation of the few recognised igneous rock shear fractures also indicates a northeasterly trend.

The regional trends of northeast and northwest also appear in stereoplots of fractures of unknown development, and once again the northeast trend is the stronger (Figure 13). In unknown fractures, the Huntingdon Formation shows a balance of both northeast and northwest trends, and the igneous rock again mainly displays a northeast trend.

A - All poles to Huntingdon
Formation fracture Planes
measured at Sumas Mountain
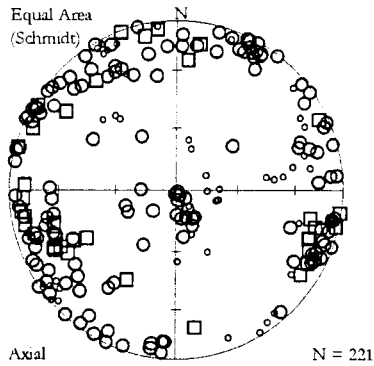
B - Density Count of poles to
Huntingdon Formation fracture
Planes
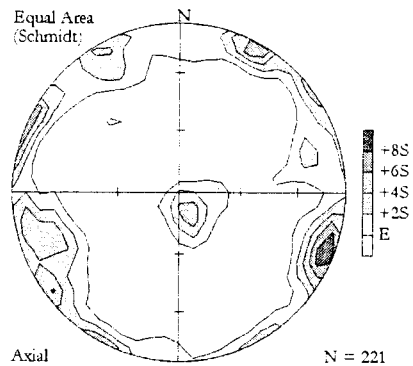
C - All poles to unnamed igneous
rock fracture Planes measured
at Sumas Mountain
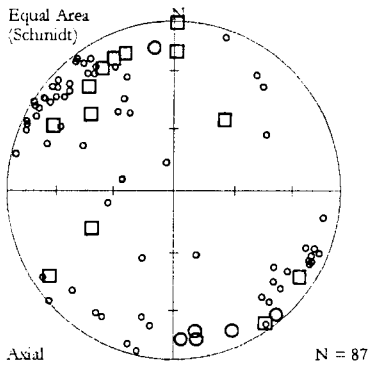
D - Density Count of poles to
unnamed igneous rock
fracture Planes
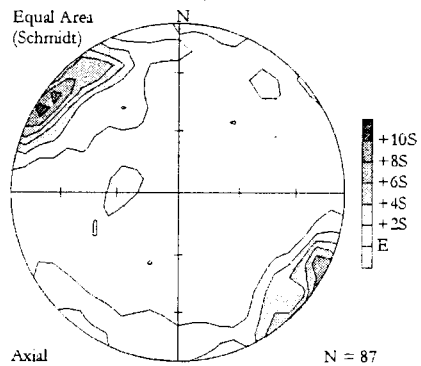
Figure 10 -Fracture planes measured at Sumas Mountain (Canada).
Large circles are extensional fractures, large squares are shear fractures, and small circles are
unknown.

A - All Poles to known Extensional Fracture Planes At Sumas Mtn.
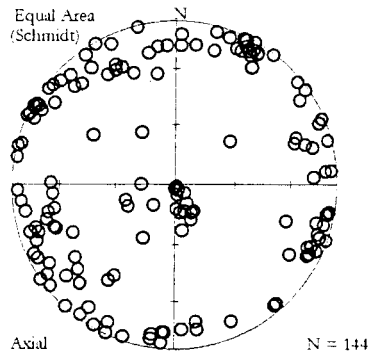
B - Density Counts of Poles to known Extensional Fracture Planes
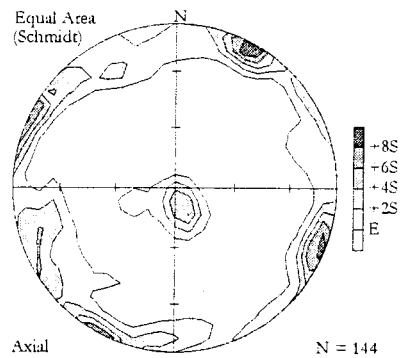
C - All Poles to known Huntingdon Formation Extensional Fracture Planes At Sumas Mtn.
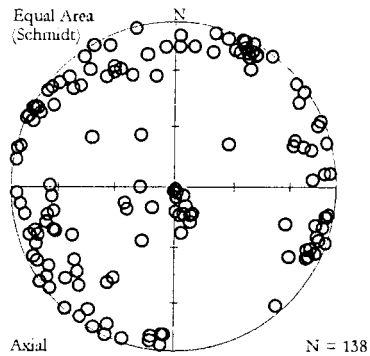
D - Density Counts of Poles to known Huntingdon Extensional Fracture Planes
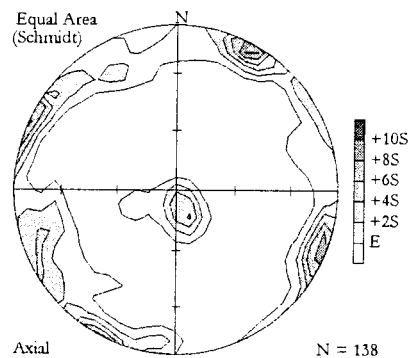
E - All Poles to known Harrison Lake Formation Extensional Fracture Planes At Sumas Mtn.
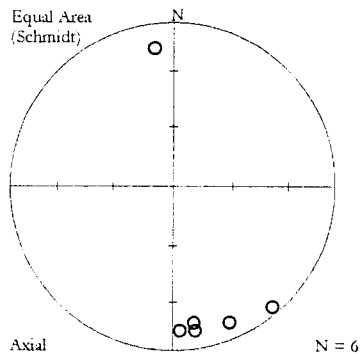
F - Density Counts of Poles to known Harrison Lake Extensional Fracture Planes
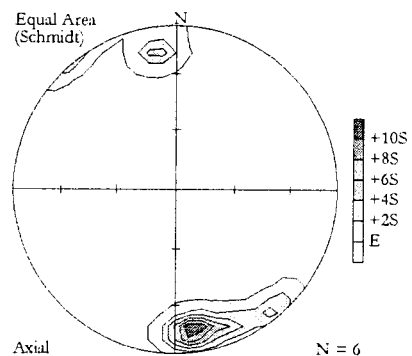
Figure 11 - Fracture planes measured at Sumas Mountain (Canada). Large circles are extensional fractures, large squares are shear fractures, and small circles are unknown.

A - All poles to known shear
fractures at Sumas Mtn.
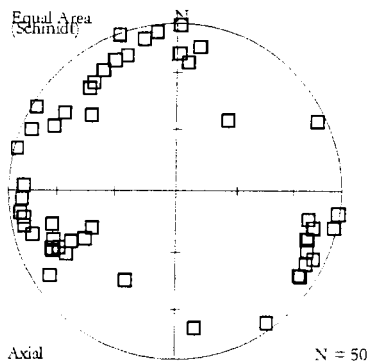
B - Density count of all poles to
known shear fractures
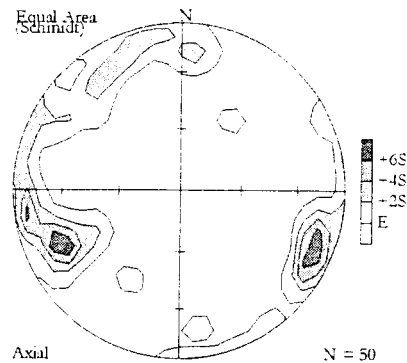
C - All poles to known
Huntingdon Formation shear
fractures at Sumas Mtn.
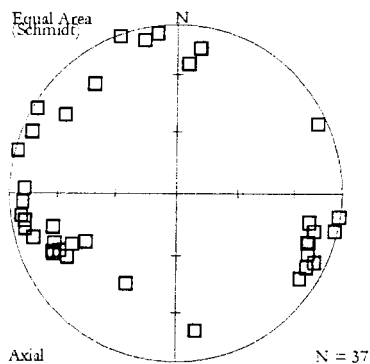
D - Density count of all poles
to known Huntingdon Formation
shear fractures
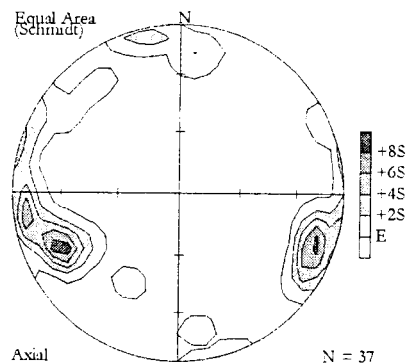
E - All poles to known
Harrison Lake Formation shear
fractures at Sumas Mtn.
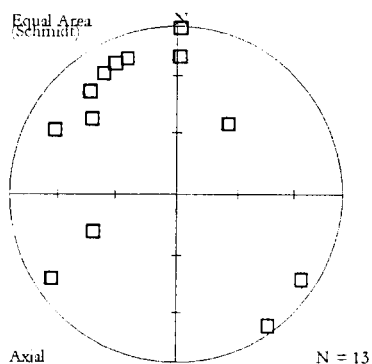
F - Density count of all poles
to known Harrison Lake Formation
shear fractures
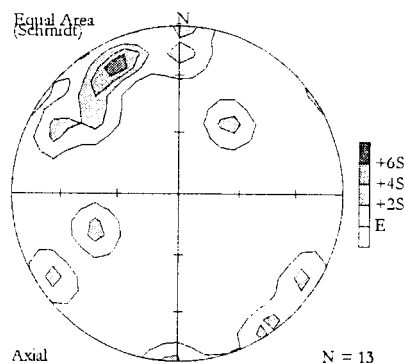
Figure 12 - Fracture planes measured at Sumas Mountain (Canada).
Large circles are extensional fractures, large squares are shear fractures, and small circles are
unknown.

A - All poles to unknown fractures at Sumas Mtn.
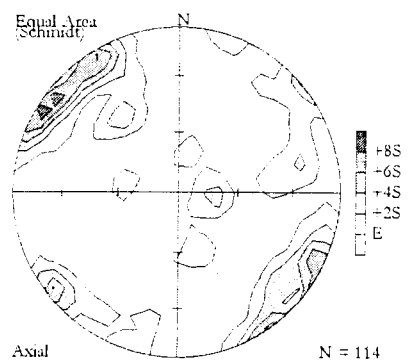
Equal Area (Schmidt)

N

Axial   N = 114

B - Density count of all poles to unknown fractures

Equal Area (Schmidt)

N

+8S
+6S
+4S
+2S
E

Axial   N = 114

C - All poles to Huntingdon Formation fractures of unknown origin at Sumas Mtn.

Equal Area (Schmidt)

N

Axial   N = 46

D - Density count of all poles to Huntingdon Formation fractures of unknown origin

Equal Area (Schmidt)

N

+8S
+6S
+4S
+2S
E

Axial   N = 46

E - All poles to unnamed igneous fractures of unknown origin at Sumas Mtn.

Equal Area (Schmidt)

N

Axial   N = 68

F - Density count of all poles to unnamed igneous fractures of unknown origin

Equal Area (Schmidt)

N

+12S
+10S
+8S
+6S
+4S
+2S
E

Axial   N = 68

Figure 13 - Fracture planes measured at Sumas Mountain (Canada).
Large circles are extensional fractures, large squares are shear fractures, and small circles are unknown.

The small number of minor faults observed in this study make statistical analysis suspect; however, principal direction analysis of these faults do show a trend northeast and southwest (Figure 14). Examples of extensional and compressional minor faulting are visible on Mosaic BP-H (Faults).

A subset of stations show data apparently unrelated to the regional fracture trends, specifically those in close proximity to either of the normal faults which define the eastern side of the horst. These stations were separated out as a fault domain. A station is defined to lie within this domain if it is between the two faults on the eastern side of the horst or within 100 m of the eastern fault (note that some stations within 100 m of map distance were removed based on elevation changes). Figure 15 displays all poles to measured bedding planes in the study area. These poles occur in two clusters. The first cluster is larger and dips just west and slightly south of 0 degrees. The second cluster is smaller and dips to the northeast. This smaller cluster contains measurements of bedding within the fault domain. The bedding in this area is interpreted to have been folded into a drag fold by the action of the fault. The average strike and dip of fault domain bedding planes is 308°/44°. This value was used to correct fractures measured at these stations back to their pre-tilting orientation (Figure 16).

In a comparison of bed-tilt corrected and uncorrected poles to fracture planes in the fault domain, the northwest and northeast trends in the rotated data correspond to local regional trends, whereas the uncorrected data do not. The drag fold, interpreted to have rotated these fracture planes, was caused by the development of the horst, thus the horst must have occurred after both of the regional fracturing trends. As the trends occurred during the Paleogene and the Neogene epochs, the horst must have formed during or after the middle Neogene. The timing of this horst is important as it is likely related to the development of a northeast-trending structural feature known locally as the Sumas Valley Graben. This discussion will use this name (Figure 2). This feature is bounded on the southeast by the northeast-trending Vedder Mountain Fault, and on the northwest by the inferred

A - Poles to bedding planes

Equal Area
(Schmidt)

N

Axial   N = 36
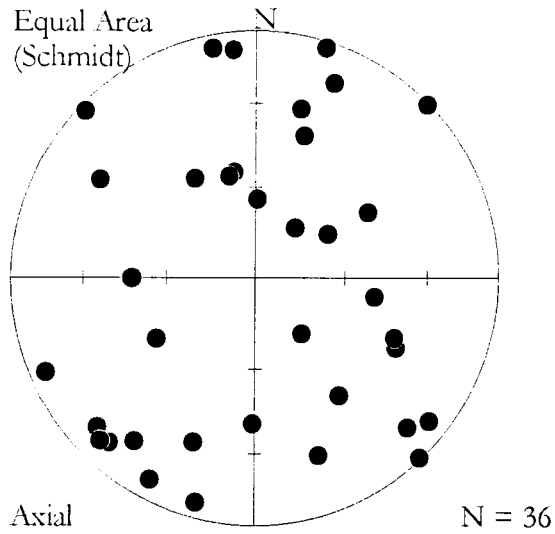
B - Density counts of Poles to bedding planes with Principle
Direction Analysis

Equal Area
(Schmidt)

N

+6S
+4S
+2S
E

Axial   N = 36
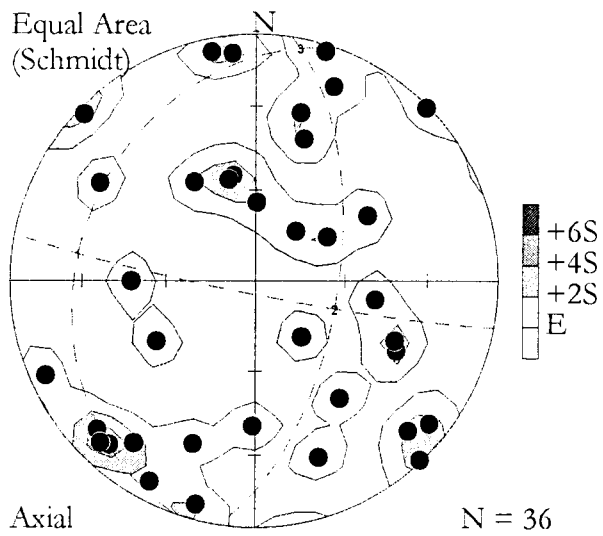
Figure 14 - Minor Faults measured at Sumas Mountain (Canada).

A - Poles to bedding planes

Equal Area
(Schmidt)

N

Axial

N = 107

B - Density counts of Poles to bedding planes

Equal Area
(Schmidt)

N

+28S
+26S
+24S
+22S
+20S
+18S
+16S
+14S
+12S
+10S
+8S
+6S
+4S
+2S
E

Axial

N = 0
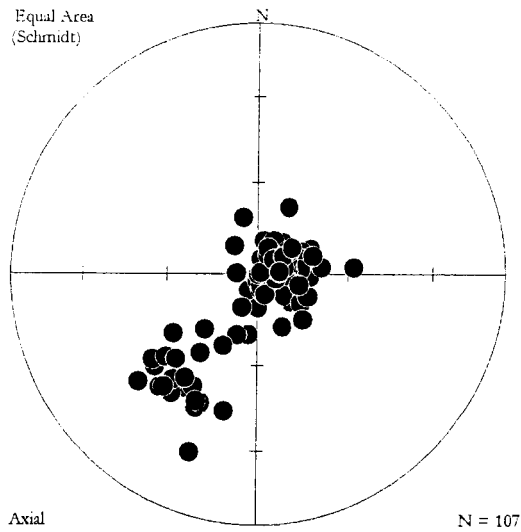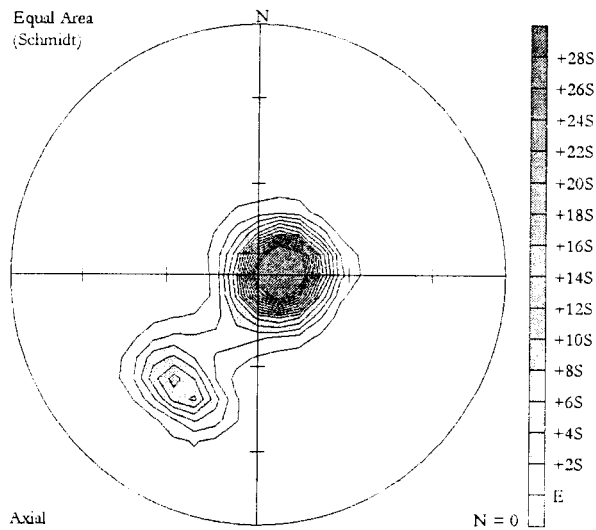
Figure 15 - Bedding planes measured at Sumas Mountain (Canada).
Note the concentration of fault domain bedding poles in the lower left quadrant.

A - Unrotated Fault
Domain Fracture Planes

B - Unrotated Fault
Domain Fracture Planes

C - Fault Domain Fracture
Plane Poles rotated by average
Fault domain bedding (308/44)

D - Fault Domain Density of
Fracture Planes Poles rotated by
average Fault domain bedding (308/44)
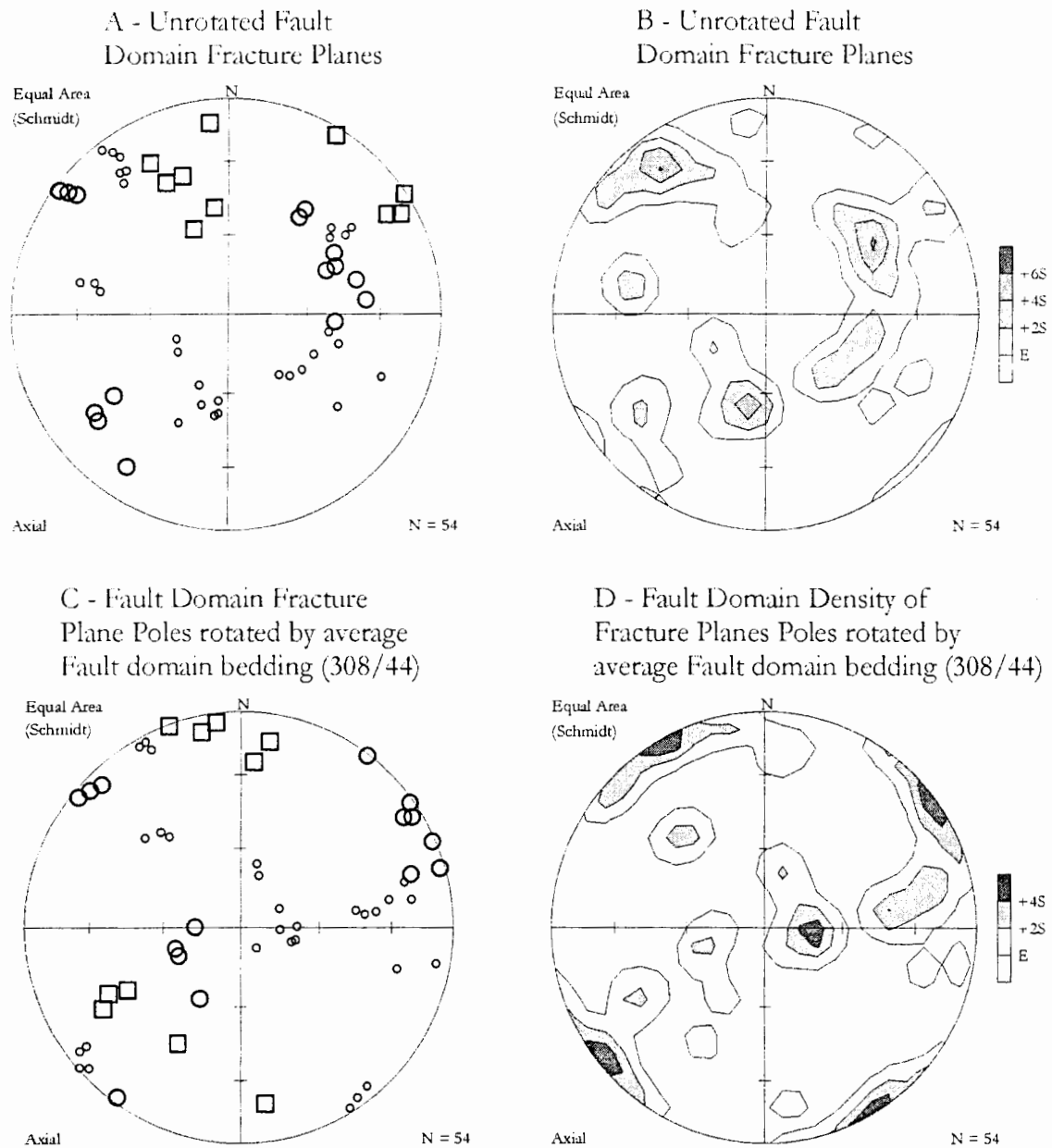
Figure 16 - Fracture planes measured at Sumas Mountain (Canada).
Large circles are extensional fractures, large squares are shear fractures, and small circles are unknown.

northeast-trending Sumas Mountain Fault (Monger and Journeay, 1994). If the Sumas Valley Graben did occur contemporaneously with the horst on lower Sumas Mountain (Canada), the graben could not have preceded the Neogene Epoch, and likely did not precede the middle of the Miocene Epoch.

Models of the Tectonic Evolution of the Chuckanut Basin

The tectonic evolution of the Chuckanut Basin is important to our understanding of the Huntingdon Formation, as well as to the tectonics of the western margin of North America during the Paleogene Epoch. Unfortunately, the evolution of the basin is not well understood.

Five models of basin evolution are reviewed in this chapter. Johnson (1984, 1985) and Mustard and Rouse (1994) have proposed sedimentation in an abnormally large strike-slip basin. Cheney (2000) proposes that the apparent strike-slip basins observed in the field are actually the erosional remnants of this larger basin. Other models for the Chuckanut Basin include: a benched forearc basin, a peripheral foreland basin, and a complex hybrid basin incorporating features from some of the other models. This section discusses of these five models, some of their features, and the implications for the Chuckanut basin.

Strike-slip Basin

During the Eocene Epoch, the Farallon (or Kula) Plate was subducting obliquely under the western margin of North America. Strain partitioning of this subduction created many strike-slip basins in the region. Using this evidence, and characteristics of the basin, Johnson (1984, 1985) interpreted the Chuckanut Basin to be a strike-slip basin. Recent work has modified the interpretation of many of the observations used to create this model. Johnson suggested the Chuckanut Formation was up to 6000 m thick and deposited entirely within the Eocene, indicating extremely rapid sedimentation, a common characteristic of strike-slip basins. However, the sedimentary package is actually probably less than 3000 m thick (Hageruud, 1998; Mustard and Rouse, 1994) and deposition probably began in the Paleocene Epoch and ended in the early part of the Oligocene Epoch. The larger

apparent thickness reported by Johnson is probably due to the existence of previously unrecognised thrust faults in the Chuckanut Hills, and thus repetition of strata in this area (Hageruud, 1998). Sedimentary evidence discussed in Chapter 4 nonetheless indicates the Chuckanut and Huntingdon formations may have had high sedimentation rates, though not as high as proposed by Johnson (1984).

Johnson suggested that the basin was constrained by the Fraser/Straight Creek fault system on the east, and by an as-yet undiscovered fault on the west. Evidence for the postulated western fault (the proposed Seattle Fault) has not been found, and motion on the eastern bounding faults has been constrained. Motion on the Fraser Fault must have occurred after 47 Ma and before 35 Ma (Monger and Journeay, 1994), entirely within the Eocene Epoch. Thus, dextral motion corresponds only to, at most, the second half of basin deposition.

Johnson recognizes that to be a strike-slip basin, the Chuckanut would have to be one of extraordinary size, larger than any other yet recognised. The largest strike-slip basins are up to 50 km wide with a length to width ratio of between 1:1 and 10:1 (Nilsen and Sylvester, 1995). The Chuckanut Basin is now understood to be even larger than Johnson reported, extending at least 150 km by 80 km, to include the early Tertiary strata in the Greater Vancouver area and on the Gulf islands. Thus, it is unlikely that the basin is an example of a simple strike-slip basin, although the tectonic regime definitely suggests strike-slip motion may have had a role in its development.

Large Regional Basin

Cheney (2000) has suggested that the sediments in the Chuckanut Basin and other smaller basins (such as the Tyee, Chumstick, Chikumchuk, and Swauk Basins) along the western margin of North America were once part of a single large basin covering much of northwestern Washington State. These smaller basins are usually interpreted to have formed as a series of strike-slip basins. However in Cheney's hypothesis sedimentation would not necessarily have been controlled by transcurrent motion, but erosional remnants of the rocks are preferentially preserved in close

proximity to transcurrent fault zones (Cheney 2000). It is beyond the scope of this study to test a claim of this magnitude (though a large detailed stratigraphic study of correlations between the basins might).

This model seems unlikely: the basins have different sedimentation styles, varying periods of deposition, many undeniable strike-slip features, and the interbedded volcanic rocks that are present in some basins are not present in all. Even if this model is correct, one would still need to identify the tectonic evolution of this postulated larger basin.

Ridged Forearc Basin evolving to Benched Forearc Basin

Ridged and benched forearc basins are similar to normal forearc basins. Sedimentation occurs in a region in front of a magmatic arc, between the arc and the trench, and subsidence occurs by lithospheric flexure or extension of the area in front of the arc (Dickinson, 1995). However, in both ridged and benched forearc basins (Figure 17) the trench slope break is topographically higher than the basin (Dickinson, 1995). If the trench slope break is higher than sea level sediment in the basin will initially be marine, but will eventually become continental. This reflects the transition from a ridged forearc basin to a benched forearc basin. A lack of marine sedimentation is a crucial feature for basin models encompassing the Chuckanut and Huntingdon Formations, as marine influence has not been observed anywhere in the basin (Mustard and Rouse, 1994; Johnson, 1984).

As discussed above, a "magmatic arc" developed to the east of the Chuckanut Basin during Paleocene time to Oligocene time and beyond (Figure 7). This arc complex was one of the major source areas for the Chuckanut Basin (discussed in Chapters 3 and 4), however a forearc model does not account for the second possible source area lying to the northwest. The model is supported by the existence of some volcanic layers within some members of the Chuckanut Formation, such as tuff beds which occur in both the Bellingham Bay and Governor's Point members of the Chuckanut Formation (Johnson 1984).

Peripheral Foreland Basin

A peripheral foreland basin can be developed by attempted subduction in the forearc setting (Miall, 1995) and can "overlie, adjoin, and may be overridden by subduction complexes and overlap marginal sediment wedges of subducting plates" (Miall 1995, 394). The uplift of the Naniamo Group, possibly during the Paleocene Epoch and/or Eocene Epoch, could represent uplift due to initial interaction with underplating accreted terranes, such as the Pacific Rim and Crescent terranes. Age constraints on these uplift and erosion events are not precise; however, if sediments from this uplift were deposited into the Chuckanut Basin, it would have been as a peripheral foreland basin. Sediments on Sucia Island contain reworked Nanaimo Group material (Mustard, pers. comm., 2002) and support the peripheral foreland basin model. Unfortunately, as is the case for the previous model, a peripheral foreland basin model does not account for the major sediment source lying to the east.

Polyhistoric, Hybrid, or Successor Basin

Hybrid basins occur in regions of complex tectonics such as subduction zones (Nilsen and Sylvester, 1995). They represent several varied styles of basin evolution acting sequentially or in concert within one basin, developing multiple or overlapping styles of sedimentation. With this model, features characteristic of the previous models may become incorporated into a single basin model. The multiple phases of tectonic evolution during deposition and multiple source areas of the Chuckanut suggest varied controls on the basin's evolution. Thus, the Chuckanut Basin may have had ridged forearc basin, benched forearc basin, peripheral foreland basin, and strike-slip basin influences or periods of development. There is support for this interpretation. Ingersoll and Busby (1995) note:

> A basin should be classified according to its tectonic setting at the time of deposition of a given stratigraphic interval; thus a basin…may change its tectonic setting rapidly and often (6).

Sedimentation in the Chuckanut Basin occurred under a number of varying tectonic
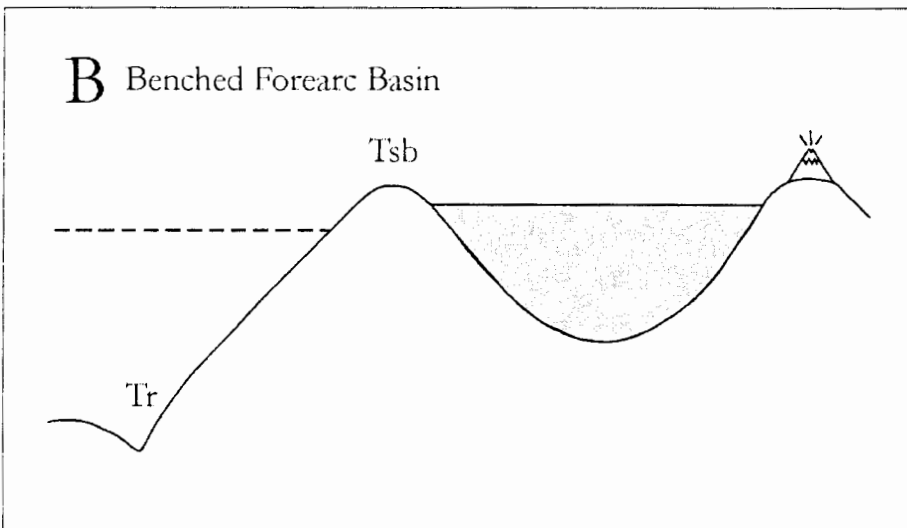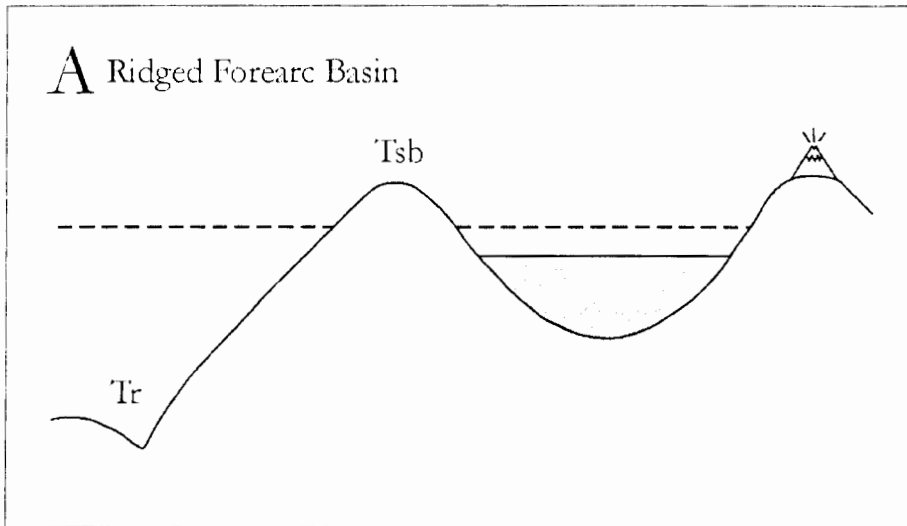
Figure 17 - Two styles of forearc deposition.
A - ridged (emergent ridge) forearc basin. Sedimentation takes place behind a raised protective ridge, but (at least initially) below sea level. **B** - benched forearc basin. Sedimentation occurs behind a ridge, but above sea level. **Tr** - trench, **Tsb** - trench slope break (altered from Dickinson 1995).

regimes. It is clear that a model which includes an evolution of tectonic styles over the age of the basin is required.

Conclusions

Brittle fractures within the field area correlate to regional fracture trends identified by Journeay and van Ulden (1998) and Journeay and Morrison (1999). These trend roughly northwest (possibly the older set) and northeast (possibly the younger set). Shear fractures in the field area are indicative of northeast/southwest compression.

Stress and strain from plate motions during deposition of the sediments were either directed roughly northeast due to oblique subduction, or roughly northwest due to strain partitioning of oblique subduction or transcurrent motion

The Chuckanut Basin is a broad, tectonically controlled structural basin, which developed as a result of several tectonic regimes. The basin contains attributes of forearc, strike slip, and possibly peripheral foreland basins, and as such, the working hypothesis for the basin's evolution is that it reflects a hybrid basin.

Chapter 3 - Huntingdon Stratigraphy and Sedimentology

Introduction

As discussed in Chapter 1 the literature contains great confusion regarding the name(s) of Tertiary-aged sediments in the Chuckanut Basin. Much of this confusion should be cleared up somewhat by the development of a formal type section for the Huntingdon Formation.

Stratigraphic Section

The Huntingdon Formation at Sumas Mountain (Canada) is exposed in a series of active quarries, housing excavations and exposed cliffs (these cliffs tend to comprise resistantly weathered sandstone and conglomerate). A complete stratigraphic section could not be extracted without an extensive drilling program. For this reason, a composite section has been produced for this study. Even with a composite section, there are gaps where no exposure occurs at the surface. The majority of the section was described and mapped in 2002; however the upper 70m was described in 1992 by Dr. Peter Mustard and was published by Mustard and Rouse (1994). The complete section is found in Appendix D, and Figure 18 constitutes a summary.

The Huntingdon Formation at Sumas Mountain (Canada) exhibits a broad coarsening-upward trend. Within this general framework are many smaller fining-upward trends. The lowest part of the section contains fine-grained sediments such as claystone, siltstone, and mudstone, with a relatively small amount of medium-grained sandstone. Sedimentary structures in the lower 40 metres are limited mostly to current ripples and horizontal planar lamination. Fossilised leaves are common and coal layers up to 30 cm in thickness occur locally. As one moves up-section, sandstone and conglomerate increase in abundance, and coarser-grained sandstones begin to increase in abundance. Coarser sandstones contain trough cross-
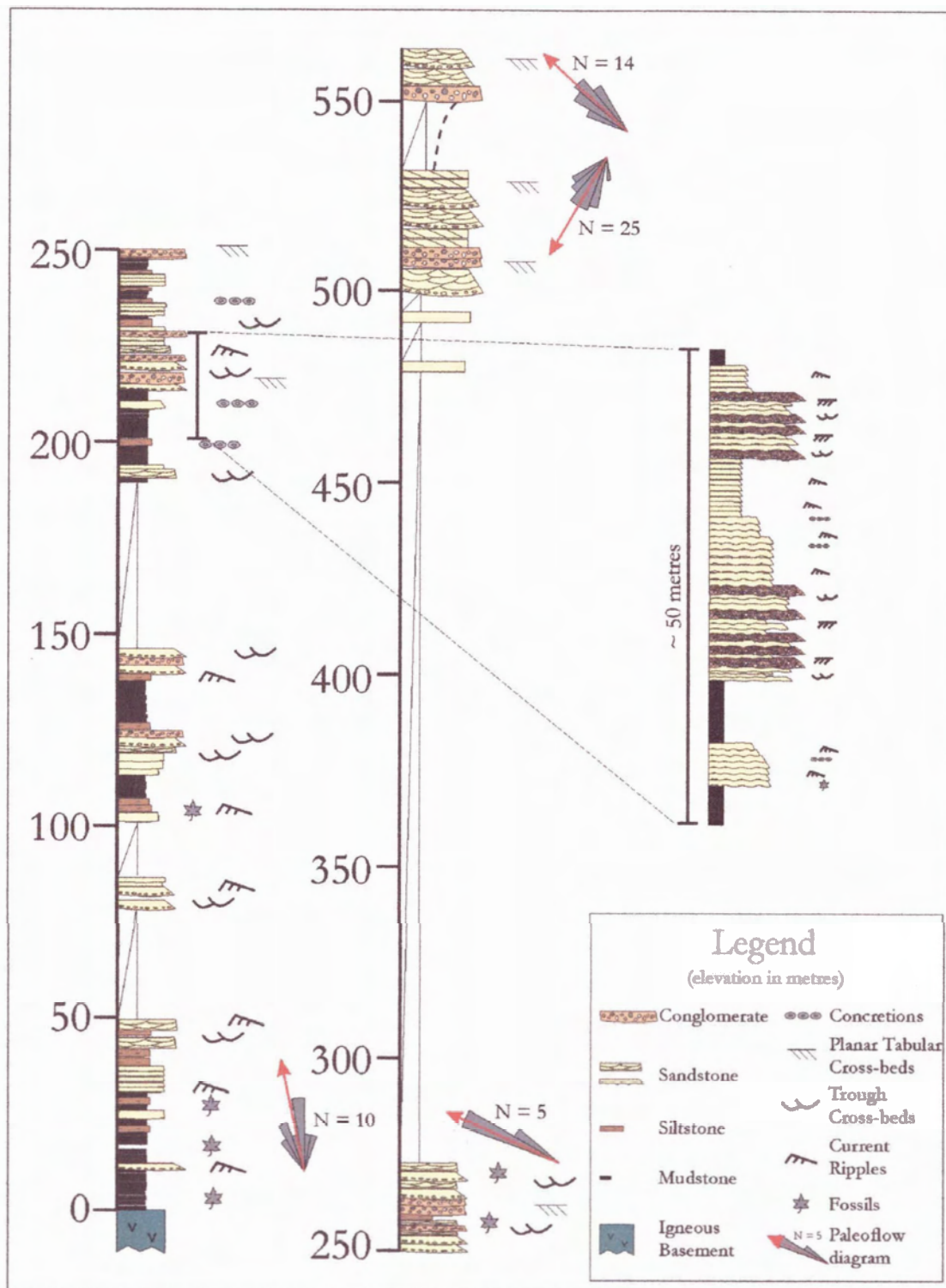
Figure 18 - Proposed composite type section of the Huntingdon Formation, Sumas Mountain (Canada).
See text for discussion.

stratification and rare planar tabular cross-stratification. The conglomerate contains trough and planar tabular cross-stratification. The first conglomerate layers appear near 125 metres; above this, many of the fining-upwards cycles begin with a conglomerate layer. No claystone occurs above approximately 150 metres, but siltstone and mudstone remain common until about 250 metres. Between 200 and 275 metres, concretions and concretionary layers are common in both mudstone and sandstone. Close to 275 metres, thick (up to 12 m) beds of multi-storey stacked conglomerate and coarse-grained sandstone occur. There is a large gap in the section between 275 metres and 475 metres. The uppermost parts of the section contain thick successions of multi-storey conglomerate and coarse-grained sandstone beds. Interpretations of the stratigraphic section are discussed at the end of this chapter.

Facies in the stratigraphic section

Lithofacies Codes

Description of facies can be greatly facilitated by the use of facies codes such as those presented by Miall (1978) and modified many times since (e.g. Miall, 1985; Miall, 1996). In Miall's assessment:

> ... sedimentological research has demonstrated that much of the apparent variability in sedimentary units disguises a limited range of basic lithofacies and biofacies types. The depositional processes which control the development of clastic fluvial lithofacies, such as traction-current transportation, with its accompanying fluid turbulence and its effects on beds of clastic grains, are common to all rivers and obey the same physical laws everywhere, with the production of similar suites of lithofacies (Miall 1996, 77).

In the early stages of fieldwork, each facies was described individually. However, as the field season progressed, Miall's lithofacies codes (e.g. Miall, 1996) were used. In general, the lithologies for each general grain size category did not vary greatly across the field area. Thus, sedimentary structures became the primary way of distinguishing various facies. Facies observed are described below, divided broadly by grain size, and listed from coarsest to finest.

Conglomerate facies

Conglomerates for this study are defined as gravel bearing rocks with greater than 30% clasts (Boggs Jr. 2001). The conglomerate facies exhibit a dark grey to black, tan, or a tan-brown weathered surface, and a light grey or whitish tan fresh surface. They are generally moderately to well lithified, but some locations contain very poorly cemented rocks that are highly friable, permitting disaggregation by hand (Figure 19). Clasts within the conglomerate facies vary generally from sub-rounded to rounded and display low to high degrees of sphericity. The clast size varies from granule (>2mm) up to 10 cm in length. In most conglomerate facies clast size ranges between 2 and 6 cm, but the range within any one bed tends not to be greater than 2 cm. The clasts comprise a variety of different rock types, mostly chert and igneous volcanic clasts, followed by (in decreasing significance), those of igneous intrusive, sedimentary, quartz, and finally metamorphic (Figure 20). Thin section analysis shows a matrix of subangular grains of lithic fragments, quartz, and feldspar. The majority of lithic fragments are chert (megachert or sutured quartz, comprising 40-50%), but detrital micas are common (15-20%). Mica grains commonly display compaction deformation around neighbouring grains. The matrix of the conglomerate facies consists of coarse upper to coarse lower sand-sized particles similar to the sandstone facies described below. Matrix grains are generally subangular. The most common grains in the matrix are chert and quartz.

All conglomerate beds overlie a sharp, commonly irregular erosional boundary and many grade upwards into medium- to very coarse-grained pebble rich sandstone (Figure 21). Most conglomerates show weak imbrication of clasts. Internal erosion surfaces within the conglomerates are common, and are typically difficult or impossible to separate.

The extent of the conglomerate facies is limited in the stratigraphically lower parts of the section, but their distribution increases up section, and multi-storey stacked conglomerates (some sections in excess of 12 metres thick) make up major portions of the upper cliffs (visible in Figure 8). In the lower section, conglomerate

Figure 19 - Recessively eroded pebbly sandstone underlying conglomerate.
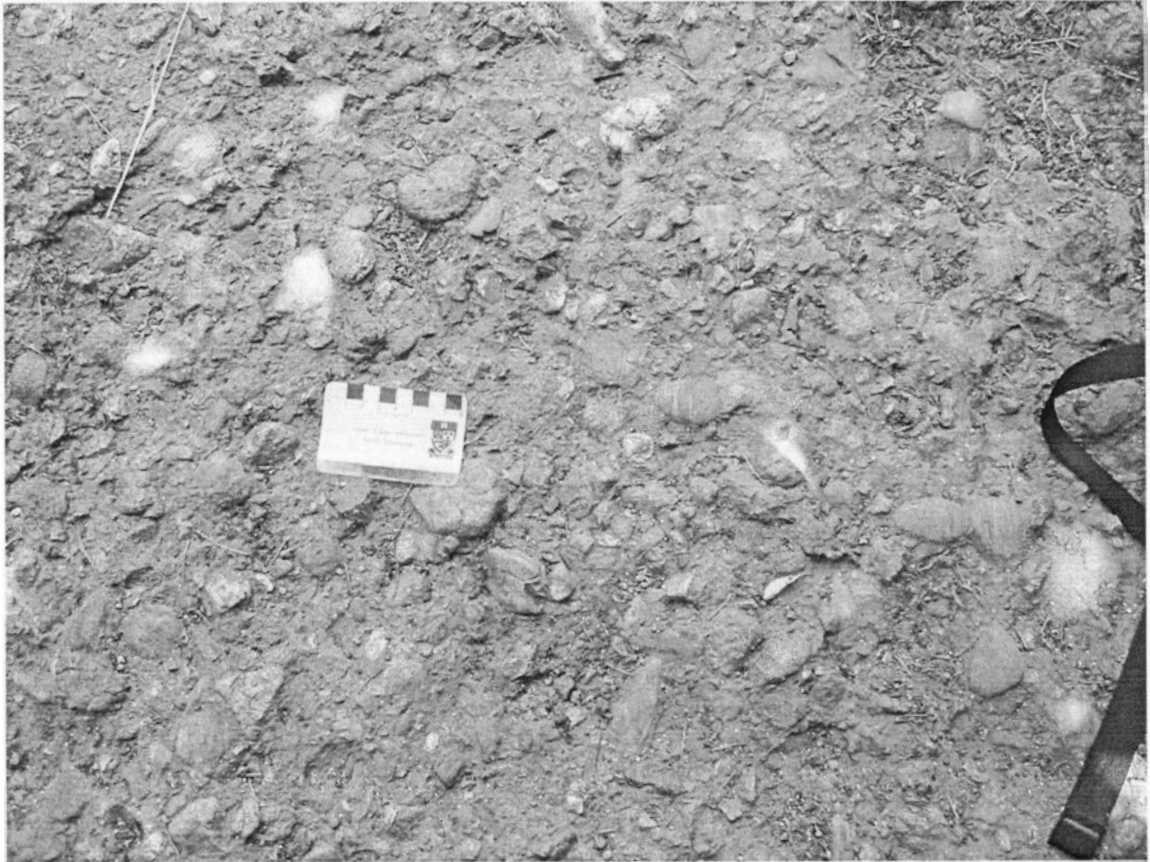
Figure 20 - Pebble conglomerate - squares on scale card are 1cm wide.

Figure 21 - Pebble conglomerate, fining upward to medium-grained sandstone.

occurs in thin (20-40 cm thick) beds, some of which are laterally extensive, but most forming lenses between one and five metres in length.

Fractures and faults within conglomerate commonly display an area of reddish alteration three to four centimetres wide on both sides of the feature. This alteration is presumably iron staining due to groundwater flow. Rarely conglomerate beds are also marked by sporadic concretionary layers, which tend to parallel bedding planes. On average these concretions are about 20 cm thick.

Two variations of conglomerate lithofacies can be identified:

Horizontally Bedded Conglomerate (Lithofacies code Gh after Miall 1996)

Horizontally bedded conglomerate occurs in layers or lenses. It rarely displays weak imbrication, but is otherwise featureless.

Cross-Stratified Conglomerate (Gt-trough and Gp-planar)

Cross-stratified conglomerate also occurs in horizontal layers or lenses. Cross stratification varies evenly between trough and planar tabular cross-stratification, but exact identification is commonly difficult because of two-dimensional exposures overlapping erosion surfaces and removal of the tops of many sets. (Figure 22 and Figure 23)

Sandstone Facies

The sandstone facies in the study area are broadly grouped into two categories: medium- to very coarse-grained sandstone and very fine- to medium-grained sandstone. Three discrete sandstone facies occur in each category: massive (apparently structureless) sandstone, horizonally stratified sandstone, and current rippled sandstone. These facies are listed with the grain size they occur with most commonly. Featureless sandstone is described with the coarser-grained sandstones facies, and current rippled sandstone and horizontally stratified sandstone are described with the finer-grained facies.

Figure 22 - Cross-stratified pebble conglomerate.
Individual cross-strata are approximately 10 centimetre thick. Bed thickness is 1.5 metres.
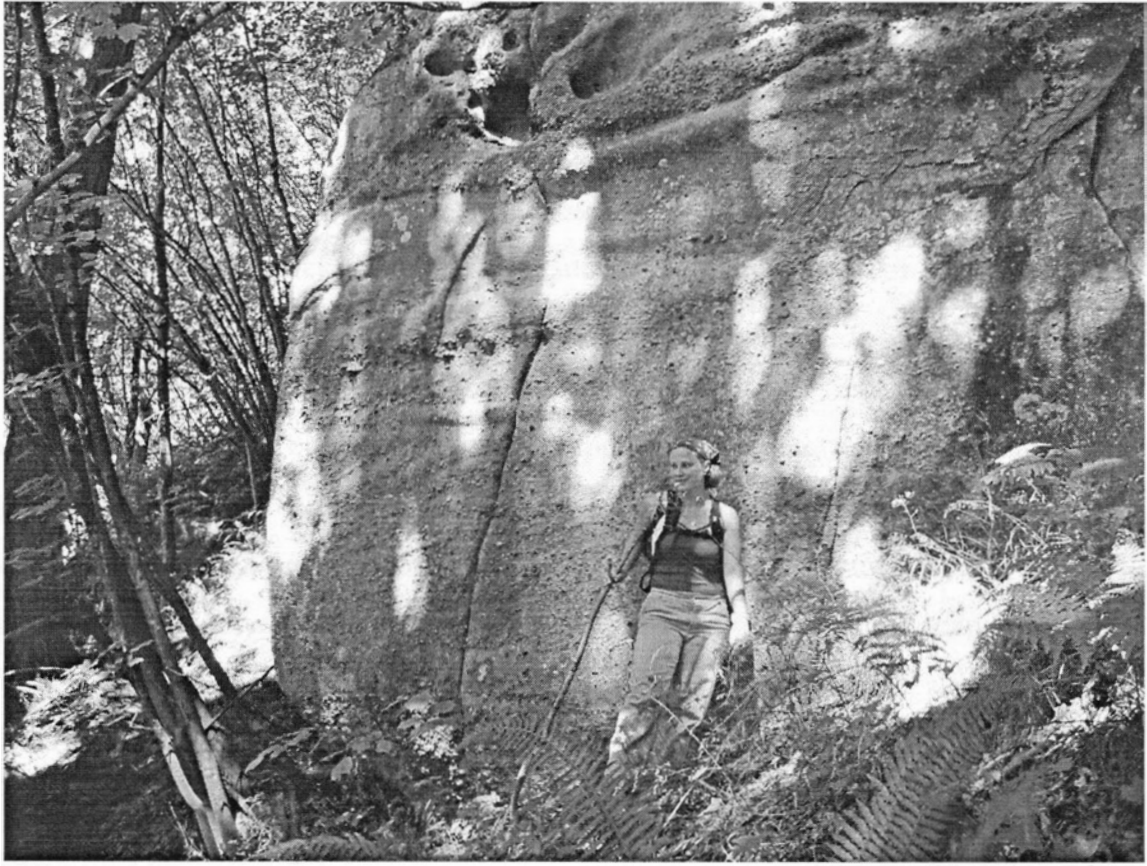
Figure 23 - Cross-stratified conglomerate.
Individual cross-strata are approximately 10 centimetre thick. Bed thickness is 1.5 metres.

Medium- to very coarse-grained sandstone facies

The greatest variability of sedimentary structures occurs within the medium- to very coarse-grained sandstone facies. Weathering colours vary from shades of tan, brown (dark brown, grey brown, white brown, tan brown, and reddish brown) to grey, dark grey to black, or tan. Fresh surfaces display shades of grey (grey, light grey), rare brown, or most commonly a "salt and pepper" appearance made up of light grey or white with dark flecks. Sandstones vary from poorly to well lithified, and many locations effervesce with the application of dilute HCl, demonstrating relatively common calcareous cement. In hand specimen or outcrop, grains of quartz, feldspar, lithic fragments, and various types of mica are visible. Individual grains are generally subangular, and sphericity is low to moderate. Grain size within these sediments ranges from medium- to very coarse-grained sand, although within any one bed the grain size range is restricted to one or two grain size divisions with a tendency to fine upwards slightly. Some beds contain a few pebbles or granules, commonly layered, at their base.

Thin section analysis of medium- to coarse-grained sandstones shows grains to be subangular to subrounded. The most common grains are lithic fragments (45%), the majority of which are chert but some mafic volcanic grains occur as well. In decreasing abundance the remaining grain compositions are quartz (20%), feldspar (15%), and detrital mica (3-5%). There is a trace amount of high birefringence accessory minerals, such as tourmaline and epidote (<3%). Cement (15%) is a varying mixture of calcite, silica, and clay, with calcite the most common. These sandstones plot as (chert) lithic arentites in Folk's 1974 classification (Mustard and Rouse, 1994).

Beds of medium- to coarse-grained sandstone tend to be between 2 and 3 metres thick but can occur in stacked bedsets. The basal contacts of these facies vary, but typically occur as a sharp horizontal surface (Figure 24), an irregular contact (Figure 25), or gradation from either conglomerate or coarser-grained sandstone (Figure 21). The irregular lower contacts commonly contain pebble to
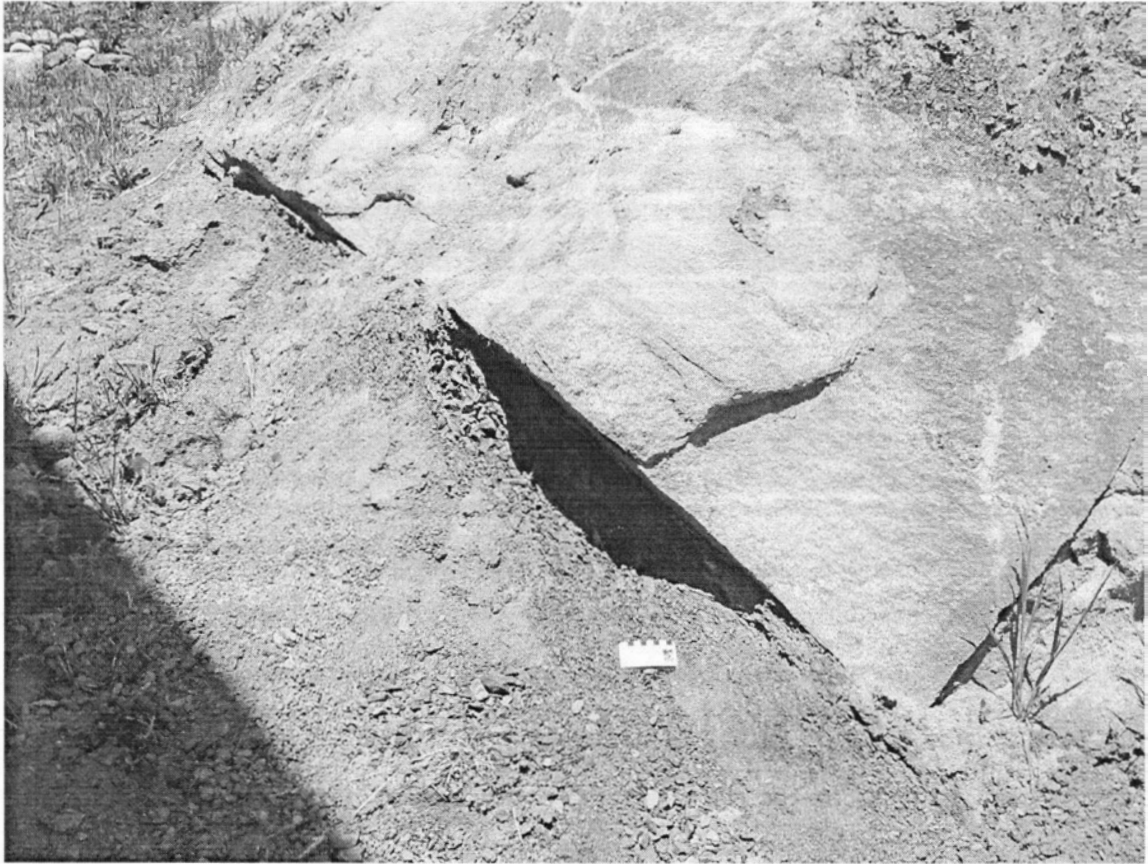
Figure 24 - Extremely regular contact between underlying blocky mudstone and overlying medium-grained sandstone.

granule sized particles or layers, or mud intraclasts directly above the surface. Some of the erosion surfaces display sole marks, flute casts, or current ripple marks if the underlying facies is fine-grained (Figure 26). Upper surfaces of the sandstone facies either fine upwards into smaller particle sized sediments, such as fine-grained sandstone or more rarely siltstone, or are erosionally truncated. Within the coarser-grained sandstone facies the overprinting of internal erosion surfaces is common. Pebble stringers demarcate many of these surfaces. These facies also contain lenses or interbedded layers of siltstone to upper fine-grained sandstone, or in some places coarser-grained sandstone to conglomerate.

In several locations, the coarse-grained sandstones contain fossil material, such as carbonaceous detritus, leaves (Figure 27), leaf fragments, branches (Figure 28), and trace fossils (Figure 29). Horizontal concretions in sandstone facies are relatively common, appear to follow bedding, and range in thickness from 10 to 50 cm. The coarser-grained sandstones are similar to the conglomerate facies, in that fractures and faults commonly have reddish alteration halves within three to four centimetres of the feature, possibly reflecting iron staining due to groundwater flow.

Sandstone facies identified in the field area are:

Cross-stratified Sandstone (St and Sp)

Individual cross-stratified layers commonly display minor fining-upwards successions. Cross-strata thicknesses vary from 1 to 20 cm. Trough cross-stratification appears to be more common, but exact identification of cross-stratification type is difficult (Figure 30 and Figure 31).

Sandstone with erosive and/or shallow scours (Se and Ss)

This is a relatively rarely used facies designation and most commonly these units can be better identified with some other lithofacies code. However, in some cases (such as the upper part of mosaic BP - B Goldstream) this code is quite useful. These sandstones occur as sandstone-filled scours with curvilinear lower contacts.

Figure 25 - Irregular erosional contact between underlying blocky mudstone and overlying coarse-grained pebbly sandstone.
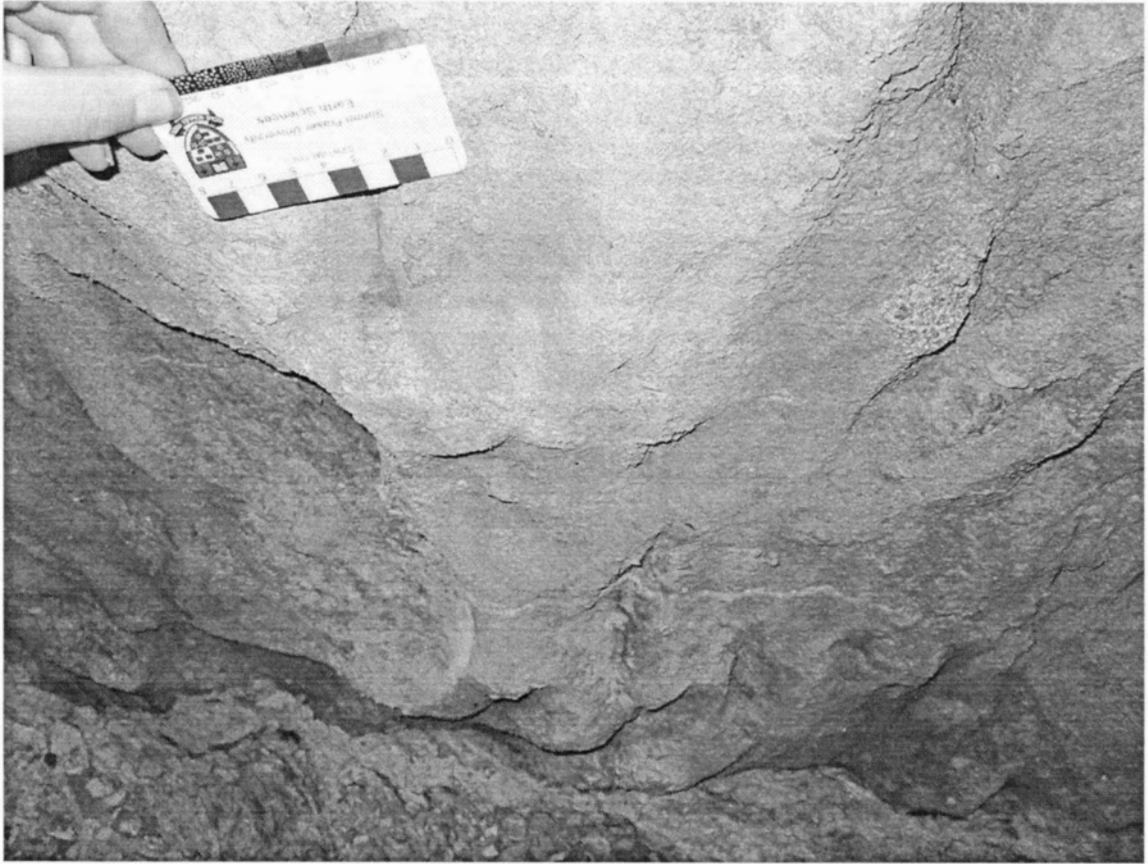
Figure 26 - Flute casts and current ripple marks preserved at the boundary between an underlying mudstone and overlying medium-grained sandstone.

Figure 27 - Fossilized leaves in medium-grained sandstone (hammer head in bottom right corner for scale).
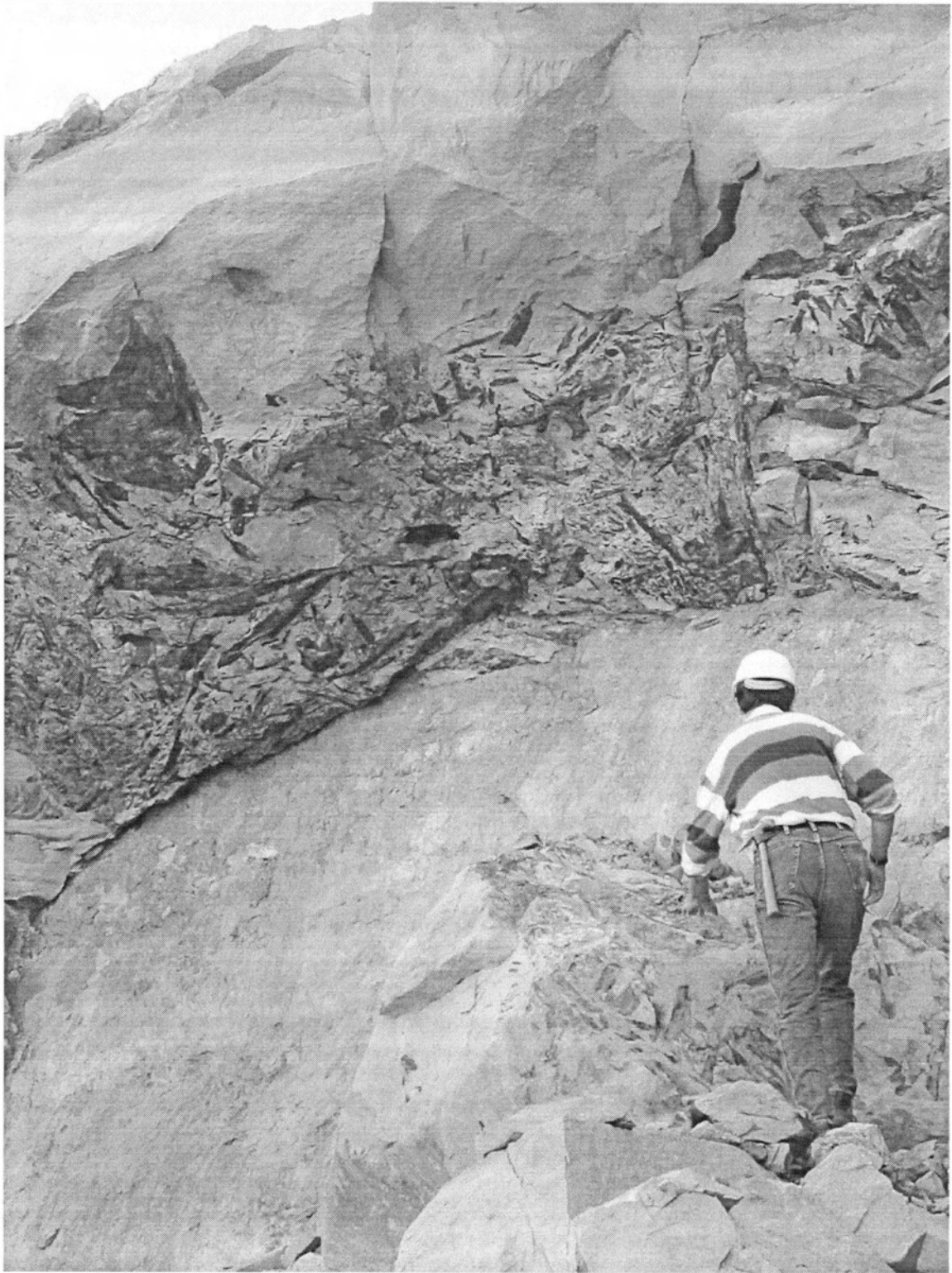
Figure 28 - Fossilized branches, roots, and leaves between layers of medium- to coarse-grained sandstone.
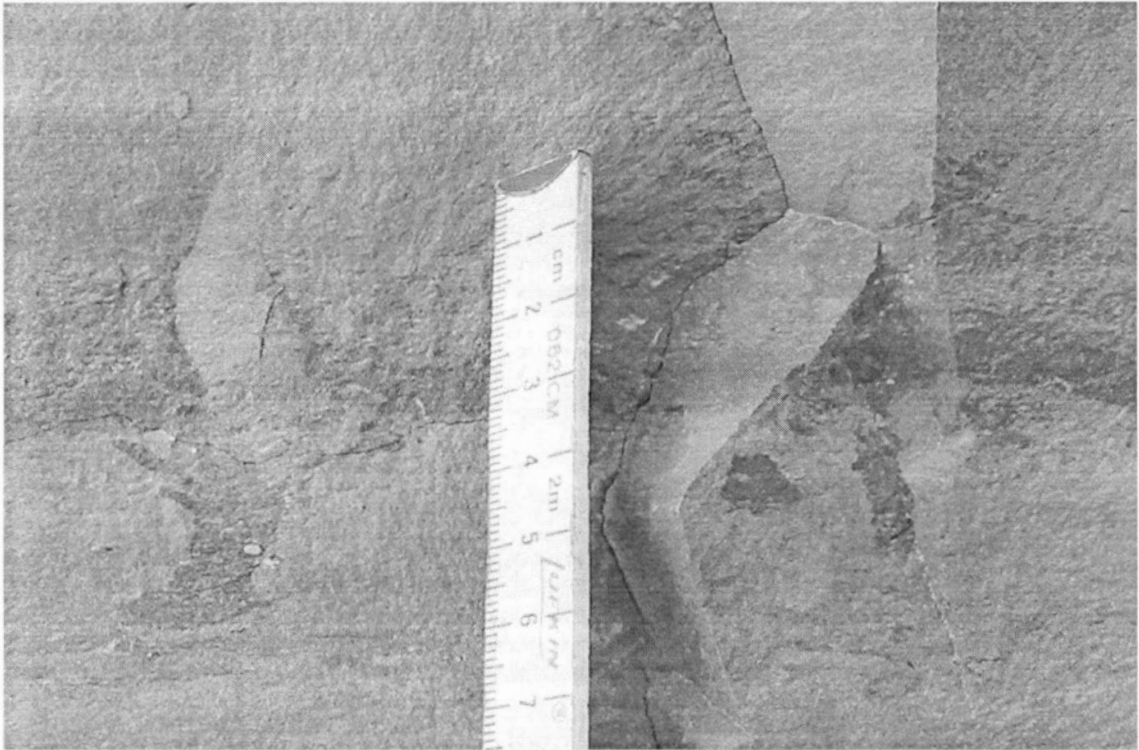
Figure 29 - Trace fossils.
Insect-generated adhesive meniscate burrows (cf., Hasiotis, 2003).
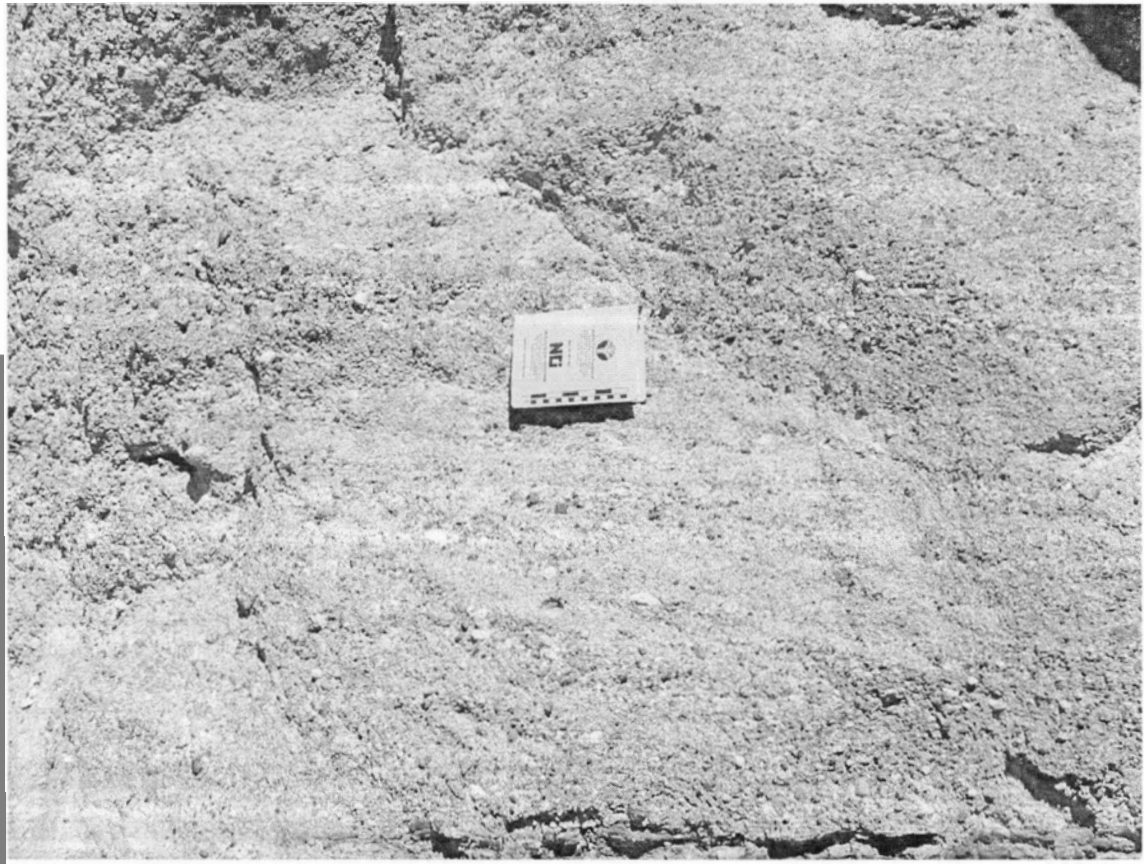
Figure 30 - Cross-stratified, pebbly, coarse-grained sandstone and conglomerate.

Figure 31 - Trough cross-stratified, medium- to coarse-grained sandstone.

Massive (apparently structureless) mL to vcU Sandstone (Sm)

Massive (apparently structureless) sandstone is common, as sedimentary structures in the study area seem to be visible only after some weathering or erosion has taken place. In many locations, freshly exposed sandstones do not display visible features, but weathered sections of the same sandstone displays very obvious sedimentary structures.

Current Rippled Sandstone (Sr)

This facies, although present in coarser-grained sandstones, is less common and is fully is described under fine-grained sandstones (below).

Horizontally Laminated Sandstone (Sh)

Horizontally Laminated Sandstone occurs more commonly in finer-grained sandstones. This facies is described below.

Fine-grained sandstone facies

The fine-grained sandstone facies differ somewhat from the coarser-grained sandstone. For this reason, they are separated in this discussion. Grain sizes vary from lower very fine- to lower medium-grained sandstone. The weathered colour is generally tan to dark grey, and the fresh colour is either grey or light grey. Where they overlie siltstone and finer-grained rock, the fine-grained sand facies are marked by sharp flat horizontal contacts (Figure 24). They also contain abundant current ripples and larger cross stratification. These sandstones tend to contain mica flakes, and in some cases also contain some traces of silt as well. Concretions, carbonaceous detritus, trace fossils, and fossilized plant material are commonly associated with this facies.

Thin section analysis of the fine-grained sandstone facies shows grains to be sub-angular and sub-spherical. The most common grains are lithic fragments (45%), comprising mostly chert with some mafic volcanic fragments. In decreasing order, the remaining grains consist of quartz (30%), feldspar (10-15%), mica (~5%), and

some accessory minerals (<3%). The sandstones are cemented with a mixture of clay and calcite. Fine-grained sandstone facies recognized in the study area are:

Current Rippled Sandstone (Sr)

Current rippled sandstone is common. The ripples are, by definition, less than 5 cm high, and are commonly stacked into simple bedsets between 30 centimetres and two metres thick. Rare rippled beds occur in the coarser-grained sandstones as well (Figure 32).

Horizontally Laminated Sandstone (Sh)

This facies occurs as horizontal laminated sheets of sandstone. The stratification in this facies is generally less than one centimetre in thickness. Individual beds can be up to two metres thick, but stacked sets are found.

Featureless ("massive") vfL to fU Sandstone (Sm)

Featureless sandstone occurs more commonly in coarser-grained sandstones. This facies is described in the previous section. Individual beds of this facies are commonly between 1 and 4 metres thick but lack of visible structure may be obscuring bed contacts.

Fine-grained sandstone, siltstone and mudstone (Fl)

This facies is predominantly very fine-grained sandstone but also contains some siltstone and/or mudstone. This facies is commonly current-rippled or featureless. Laminations in this facies can be less than one centimetre thick and beds vary from less than 0.5 metres to stacked successions several metres thick.

Fine-grained facies

Identification of very fine-grained facies (silt sized and finer) in the field can be problematic. In some areas cliff access is limited, and recognising which layer talus is derived from can be difficult. At Sumas Mountain (Canada) four fine-grained facies are identified, three of which are somewhat similar:

Figure 32 - Current ripple laminations and planar parallel horizontal lamination in fine-grained sandstone. The irregular boundary of a conglomerate layer is visible in the upper left corner.

Figure 33 - Medium- to fine-grained sandstone, fining upwards into siltstone and blocky mudstone.

Mudstone and Siltstone, (Fsm, Fm, and Fr)

The mudstones and siltstones in this area are generally tan, or tan brown on weathered surfaces and dark grey to grey fresh surfaces (Figure 33). These fine-grained sedimentary rocks commonly occur above sandstone beds (Figure 25) or rarely, conglomerate beds. Mudstone and siltstone beds can be quite thick - exposures greater than five metres thick were observed in the pits. Presumably greater thicknesses exist but if exposed are quickly covered by weathered material, as the fine-grained mudstones and siltstones do not resist weathering well. Both facies weather recessively, creating small hollows or caves. The mudstone specifically contains abundant fossil leaves, trace fossil burrows, and somewhat rarer interbedded carbonaceous layers. In some locales, mudstone also contains fossilized in-situ roots (Figure 34). Concretions and concretionary layers are relatively common and tend to be 20 to 50 cm thick.

Claystone

Claystone occurs only in the lower section of the Clayburn Industries pits and has a distinctive reddish colour on both weathered and fresh surfaces (Figure 35). This facies is comprised of apparently structureless claystone. Beds occur from 5 and 50 cm thick, but are seldom thicker than 30 cm. The economic claystone deposits were the first material mined on Sumas Mountain (Canada) and are still economically viable today. These deposits are one of the few economic clay deposits in western North America and have been mined for at least 95 years (Kerr, 1942).

Other facies

Coal (C)

Thin layers of coal are found in the lowest portions of the stratigraphy (Figure 36). These beds are never more than 30 cm thick and are interbedded with claystone, mudstone, siltstone, and fine-grained sandstone. In places the coal retains recognizable fossilized tree remains, including growth rings. On weathered surfaces,

sulphurous material has collected on the layers. There is neither enough volume nor the sufficient grade required for economic recovery of the coal.

Paleocurrents

Paleocurrents from twenty sites were measured during the course of the study. These were added to a handful of measurements from a previous study by Mustard and Rouse (1994). Several rose diagrams appear the stratigraphic section (Figure 18 and Appendix D). Paleocurrent-bearing structures that were measured include: large scale cross-stratification, sole marks, and apparent A-B plane pebble imbrication. Rose diagrams of paleocurrent measurements are given in Figure 37 and tabulated paleocurrent information is provided in Appendix C. Two summary rose diagrams were developed from the paleocurrent information the first a summary of all paleocurrent azimuths (Figure 38 - A) and the second a summary of all orientations from planar cross-strata (Figure 38 - B).

Paleocurrent measurements in the study area indicate paleoflow directions generally westerly, with the average direction lying almost due west. Cross-strata alone tend to indicate a direction closer to northwest. Paleocurrent summary diagrams (Figure 38) seem to indicate a wide variation in flow. This variation is not as strong if paleocurrent measurements are grouped by geography (Figure 37) or by relative stratigraphic level. In general, paleoflow measurements in the lower parts of the section trend more westerly while measurements in the upper part of the section trend more northerly.

Interpretations

Interpretations based on material presented in this chapter are discussed at the end of Chapter 4.

Figure 34 - Mudstone with in situ fossilized root (squares on scale card are 1 cm).

Figure 35 - Distinctive reddish economically mined claystone layers (arrowed).

Figure 36 - Coal layer found in the lower section of the pits.
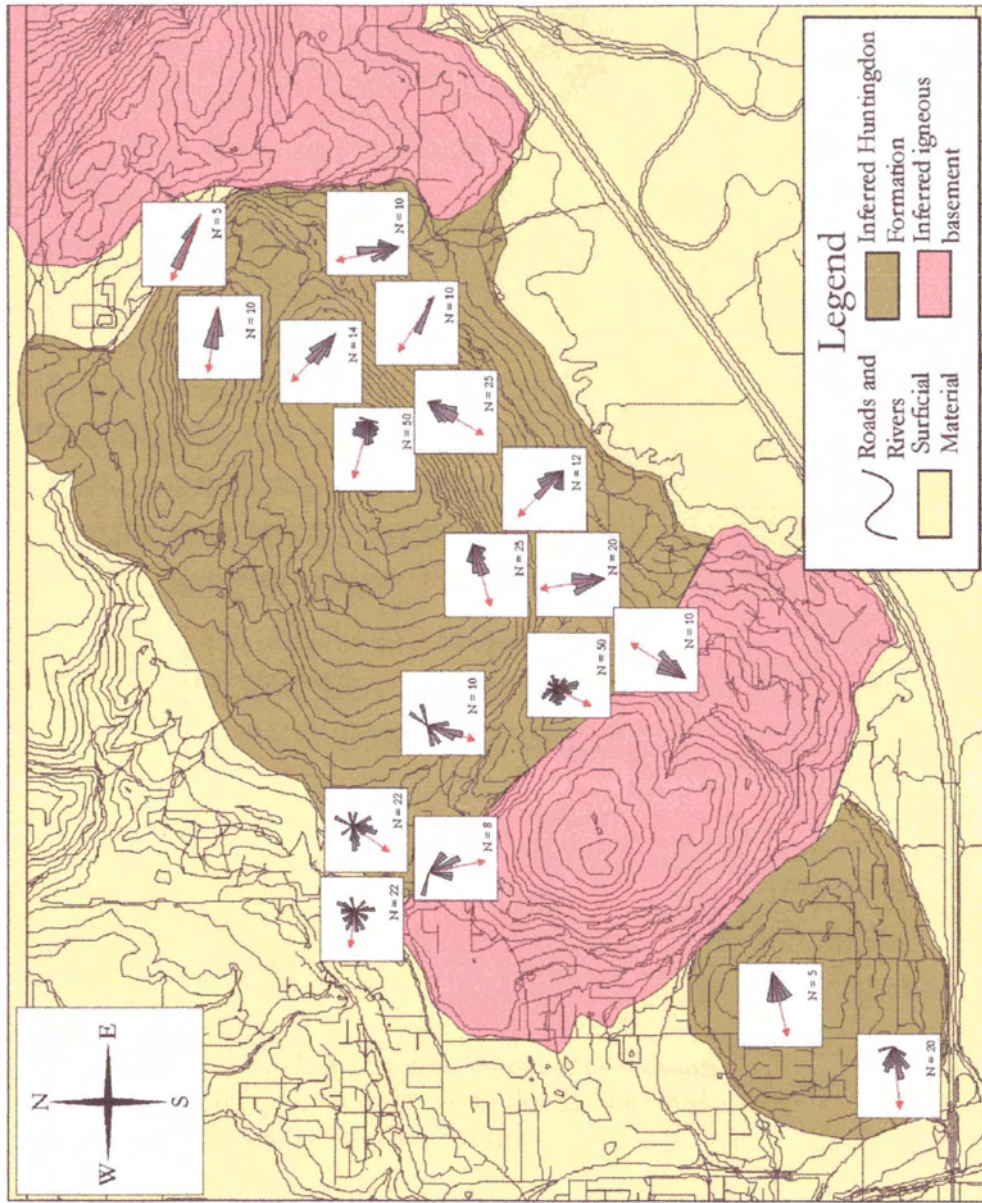
Figure 37 - Paleocurrent measurements at Sumas Mountain (Canada).
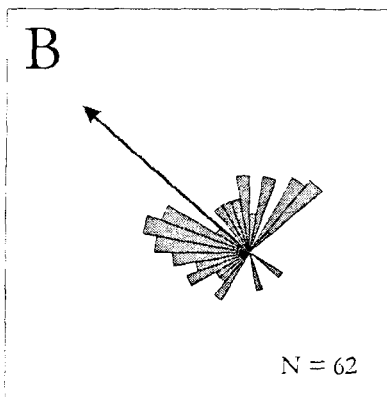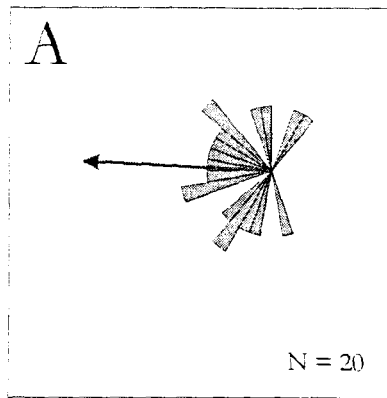
Figure 38 - Summaries of paleocurrent measurements at Sumas Mountain (Canada).
A is a summary of all paleocurrent azimuths in the study area. **B** is summary of all orientations from measured cross-strata planes.

Chapter 4 - Architectural Element Analysis, Facies Associations, and Interpretation of Sedimentary Environments

Introduction

Chapter Three defined and described the lithofacies observed in the study area. The purpose of this chapter is to describe and interpret the architectural elements (macroforms). From the assessment of architectural elements, facies associations constructed from these elements can be made. Architectural Element Analysis (AEA) has been developed in a large part by Andrew Miall, and this study adheres to Miall's approach. Alternative methods of AEA have been described in the literature, the most notable example is the approach advanced by John Bridge (1993).

Background of AEA

The use of facies models has been the mainstay of sedimentary geology for more than 25 years; however, the utility of making predictions about the geometry of sedimentary bodies using only vertical sections is limited. Architectural Element Analysis (AEA) was a technique developed primarily to help geologists understand and predict the three-dimensional extent of fluvial deposits. Development of AEA was originally largely driven by the search for oil and strata-bound ore bodies (Miall 2000). Facies analysis is not to be replaced by AEA; rather AEA is a tool to extend facies analysis.

Modern facies analysis was developed and refined in the 1960s and 1970s as a means to classify recurring sedimentary bodies and make predictions about their spatial distributions (Walker, 1992). However by the 1980s many authors (e.g. Allen, 1983) observed that facies analysis based solely on vertical sections and cores was of limited use for determining the physical extents of sedimentary bodies. The need for an enhancement of facies analysis was evident.

Another drawback of traditional facies analysis, specifically with respect to fluvial systems, was that by the early 1980s there were at least a dozen formal facies

models to explain fluvial sedimentation (e.g. Miall, 1980). These models reflect a set of fixed points along a multidimensional spectrum (Miall, 1985). Miall (1985) points out (though with some hyperbole) that the logical conclusion of an expanding series of fixed points along a spectrum would eventually be a unique facies model for each separate fluvial system in the real world.

Architectural element analysis is meant to bridge a gap in fluvial facies analysis; it accomplishes this by grouping facies and sedimentary structures into features of a slightly larger scale (Macroforms or Architectrual Elements, as discussed below). Traditionally, sedimentology involves identification of recurring facies (micro- and mesoform features), the results of processes in the environment the facies were deposited in. The sedimentologist deduces characteristics of the environment from preserved aspects of the facies. Unfortunately, (or fortunately) the facies observed in modern and ancient rivers are relatively few and can be similar even in markedly varied fluvial environments. Interpretation of fluvial style based on such similar micro- or mesoform scale features can be difficult. There is, however, variance in the spatial arrangement of these same facies between different fluvial environments. If one can describe and characterize recurring sedimentological features of a scale intermediate between sedimentary structures and entire fluvial environments, then one can facilitate a more refined appraisal of ancient fluvial styles. This, in turn, allows the development of a more accurate description of the depositional environment without resorting to force-fitting fluvial systems into previously developed models. Examples of such models include the spectrum of fluvial facies models (e.g. wandering gravel bed river or gravel-sand meandering river) described by many authors (cf. Miall, 1980; 1985; 1997). AEA allows one to define basic similarities or "elements" common to modern fluvial systems and use these to develop a unique description of any given ancient fluvial system.

The term "architectural element" (AE) was first applied by Allen (1983). This study and two others (Friend, 1983; Ramos and Sopeña, 1983) inspired the paper by Miall (1985) that laid out a prototype approach for the concept of AEA.

Architectural Element Analysis

AEA is defined by two interrelated core concepts: (1) Hierarchical Bounding Surfaces and (2) Architectural Elements (Miall, 1985; 1988; 1997; 2000). Bounding surfaces are the borders that separate, divide and group individual architectural elements.

1. Bounding Surfaces and Scale

A bounding surface is interpreted as a surface of non-deposition or erosion, which separates two sedimentary units. It can represent any interval of time ranging from a few seconds to hundreds of thousands of years and bound elements as small as individual ripple marks to the size of entire river complexes (Miall 2000). In essence bounding surfaces are discontinuities with scales varying in terms of both distance and time.

Allen (1983) defined microforms, mesoforms, and macroforms to represent different scales of fluvial sedimentary structures. Microforms include smaller features such as current ripple marks and current lineations. Mesoforms are larger "flow regime bedforms" such as dunes. Macroforms reflect processes acting over much longer periods of time, such as channel fills, channel bars, and islands (Miall 1985). Macroforms are broadly equivalent to architectural elements (AE) (described in depth in the next section).

Bounding surfaces are the hierarchical delineating surfaces of microforms, mesoforms, macroforms, or larger. Allen (1983) initially recognised three scales of bounding surfaces. Miall (1985) expanded this into seven and then into eight hierarchical scales of bounding surfaces (Miall, 1996). The divisions between hierarchies are loosely on the inferred length of time required to achieve each depositional event or erosional hiatus (Miall 2000). The characteristics of bounding surfaces are described below and example surfaces of 1st to 6th order are shown on Figure 39.

1.5 m

Figure 39 - Examples of bounding surfaces from 2nd to 5th order.
Green lines represent 2nd order bounding surfaces, yellow lines represent 3rd order bounding surfaces, the blue line represents a 4th order bounding surface separating two architectural elements, and the red line represents a 5th order bounding surface, in this case an irregular erosion surface. Note bounding surfaces are truncated by surfaces of higher order. Bounding surfaces in this diagram are taken from Figure BP - K Powerline.

1st Order Bounding Surfaces

These surfaces represent minor boundaries within microform and mesoform deposits. This surface is unchanged from Allen (1983). Very little erosion is apparent at 1st order boundaries, unless it is due to reactivation of the bedform, or to minor reorientation of the current. This surface represents virtually continuous sedimentation in the rock record, and any time gaps are on the order of minutes to hours.

1st order bounding surfaces are cross-set bounding surfaces. Such surfaces are small, plentiful, but commonly difficult to discern in outcrop. As a result 1st order surfaces are not shown on photomosaics in this study.

2nd Order Bounding Surfaces

2nd order surfaces also represent minor boundaries within microform and mesoform deposits. 2nd order boundaries represent coset bounding surfaces reflecting relatively minor changes in flow condition or flow direction. Lithofacies may vary across the boundary, but evidence of significant erosion is not present, comparable to that of the 1st order surfaces.

3rd Order Bounding Surfaces

3rd order surfaces are boundaries within macroform deposits. They are cross-cutting erosion surfaces typically dipping at less than 15°. Facies above and below the boundaries are similar. 3rd order surfaces may also delineate minor bar or bedform successions draped with mudstone or siltstone. At this scale the surface indicates changes in river stage or macroform orientation and can be thought of as the growth increments or accretion surfaces within the AE/macroform.

4th Order Bounding Surfaces

4th order surfaces are the upper bounding surfaces of AEs/macroforms. They tend to be flat to convex upward. Basal scour surfaces of minor channels or chutes are also 4th order surfaces. This order of surface represents periods of time longer than 1st and 2nd order surfaces (on the order of 100 to 1000 years).

5th Order Bounding Surfaces (3rd order of Allen (1983))

These surfaces bound major sand sheets (e.g. channel fill complexes) and are flat to slightly concave. 5th order surfaces commonly contain local cut and fill features, as well as basal lags. Time periods represented by 5th order surfaces are relatively long, on the order of millennia.

6th, 7th, and 8th Order Bounding Surfaces

Surfaces of this scale lie in the realm of sequence stratigraphic analysis, and are essentially equivalent to unconformities. 6th order surfaces represent groups of channels or paleovalleys. Stratigraphic units such as members or submembers may also be bounded by 6th order surfaces. 7th order surfaces bound entire depositional systems, such as the surface between the Huntingdon-Chuckanut System and the Cretaceous Nanaimo Group. 8th order surfaces bound major basin and fill complexes, may represent long periods of time (10^6-10^7 years), and encompass deposits of vastly different environments of deposition. 6th to 8th order surfaces were not encountered in any of the outcrops in this study, though the nonconformity identified by Kerr (1942) would represent an 8th order surface.

Architectural Elements and Facies Associations

Facies in this chapter are grouped into two hierarchical scales. The first scale is that of architectural elements (genetically related groups of lithofacies, separated by hierarchical bounding surfaces as described below). These architectural elements are broadly equivalent to the macroforms described by Allen (1983). The second scale is that of facies associations, defined here as groups and successions of architectural elements.

Architectural Elements

Architectural Element Analysis is based on the identification of architectural elements (AE). AEs are characterised by geometry, facies composition, and scale. As noted in the previous section, they are equivalent to macroforms, and consist of genetically related lithofacies. Internal minor (1st to 3rd order) bounding surfaces extend from the top to the bottom of the elements and they are bounded by surfaces

of 4th, or higher, order. Architectural elements develop by relatively long-term accretion over decades or centuries (Miall 2000). Larger elements may contain several orders of bounding surfaces and are delineated by major (5th or higher order) bounding surfaces (Miall 1988). In general sedimentary structures within each element show similar orientations; however, large elements may show greater variability in internal orientation (see element CH below).

AE's are "assembled" out of a set of similar facies. As suggested by Miall (1985), facies codes can be useful in assembling AEs. Facies codes used in this study are described in Chapter Three. This study uses Architectural Elements suggested by Miall (1985; 1996; 2000). Sample AEs are presented graphically in Figure 40. Detailed descriptions of architectural elements observed in this study, broadly grouped from most to least common, are summarized below.

FF – Floodplain Fines

Floodplain fines are the most common element in the field area (though not in the photomosaics). They are typically composed of fine-grained sandstone, siltstone, and/or mudstone (lithofacies Fl, Fsm, and Fm - see Chapter Three), but may also contain thin coal seams.

The FF element forms in very broad horizontally stratified sheets. These elements generally vary from one to ten metres in thickness, and extend many tens of metres laterally at a minimum. Most are likely many hundreds of metres to kilometres in horizontal extent. These fine-grained sediments were deposited in waning flow conditions during floods or from suspension in still waters on the floodplain, either after flood events or within permanent swamps or ponds (Miall, 1996).

There are many examples of FF elements in the study area. Mosaic BP - E (Greta), and Mosaic BP - C (Upper Banshee) each contain multiple examples of the FF element. In the stratigraphically lower parts of the study area, localized occurrences of economic claystone (Fc) have been mined for almost 100 years.
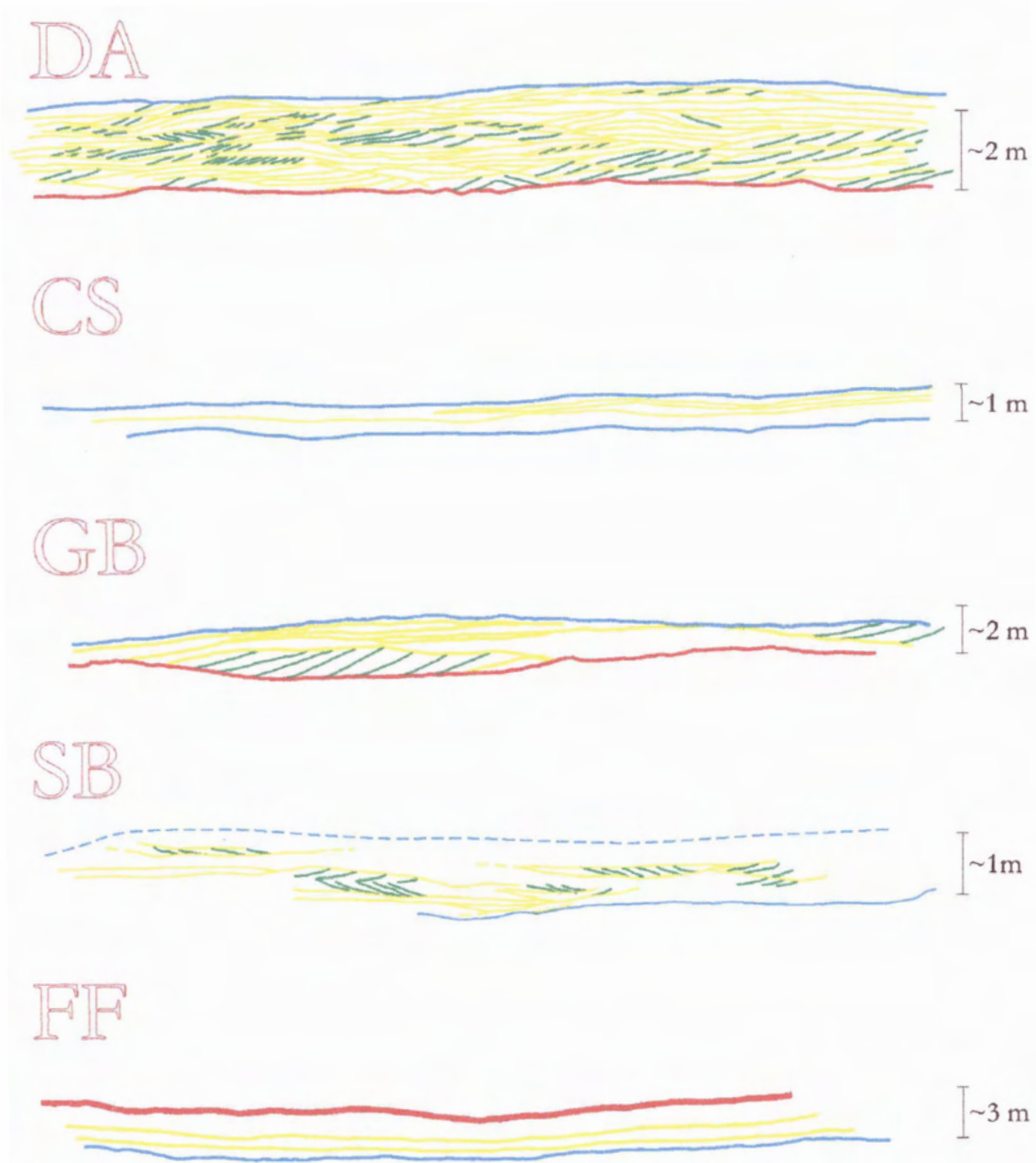
Figure 40 - Some sample Architectural Elements from the study area.
Vertical scale and horizontal scale are equivalent.
DA - Downstream Accretion (from Mosaic I - Lower Banshee)
CS - Crevasse Splay (from Mosaic I - Lower Banshee)
GB - Gravel Bar or Bedform (from Mosaic D - Kelly)
SB - Sandy Bedform (From Mosaic G - Mckee)
FF - Floodplain Fines (From Mosaic E - Greta). The shape of this element is slightly
distorted by photographic effects in the field. It is convex upwards.

CH - Channel

CH elements are an amalgamation of several other elements and may contain several different facies. Though it can be complex, the CH element constitutes the most basic element, and, obviously, represents a channel filled with sediment, a common characteristic of fluvial successions. In many cases the CH element occurs with a convex upward, lower bounding surface, typically of 5th or greater order. A CH element can contain any lithofacies and any of the other architectural elements, including other CH elements depending upon channel size.

As any lithofacies can occur in CH elements a wide variety of sedimentary deposition (many described below) can lead to the development of a CH element. The CH element is not one of the more useful elements for fluvial style interpretation, as most fluvial deposits are technically part of a CH element. It is more useful to differentiate the smaller elements (e.g. SB or DA see below) within a CH element. The CH element is used when sedimentary structures are obscured or too complex to usefully display.

One of the few examples of a CH element defined in this study is found on Mosaic BP - B (Goldstream). It represents a relatively large channel form between 15 and 20 m wide and greater than 3 m high with an arrangement of cross-stratification too complex to show on the mosiac.

SB – Sandy Bedforms

SB elements are typically convex upward lenses or sheets consisting of a range of sandstone-dominated "flow regime bedforms." They range from 0.5 to 3.0 metres in height, and can be tens of metres to hundreds of metres in lateral extent. Common lithofacies within SB are cross-stratified sandstone (typically St, less commonly Sp), horizontally laminated sandstone (Sh), and rippled sandstone (Sr). Element SB is deposited by a variety of flow conditions, but is, in general, formed by vertical aggradation of sediment carried either by traction or suspension/saltation (Miall 1996). Many SB elements were observed in this study. Examples include a

stacked set of forms in Mosaic BP - F (Thiessen), Mosaic BP - B (Goldstream), and BP - G (McKee).

GB – Gravel Bars and Bedforms

GB elements form a range of mesoforms or macroforms containing mostly horizontally bedded conglomerate (Gh), or cross-stratified conglomerate (Gp or Gt). These elements comprise bars and sheets. In this study GB typically forms multi-storey sheets up to tens of metres thick, and in some cases 1.5 km in lateral extent. GB is interpreted to form through the deposition of pulses or lobes of gravel mobilized on the bed of a river by shear forces and carried as bedload during periods of high flow (Miall, 1996). This sediment is moved by traction or extremely limited suspension. Higher flow velocities form crude horizontal stratification (lithofacies Gh), whereas slightly lower flow velocities form cross-stratification (lithofacies Gt or Gp) (Miall, 1996). Many mosaics contain element GB though the best examples can be seen on Mosaic BP - D (Kelly).

DA – Downstream Accretion

DA elements are characterized by erosional bases with gradational tops, unless cut into by another element. DA elements may be formed of gravel or sand, and may display a fining-upwards profile. Accretion surfaces will be evident if the outcrop orientation is favourable. DA elements tend to form convex upward lenses or sheets, vary between 1 and 3 metres high, and have lateral extents of tens of metres to hundreds of metres. The crucial test for accurate identification of a DA element is that accretion surface strikes are oriented perpendicular to the dominant current direction, indicating that the element developed by accretion in a downstream, not lateral direction. Like element LA (described below) this element can be extremely difficult to recognize in the field, as favourable orientation of paleocurrent indicators can be difficult to find.

Lithofacies codes within DA elements include cross-stratified sandstone (St or Sp), horizontally laminated sandstone (Sh), current rippled sandstone (Sr), and sandstone with erosive and/or shallow scours (Ss). DA may include gravel

lithofacies as well, such as cross-stratified conglomerate (Gt or Gp). DA elements form by lateral (downstream) aggradation of bars or lenses in the channel bottom, typically during high flow periods. Sediments are transported as bedload or by saltation.

DA elements are quite common in the study area. Mosaic BP - D (Kelly) and Mosaic BP - C (Upper Banshee) contain good examples.

CS - Crevasse Splay

A crevasse splay is a fan- or lens-shaped deposit formed by the breaching, or overtopping, of a river's bank (commonly levees) during flood conditions (Miall, 1996). Depending on the size of the river, splays may be kilometres wide and metres thick, though typically much less. In this study the CS elements are between one and two metres in thickness, though of unknown lateral extent; exposures indicate they are at least tens and possibly hundreds of metres wide, and most exposures end before beds thin or pinch out. The margins of a splay may interfinger with floodplain or levee deposits (Miall, 1996) though this was not observed in the study area. Sedimentation within a splay occurs by saltation, traction, and deposition of suspended sediment, all during waning flow conditions. In many ways a crevasse splay deposit is similar to an alluvial fan.

Lithofacies expressed in CS elements are commonly horizontally laminated sandstone (Sh), rippled sandstone (Sr), sandstone with erosive and/or shallow scours (Ss) and rare cross-stratified sandstone (St). The splays may show 3rd order internal bounding surfaces and, typically, a fining upwards profile; some beds should show normal grading. Higher elevation areas are abandoned as the splay progrades.

CS elements are generally found in association with FF elements and represent a significant amount of the deposits of the Huntingdon Formation at Sumas Mountain. Examples of CS elements occur in Mosaic BP - C (Upper Banshee) and Mosaic BP - E (Greta).

CR - Crevasse Channel

Crevasse channels are minor channels that form as a river breaches its banks or levees and spills out onto the floodplain. The size of the CR and its sedimentary deposits depend upon the size of the river spawning the flood (Miall, 1996). CR elements should form lens or fan-like layers with lateral extent between tens of metres and hundreds of metres (Miall, 1996). Sediment in a crevasse channel is transported by traction, saltation, and suspension. Sediment size in a CR element can be similar to the sediment size in the main channel (Miall, 1996), but may decrease with distance from the main channel (Bridge, 2003). This larger sediment size could occur because the splay channel cuts deep enough access bedload, because flood conditions cause an increase in mean sediment size causing parts of the CR deposit to mimic the coarseness of the main channel's deposits, or because the effect of flow is concentrated in a narrow channel. In rare cases, CRs can form many kilometres from the original channel (Miall, 1996). Deposition in CR occurs by similar methods as the main channel, albeit on a smaller scale. The upper parts of the CR deposit may fine upwards as the flow wanes. The CR element is closely related to the CS element. Each CS element must have been fed by a CR element, though the preservation potential of the first is far greater than the second.

A single CR element was identified in the study area (Mosaic BP - C, Upper Banshee). The channel is approximately two to three metres thick and at least tens of metres in lateral extent. It contains sandstone with erosive and/or shallow scours (Ss), cross-stratified sandstone (Sp), and thin lenses of cross-stratified conglomerate (Gp).

LA – Lateral Accretion

LA elements have erosional bases and gradational tops, unless truncated by an overlying surface. LA deposits generally form a classic fining-upward profile. Their widths are approximately 2/3 of the channel (Miall 1996). Facies assemblages within such elements tend to vary markedly. Ideally any dominant paleoflow indicators will trend 90 degrees to the dip of the accretion surfaces. This element

forms the typical "point bar structure macroform." It may be difficult to recognise in the field, as paleoflow indicators may not be available.

A LA element can contain a variety of lithofacies including cross-stratified sandstone (St or Sp), horizontally laminated sandstone (Sh), current rippled sandstone (Sr), and sandstone with erosive and/or shallow scours (Ss). The top of the element may fine- to very fine-grained sandstone, siltstone, and mudstone (Fl), though this classic fining-upwards pattern of the LA deposit may or may not be present. LA elements may vary if viewed on the upstream or downstream sides (Jackson 1976). At Sumas Mountain (Canada) only one LA element was identified. This example is about 3 metres thick, between 40 and 50 metres across, and occurs in Mosaic BP - F (Thiessen).

Methods of Architectural Element Analysis

The primary method for developing AEA is through the use of photomosaics. Figure 41 (Mosaic A, Laurenzi) is an example of the development of a photomosaic. A digital camera was used to take overlapping photos of a suitable outcrop (Figure 41 - A). For the purpose of demonstration, the outcrop in this figure is much smaller than the one would normally use for AEA.

After downloading the photographs to a computer, they were merged using a digital editing program (Figure 41 - B). This study used Canon Photostich. The enlarged image of the mosaic was printed from a plotter and a mylar overlay was then taped over it. Preliminary identification and scaling of some bounding surfaces was completed in the lab. The overlay and image were then taken back to the outcrop, where a detailed analysis was performed, bounding surfaces sketched on the overlay, lithofacies codes added to denote the appropriate facies, and preliminary interpretation of bounding surface hierarchies and architectural elements initiated. Interpretation of the elements and bounding surfaces was completed after paleocurrent analysis and other relevant field evidence were added to the overlay. The mylar overlay was then scanned (Figure 41 - C), digitized, and final interpretations made using a graphics program (Figure 41 - D), in this case

CorelDraw 10.

Not every level of bounding surface is drawn on each mosaic. For example, 1st and 2nd order surfaces are always too small and numerous to include on a large mosaic. As well, if the sedimentary relationships were too complex to be easily represented (or deciphered), the bounding surfaces were not drawn, so as not to obscure information. On the example mosaic, 2nd order surfaces (green lines) were observed in the lower left part of the outcrop, but were not visible elsewhere on the mosaic.

The example mosaic contains two architectural elements common in the study area and in their typical spatial association: the downstream accretion element (DA) and the gravel bars and bedforms element (GB). The 4th order erosion surface between these elements (blue line, labelled A^1) displays some erosional relief.

Photo Mosaics

Photomosaics described below are labelled Figure BP - B to figure BP - F and can be found, with the legend (Figure BP - N) in the back pocket of this thesis. Figure BP - G to Figure BP - M are photomosiacs completed in the study area but made up of elements and associations already well represented by the six mosaics described below.

Mosaic BP - B (Goldstream)

The Goldstream mosaic exhibits the broad coarsening-upward trend common in many outcrops (but visible on few mosaics) in the study. Most outcrops tend to be capped by erosionally resistant conglomerates. The lowest parts of the section are dominated by fine-grained sediment (blocky mudstone alternating with very fine-grained sandstone), erosionally overlain by medium- to coarse-grained, commonly pebbly sandstone and capped by a major erosion surface overlain by conglomerate. At this location, the uncommonly large exposures of fine-grained sedimentary rock (Element FF) were exposed by recent subdivision development.

The major 5th order bounding surfaces in the Goldstream mosaic are broadly flat lying, except for the channelized sections above the surface labelled "C". In

general the morphologies of the 4th order surfaces are flat to concave-upward, hinting at an overall lens-like morphology of the sheets.

The lower fine-grained section is largely featureless, although some of the silty fine-grained sandstone displays current ripples (Sr) and horizontally laminated sands (Sh) where favourable weathering occurs. These facies together are interpreted as floodplain fines (FF) or crevasse splay (CS) elements .

Between the 5th order bounding surfaces labelled "B" and "C", the most common bedform is trough cross-stratified sandstone, although rare sections of planar tabular cross-stratification also occur locally. These are interpreted as SB elements, though one lens-like section of conglomerate is interpreted as a GB element. Above the 5th order surface C, a portion of a downstream accretion (DA) element is preserved beneath a channel scour though most of the elements above surface C are gravel bar and bedforms (GB). The cross-stratification within the DA element is similar to the orientation of the GB element, this is interpreted to mean both formed by similar processes, likely downstream accretion. Within the Channel element (CH), a complex arrangement of 2nd and 3rd order surfaces defining trough cross-stratified sandstone and conglomerate makes recognition of elements difficult (too complex to be individually delineated on the mosaic).

This mosaic represents some of the typical associations observed throughout the field area. Association A1, A2 (channel sequences) and B1 (floodplain) are present. The upper part of the mosaic has been cut into by a subsequent gravel bars and bedforms element (GB), the first of a 10 metre high series of multi-storey GB elements that lie stratigraphically above this mosiac.

Mosaic BP - C (Upper Banshee)

Mosaic BP - C has a scale which varies along the length of the mosaic; as the surface of the exposure is irregular and the camera position was constrained. The succession illustrated in this mosaic generally fines upward. The lowest portion contains a complex section of erosionally amalgamated, coarse-grained, trough cross-stratified sandstone (St) and is interpreted as a group of downstream accretion

elements (DA). Cross-strata and accretion surfaces in these elements indicate that strike of accretion surfaces formed perpendicular to the regional paleoflow direction indicating downstream accretion. An erosive contact (5th order surface labelled "B") is overlain by fine- to medium-grained, trough cross-stratified sandstone (St), which fines-upward to fine-grained current rippled sandstone (Sr), and ultimately to silty, very fine-grained sandstone (Fl). These units are interpreted as several Crevasse Splay elements (CS). The 5th order bounding surface labelled "C" is an erosive contact. Interstratified sandstone and conglomerate above this contact are interpreted as crevasse channel (CR) element. The planar tabular cross-stratified conglomerate (Gp) within the CR element occurs as thin (10 cm thick) lenses of sediment; this is surrounded by planar tabular cross-stratified sandstone (Sp) and sandstone scours (Ss). This element is interpreted as CR because of the odd stacked lens arrangement of the lithofacies and internal bounding surfaces, the way it grades into the overlying CS element, and the erosional basal contact. This element grades vertically into the horizontally bedded and interbedded sandstones and mudstones of crevasse splay (CS) and intercalated floodplain fines (FF) elements. At the erosional 5th order bounding surface labelled "D", these fine-grained sediments are cut into by a thick layer of Sandy Bedform elements (SB) and Gravel Bars and Bedforms elements (GB).

Mosaic BP - D (Kelly)

The Kelly mosaic is stratigraphically the highest in the study interval. The lowest portions of the mosaic correlate to the highest portions of Mosaic BP - C (Upper Banshee). The lowermost rocks (below the 5th order bounding surface labelled "B") comprise coarse-grained trough cross-stratified sandstone (St), planar tabular cross-stratified conglomerate (Gp), and minor planar tabular cross-stratified and current rippled sandstone (Sp and Sr). These are interpreted as a stacked series of Downstream Accretion elements (DA) and Gravel Bars and Bedforms elements (GB) because the accretion surfaces in the DA elements are similar to surfaces in the GB elements. These DA and GB elements are lens like in overall morphology, and

seem to interfinger somewhat. This group of elements represents facies association A1 and probably normal to high stage deposition in the channel bottom.

Above the irregular erosion surface "B" lies current rippled, horizontally laminated and featureless, fine-grained sandstones (Sr, Sh, and Sm). These are interpreted as a (small) Crevasse Splay (CS) element because of the wide thin morphology of the deposit, the relief of the surface, and the relative coarseness of the deposit. These fine-upwards into the blocky mudstone (Fsm) of a Floodplain Fines (FF) elements.

The 5th order bounding surface labelled "C" is an extremely irregular erosion surface (up to 1.5 metres of elevation variations over less than 10 metres). Above this is planar tabular cross-stratified conglomerate (Gp) interpreted as Gravel Bars and Bedforms elements (GB) because of the coarse-grained sedimentary rock and lens like morphology of the elements. Overlying the GB elements is a series of lens shaped sandstone beds interpreted as Downstream Accretion macroforms (DA). Once again accretion surfaces of the DA elements, though inaccessible are visually similar to nearby GB elements and form the basis for the interpretation.

The final 5th order boundary in this mosaic (labelled "D") is overlain by planar tabular cross-stratified and/or scoured, coarse-grained pebbly sandstone interpreted as Downstream Accretion elements (DA) for reasons similar to the stratigraphically lower DA elements.

Mosaic BP - E (Greta)

The Greta Mosaic is a good example of the extensive fine-grained deposits that make up much of the lower part of the succession in the study area. The lowest rocks in this mosaic comprise a series of interbedded silty fine-grained sandstone (Fl) and blocky mudstone (Fsm). These laterally extensive layers are interpreted as several stacked Floodplain Fines (FF) elements. They are cut by the 5th order bounding surface labelled "B", and overlain by trough cross-stratified sandstones with some featureless sandstones, interpreted as a Sandy Bedform elements (SB) because of the thickness of the elements, the channel-like morphology to some sections, the

erosionally truncated morphology of bounding surface B⁻¹ (left end), and the lag at
the base of the SB elements. This lag includes a "jam" of fossilized branches and
mud rip-up clasts. Above the SB deposits is inter-bedded mudstone and silty fine-
grained sandstone (Fl) interpreted as Floodplain Fines (FF).

This mosaic represents Facies Association C (transitional), the succession
records deposition on a floodplain, cut into by a minor sand-dominated channel,
then grades back into floodplain deposition.

Mosaic BP - F (Thiessen)

Mosaic 6 broadly displays a coarsening-upward trend. The lowest part of the
mosaic contains laterally extensive horizontally laminated blocky mudstone (Fsm),
interpreted as a Floodplain Fines (FF) element. Above this is a medium-grained
apparently featureless sandstone unit (Sm) with some trough cross-stratification
interpreted as a Crevasse Splay element (CS), because of its gradational relationship
with the FF elements above and below it. This in turn grades into the siltstones and
mudstones of another similarly identified Floodplain Fines element (FF). Above the
4th order surface labelled "A³" is the only recognized Lateral Accretion element in
the study area. It consists of planar cross-stratified medium- to coarse-grained
sandstone fining upward to silty fine-grained sandstone. The strikes of the accretion
surfaces of these two LA elements are parallel to the regional paleocurrent directions
in the area. Above the erosional 5th order bounding surface labelled "B" is trough
cross-stratified conglomerate interpreted as a Gravel Bars and Bedforms element
(GB), overlain in turn by two stacked Sandy Bedform elements (SB), both made up
trough cross-stratified sandstone. The lower of the two Sandy Bedform elements
contains abundant pebble lags. These three upper elements are all recognised on the
basis of their lithologies and slightly concave upward upper surfaces.

Facies Associations

This thesis recognises various associations of architectural elements (and by
extension lithofacies) common in the study. As a shorthand when describing facies
associations, the symbol "}" denotes an erosive contact and "→" a facies change.

Association A1 (Channel sequence 1)

}GB → DA (pebbly) →SB

Association A1 represents a typical succession of facies within a fluvial channel. It begins with element GB (Gravel Bars and Bedforms) and is always erosively based. The GB element fines upward into a DA (Downstream Accretion element), which represents a change to sediment accumulation by downstream accretion and may reflect a change in depth of flow in the channel due to aggradation of the (lower) GB element. The DA element is commonly pebbly in these cases. The fining upwards cycle persists and the next element in this sequence is a SB (Sandy Bedform), representing continued shallowing of the flow and deposition on the top of a bar, near the river's edge, or in a secondary channel.

Association A2 (Channel Sequence 2)

}GB→ SB (pebbly) → SB

Association A2 is similar to A1, the sole difference being that directly overlying the GB element is a pebbly SB element. This reflects that sedimentation in this sequence followed vertical aggradation rather than downstream accretion.

Association B (Floodplain Sequence)

CS → FF→ (CR→) CS → FF

Association B1 is stacked successions of CS (Crevasse Splay) elements fining-upwards into FF (Floodplain Fines) elements. It also contains rare examples of element CR. This association represents accumulation of sediments on a floodplain. Association B1 can start with either CS or FF, may lack one of the elements, and the thicknesses of individual elements can vary between 30 cm and several metres. In an ideal sequence this association might be based by a CR element, indicating the channel was nearby. This might fine upwards into CS element and then finally a FF element indicating deposition was slowing and becoming less proximal. This does not necessarily mean the channel was migrating away - it could mean that the point of flood initiation was distal, rather than the nearest channel. This association is the

most common in the quarries and is assumed to be the most common in the field area, although recessive weathering obscures most outcrops.

Association C (Transitional sequence)

SB→ CS→ FF

Association C typically begins with SB, and may or may not be an extension of Association A1 or A2. The SB element fines upward into a CS element, and then into a FF element. This association is interpreted to represent the transition between deposition on channel margins, or subsidiary channels, and floodplain deposition. It may lead into association B1.

Association D (Point Bar)

LA → FF

This last association is rare in this area, occurring as two related elements in one short section of a single mosaic (Mosaic 6 - Thiessen). The elements show a typical coarse- to fine-grained sandstone-dominated point bar sequence. Deposition begins as LA (Lateral Accretion) elements and fines vertically and laterally into FF elements. The rarity of this association suggests that such processes were minor in this fluvial system.

Idealized Facies Succession

}GB→DA or SB (pebbly)→ SB → CS- > FF

An idealized complete facies association typifying the study area would begin with an erosively based GB element, followed by transition into either a pebbly DA or SB element. This is generally overlain by a SB element (without pebbles), a CS element, and ultimately be capped by a FF element. This sequence would represent the continuous deposition of facies from the channel bottom to the distal floodplain (Figure 42). The preservation of such a sequence is unlikely and it is not found in the study area.

Interpretation of Sedimentary Environment

Several data sources were used to interpret the sedimentary environment of the Huntingdon Formation. These include the stratigraphic section, provenance data, and architectural element analysis.

Stratigraphic Section

The Huntingdon Formation at Sumas Mountain (Canada) follows a broadly coarsening-upward succession, made up of smaller fining-upwards successions. The overall coarsening-upwards succession could be interpreted in several ways. It could indicate high sedimentation rates and overall aggradation and progradation of the deposit, that is, the top of the deposit is of more proximal derivation than the base. It could indicate a general increase in the competency of the fluvial system, represented by preservation of larger grain sizes. The cycle could also indicate tectonic instability impinging on the system or its source area, affecting the local base level. Finally, coarser facies could only appear to be more common in the upper parts of the section; perhaps finer material stratigraphically equivalent to the upper section was preserved (or exposed). This would cause the section to appear to coarsen upwards.

Of these four scenarios, the most likely are that the Huntingdon Formation was prograding westward over time due to high sedimentation rates and/or that base level is being affected by tectonic instability. These two scenarios are interrelated, high sedimentation rates could be caused by subsidence or uplift increasing accommodation space. The Huntingdon Formation at Sumas Mountain contains extremely common floodplain deposits of fine-grained sediments. Preservation of floodplain deposits is increased during periods of net aggradation (Bridge, 2003). Thus, the abundance of floodplain deposits in the Huntingdon Formation supports the interpretation that high sedimentation rates this in turn could cause progradation of the system and eventually a change to more proximal sedimentation styles.

Architectural element analysis is confined to the exposures and outcrops in the aggregate quarries. These exposures occur only in the lower half of the section,
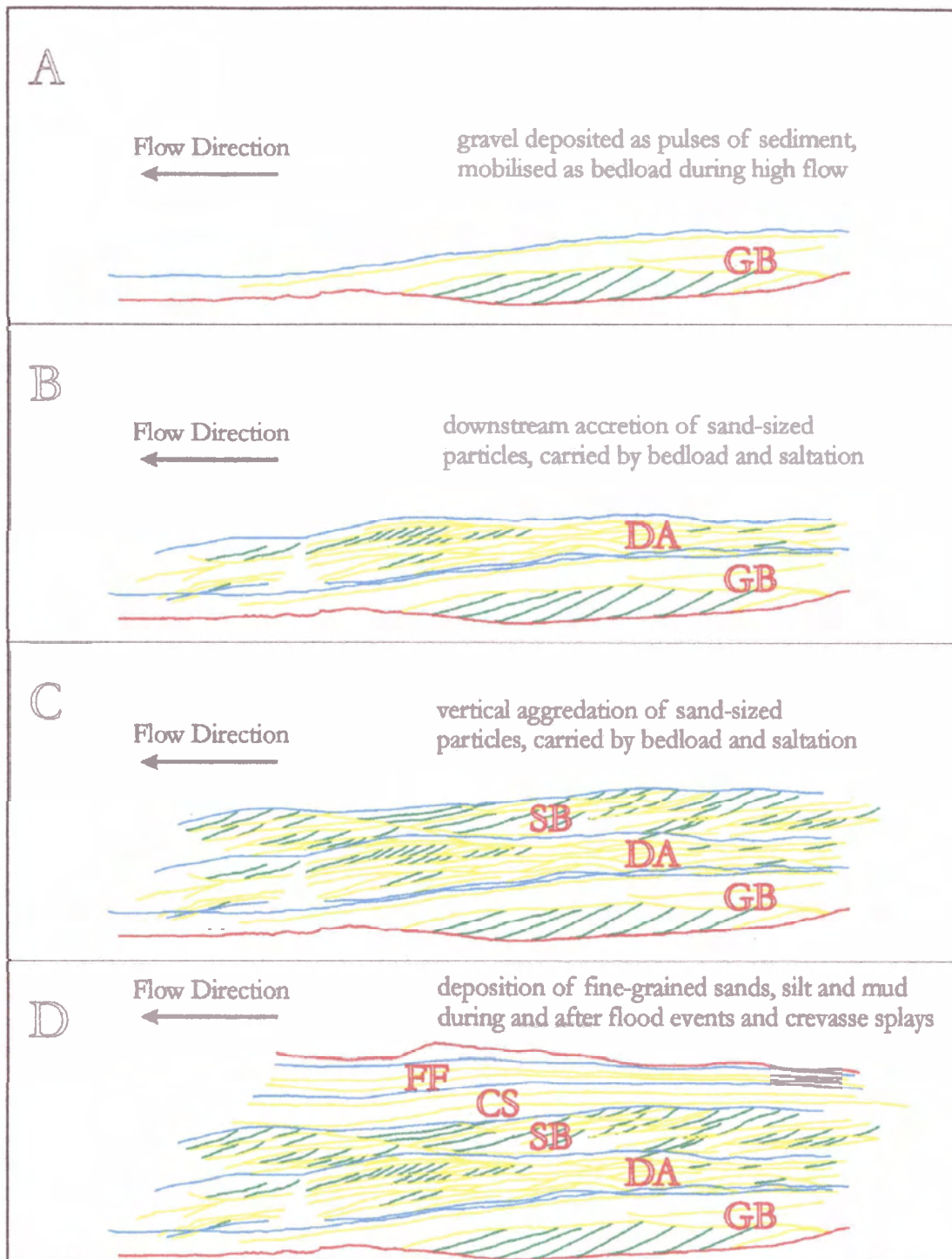
Figure 42 - Development of an idealized facies progression.
A Deposition of gravel bedforms during high stage cuts into layers below
B common fluvial sedimentation is achieved by Downstream Accretion of sandy bars
C shallow flow conditions near the river edge or on top of bars deposits Sandy Bedforms
D Crevasse splays and Floodplain Fines are deposition during and after flood events, which
in turn may be cut into by gravely sediments.

below 268 metres. Thus the stratigraphic section, outcrop descriptions, and provenance data are the only tools available to describe the sedimentary environment of the upper section, although the highest mosaics, BP - D (Kelly) and BP - C (Upper Banshee) do show more of the coarser-grained rocks. As the uppermost parts of the Huntingdon Formation contains fewer fine-grained sediments and thick continuous sections of multi-storey conglomerate and sandstone, floodplain processes are probably not as important as they are in the lower 2/3 of the stratigraphy. This coarser more proximal character of the upper part of the section is different enough from the lower parts that it is interpreted as a change in fluvial style. If fluvial style is a spectrum (with multiple axes) the erosionally amalgamated multi-storey coarse-grained sandstones and conglomerates of the upper section correspond more closely with the shallow gravel braided river style (Miall 1996) than the lower parts of the section. A hint of this change in style is reflected in the relative coarseness of the rocks in the stratigraphically highest photomosaics (BP - C Upper Banshee and BP - D Kelly). The fluvial style of the lower section is discussed under Architectural element analysis below.

Provenance

Clast Lithology

The most common pebbles in the conglomerates are chert composition, followed by igneous and quartz. Grains in sandstone comprise chert, quartz, feldspar, and volcanic lithologies. Grains in the sandstones and conglomerates tend to be sub-rounded and sub-spherical, indicating a moderate to low maturity. These compositions suggest a local source for the sediments of the Huntingdon Formation, probably derived from the Vedder Complex or Cascade sources to the south or east (Mustard and Rouse; 1994).

Paleocurrent Measurements

The number of paleocurrent measurements in this study is relatively small (around 20 individual sites) and may not be enough to be statistically significant.

However, the measurements collected give interesting results. In general paleoflow in the Huntingdon Formation was towards the west, though many measurements indicate flow directions well north, or south, of west. This relatively large variation in measured flow orientations appears to indicate a fluvial system of at least intermediate sinuosity (Figure 38-B), but if the measurements are placed in geographic and stratigraphic context (Figure 37) flows in any one area tend to have similar orientations. Thus the Huntingdon Formation is a fluvial system with relatively low sinuosity, but the paleoflow orientations migrate through time. In general the paleocurrents are more westerly in the lower parts of the section and more northerly in the upper parts of the section.

Architectural Element Analysis

Because the Huntingdon Formation (in common with many fluvial systems) does not fit well into the "spectrum" of fluvial facies models presented by Miall (1985, 1996), architectural element analysis is a fitting tool for this study as it facilitates the development of a unique model. At best, the system falls somewhere between a shallow gravel braided river, a wandering gravel bed river, and a low sinuosity braided-meandering with alternate bars river (all from Miall, 1996). However, the deposits of the Huntingdon Formation vary significantly from all of these fluvial styles.

In shallow gravel braided rivers' deposition is dominated by gravel and should only have minor amounts of sand or finer-grained sediments. In the Huntingdon Formation, gravels are common but they are not the dominant sediment type. Also the extremely common FF elements of the Huntingdon do not fit well with this model. Gravel meandering river deposits consist mostly of coarse-grained sediments such as gravel, and should have a minimum of sand or finer-grained sediments. The Huntingdon Formation is dominated by sand deposits, with relatively small amounts of gravel (at least in the lower parts of the section). The most common AE's in a wandering gravel bed river should be GB, DA and LA; the Huntingdon contains plentiful GB and DA, but only minor amounts of LA. Also, a wandering gravel river

should displays sinuosity higher than that postulated for the Huntingdon Formation. A low sinuosity braided meandering river (Miall, 1996) is dominated by sand, has low sinuosity, and has common DA, SB, and possibly FF elements similar to the Huntingdon Formation. However, the LA element should also be common in this type of river, and it is not commonly recognised in this field area. The low sinuosity braided meandering model also does not contain coarse GB elements, again in contrast to the Huntingdon Formation.

The correct identification and differentiation of Downstream Accretion (DA) elements and Lateral Accretion (LA) elements is a key part of interpretation with AEA. This identification requires accurate paleoflow information for the channel in which the macroform developed. This paleocurrent information is then compared to the strike of the accretion surfaces. If the strikes of these surfaces are roughly parallel to paleoflow direction, the element was formed by lateral accretion; if the strikes are perpendicular, the element represents downstream accretion (Miall 1996). Unfortunately, like elsewhere, this information can be quite difficult to gather in this study area; even Miall suggests in one of his studies that interpretation of a set of DA elements is "tentative" (e.g. Miall 1988). Features such as cross-strata are commonly difficult to make out because of weathering (or lack thereof), and some elements are found several metres high on unstable cliff faces; measurement of these features is commonly not feasible. One method used to infer accretion style in this study is to compare potential DA or LA elements to nearby GB elements. GB elements generally form through downstream accretion and only rarely by lateral accretion, the accretion surfaces of nearby DA elements are likely to have similar orientations and LA elements roughly perpendicular orientations. Comparison to cross-stratification within SB elements can also be used in this way. The problem of differentiation between lateral accretion and downstream accretion is a major difficulty, not just with AEA, but in fluvial facies analysis in general.

The most common architectural elements identified in the study area, in decreasing order, are Floodplain Fines (FF), Sandy Bedforms (SB), Gravel Bars and

Bedforms (GB), Downstream Accretion (DA), and Crevasse Splay (CS) elements. There are lesser amounts of Crevasse Channel (CR), and Lateral Accretion (LA) elements. The most important facies associations are B1 (Floodplain), A1 (Channel Succession 1), and A2 (Channel Succession 2). These channel progressions indicate sand sedimentation was dominant, but that gravel was also important, probably during high water levels and flood events.

Although not immediately the most common in the mosaics, the Floodplain Fines element is identified as the most common element in the study area for two reasons. The first is that the finer-grained sedimentary rocks of the Huntingdon Formation are much less resistant to weathering than the sandstone or conglomerate. These finer-grained rocks typically weather recessively, forming small caves or grottos with coarse-grained overhangs (Figure 43). Most exposures of Eocene material on Sumas Mountain (Canada) are capped, floored, or otherwise reinforced by a conglomerate or sandstone layer. Thus, sandstone and conglomerate are over-represented in available exposures. The second reason FF elements are considered more common is they are the more common in the extensive aggregate pit exposures, where close to 100% of the rock is exposed. Outcrops near these pits generally reflect the style of the rest of the study area and expose insignificant amounts of the finer rocks. FF is considered to be the most common element, at the very least in the bottom half of the section (below 268 metres), but is likely most common for the majority of the section. Evidence points to an extremely active floodplain as a feature of the fluvial system which deposited at least the lower portion of the Huntingdon Formation at Sumas Mountian (Canada).

The interpretation of an extremely active floodplain is an important part of how the depositional model of the Huntingdon Formation differs from established models. Though FF and CS are common, no levee structures were recognised in the study area. The thickness of channel architectural elements is similar to the depth of

Figure 43 - Overhang/cave created by the recessive weathering of fine-grained sedimentary rocks.

the fluvial system (Miall 1996). As architectural elements in the study area are, in general, between 2 and 3 metres thick (though erosionally amalgamated successions can be much thicker), channels in the study area were relatively shallow. Paleocurrent analysis suggests channels of low sinuosity. Thus an entrenched and meandering fluvial system such as those normally associated with extensive floodplain deposits is not indicated. Instead the fluvial system was likely a series of shallow complexly overlapping thin channel systems. Inundation of the floodplain could have occurred as a result of relatively rapid basin subsidence, not by the breaching of well developed levee complexes..

The active floodplain indicated by the common FF elements is indicative of progradation, aggradation (Bentham et al. 1993, Bridge, 2003), and tectonic instability. Most rivers have extremely high sediment supplies, the preservation of any one set of features is very low, as sediments are constantly deposited, eroded, and re-deposited as the river system migrates back and forth over the floodplain. The limiting factor for fluvial sedimentation is commonly basin volume or accommodation space; fluvial systems with high rates of sedimentation may be experiencing relatively rapid subsidence. Because rapid subsidence is one of the defining characteristics of a strike-slip basin, the observation of an extremely active floodplain supports the hypothesis of hybrid basin evolution presented in Chapter 2 with a component of strike slip basin characteristics.

The fluvial system of the Huntingdon Formation at Sumas Mountain can be divided into two broad regimes: below about 300 metres and above about 300 metres. The fluvial system which deposited the lower parts of the Huntingdon Formation (Figure 44) is interpreted as a series of shallow complexly overlapping thin channel of relatively low sinuosity, it is a mixed load sand-dominated system with common occurrences of gravel, as suggested by common GB, DA and SB elements (Facies Association A1 and A2). This system included an extremely active, alluvial flood plain, some parts of which were paludal to lacustrine in character. Floodplain deposits are typified by abundant FF elements, coal horizons in the
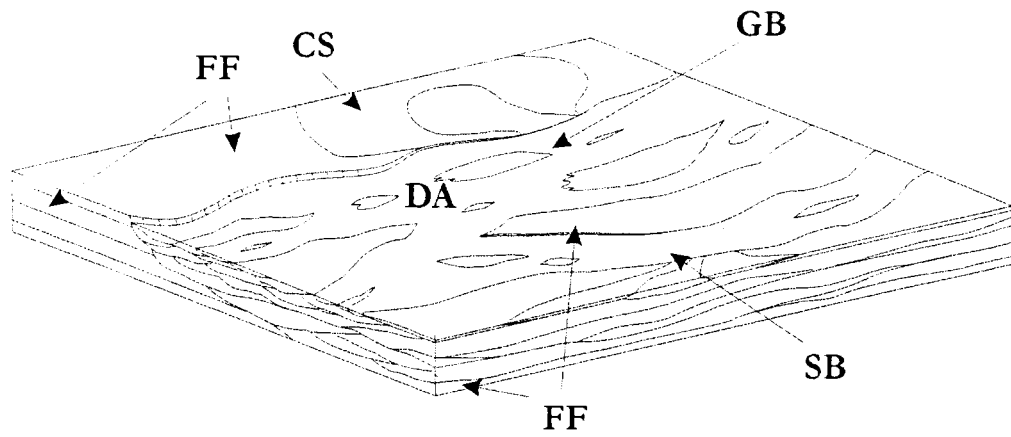
Figure 44 - A model of sedimentation for the lower Huntingdon Formation at Sumas Mountain (Canada).

lowest parts of the section, and little evidence of paleosol development; however, there must have been some subaerial exposure of the floodplain as trace fossils and the occasional rooted horizon are found in the area.

The portion of the Huntingdon Formation above 300 metres has not been analyzed with AEA and its fluvial style is interpreted under Stratigraphic Section, above.

Discussion of Architectural Element Analysis

Architectural element analysis was useful at Sumas Mountain (Canada). Interpreting a unique facies model for the bottom part of the section was greatly facilitated by AEA. However, there are many difficulties encountered when using this technique. Several are discussed here, but for an extensive list and some critical discussions see Bridge (1993) or Miall and Bridge (1995). The largest problem in AEA is the need for high quality three-dimensional exposures. The top half of the section at Sumas Mountain does not have any exposures either large enough or easily accessible. The lower half of the section has extensive exposures in the quarries, but not all of these are ideal because of a lack of visible structures or difficulty in photographing the exposure. The best exposure in the study area is the one depicted in mosaic BP - B (Goldstream). This exposure was cleared in a subdivision development, and has or will soon be covered. Even the best exposures at Sumas Mountain were not ideal for AEA; if there were three-dimensional extents to the outcrops, more work on quantifying the three-dimensional nature of the deposits could have been completed. With drill core the use of AEA is extremely limited, as the identification of bounding surfaces and elements is extremely challenging.

Another difficulty with AEA is the correct identification of DA and LA elements discussed above. The differentiation of these notoriously difficult to identify features is an important problem facing fluvial sedimentology.

The final problem discussed here is one AEA was largely designed to remedy. Using traditional facies analysis it can be difficult to relate simple vertical successions of facies to river planform. AEA was designed to be a bridging step, allowing one to

interpret larger features, architectural elements, in the hopes that it would make identifying fluvial style easier. AEA succeeds in this to a certain extent; however Hickin (1993) points out that to make predictions about a river planform, one needs to make observations of features at that scale. Using macroforms to predict planform can be very difficult, and in some cases may not be possible.

One of the main reasons AEA was developed was to help predict three-dimensional sedimentary structures in fluvial sandstone bodies. However, there has not yet been enough quantitative research done with AEA, and more is required before we rely on AEA and its ability to predict forms in three dimensions (Miall 1985, 1993, and 2000). To this end the current utility of AEA to predict the three-dimensional extent of forms is limited. It is not much use without well-exposed outcrop or extremely closely spaced core.

Chapter 5 - Conclusions

Tectonic Setting

Brittle fracture analysis of the Huntingdon Formation at Sumas Mountain (Canada) indicates that the rocks were subjected to two regional stress regimes, identified by Journeay and van Ulden (1998) and Journeay and Morrison (1999). These two regimes may have occurred during early Paleogene time and middle Miocene time, respectively. If correct, this indicates that normal faults - both within the Huntingdon Formation as well as separating the Huntingdon from unnamed igneous rocks at Sumas Mountain - occurred sometime after the mid-Miocene Epoch. If these normal faults are related to the formation of the feature known as the Sumas Graben, this feature may also be younger than middle Miocene time. The results of this study suggest that the Chuckanut Basin's tectonic development is that of a hybrid basin with a complex tectonic history. This history includes development as a benched forearc basin, a strike-slip basin, and possibly as a peripheral foreland basin.

Stratigraphy and Sedimentology

The development of a type section for the Huntingdon Formation should clear up some of the confusion surrounding the stratigraphic nomenclature of the Tertiary in the Greater Vancouver area.

Rocks in the study area are entirely sedimentary and siliciclastic. Facies identified in the field area are divided into five broad divisions: Conglomerate Facies, Medium- to Very Coarse-grained Sandstone Facies, Very Fine- to Medium-grained Sandstone Facies, Fine-grained Facies, and Other. These facies are further subdivided on the basis of differing sedimentary structures and are the basis for the architectural elements described below.

Interpretation of Sedimentary Environment

The sedimentary rocks of the Huntingdon Formation at Sumas Mountain (Canada) are interpreted to have been deposited during the Paleogene. In the lowest

part of the section the most common fluvial architectural elements in the study area are Floodplain Fines (FF), Sandy Bedforms (SB), Gravel Bars and Bedforms (GB), Downstream Accretion (DA), and Crevasse Splay (CS) elements. There are relatively fewer occurrences of Crevasse Channels (CR), and Lateral Accretion elements (LA). The differentiation between the LA elements and the DA elements is extremely important in the use of Architectural Element Analysis. The most common facies associations are B1 (Floodplain), A1 (channel progression 1), and A2 (channel progression 2).

Using Architectural Element Analysis, the fluvial style of the system which deposited the lower part of the Huntingdon Formation is interpreted as a dominantly sand and gravel, mixed load fluvial system with an extremely active floodplain. These sediments were deposited by a series of shallow, complexly overlapping thin channels of relatively low sinuosity. High floodplain activity may have been sustained by subsidence or tectonic instability. The upper part of the section is interpreted using the stratigraphic section as photomosaics were not possible with the exposures available. The upper part of the section has a different character than the lower and was likely deposited by a system similar to a shallow gravel braided river. Abundant Floodplain Fines elements at Sumas Mountain (Canada) indicate a high rate of sedimentation. Paleocurrent measurements suggest that this fluvial system was of low sinuosity but that flow migrated from broadly westward to broadly northward over the course of the Paleogene Period.

Future Work

Much work remains to be done on the Huntingdon Formation. The relationship between the Huntingdon and the Chuckanut Formations, though discussed in some of the literature, could be explored more fully. Work attempting to correlate outcrops over the entire Greater Vancouver region would be a valuable addition to our knowledge of the area. A study using AEA in building excavations in the Vancouver area could be very useful in developing a greater understanding of the

sedimentary environment, especially if mosaic density was close enough to correlate easily between mosaics.

References

Allen, J.R.L., 1983, Studies in fluviatile sedimentation: bars, bar-complexes and sandstone sheets (low-sinuosity braided streams) in the Brownstones (L. Devonian), Welsh Borders: Sedimentary Geology, v. 33, p. 237-293.

Anderson, D., 1991, Report of the commission of inquiry into Fraser Valley Petroleum Exploration: Province of British Columbia. 181p.

Bentham, P.A., Talling, P.J., and Burbank, D.W., 1993, Braided stream and flood-plain deposition in a rapidly aggrading basin; the Escanilla Formation, Spanish Pyrenees, in Best, J.L., and Bristow, C.S., eds., Braided rivers: Geological Society Special Publication No. 75. Geological Society of London, p. 177-194.

Boggs Jr., S., 2001, Principles of Sedimentology and Stratigraphy 3rd ed: Prentice Hall, Inc. 646p.

Bridge, J.S., 1993, Description and interpretation of fluvial deposits; a critical perspective: Sedimentology, v. 40, p. 801-810.

—, 2003, Rivers and Floodplains: Form, Processes, and Sedimentary Record: Blackwell Science Ltd., 491 p.

Bustin, R.M., 1990, Stratigraphy, sedimentology, and petroleum source rock potential of the Georgia Basin, southwest British Columbia and northwest Washington State: Geological Survey of Canada Paper 1990-A. 103-108 p.

Burwash, E.M.J., 1918, The geology of Vancouver and vicinity [Ph.D thesis]: The University of Chicago press, 106p.

Cheney, E.S., 2000, Tertiary geology of the eastern flank of the Central Cascade Range, Washington: Fieldtrip guide Book Geological Society of America Cordilleran Section Annual General Meeting 2000. p. 205-227

Daly, R.A., 1910, Geology of the North American Cordillera at the forty-ninth parallel: Canadian Department of the Interior, Report of the Chief Astronomer, 1910, p. 1-799.

Dawson, J.W., 1895, On Collections of Tertiary Plants from the Vicinity of the City of Vanocuver: B.C., Royal Society of Canada Transcripts And Procceedings, 2nd Series Vol. I, section IV, p. 137-151.

Dickinson, W.R., 1995, Forearc Basins, *in* Busby, C.J., and Ingersoll, R.V., eds., Tectonics of Sedimentary Basins: Blackwell Science, Cambridge, Masachusetts, 221-262.

Dostal, J., Church, B.N., Reynolds, P.H., and Hopkinson, L., 2001, Eocene volcanism in the Buck Creek basin, central British Columbia (Canada); transition from arc to extensional volcanism: Journal of Volcanology and Geothermal Research, v. 107, p. 149-170.

Engebretson, D.C., Cox, A., and Gordon, R.G., 1985, Relative motions between oceanic and continental plates in the Pacific Basin: Geological Society of America Special Paper 206, 60 p.

England, T.D.J., and Bustin, R.M., 1998, Architecture of the Georgia Basin, southwestern British Columbia: Bulletin of Canadian Petroleum Geology, v. 46, p. 288-320.

Ewing, T.E., 1980, Paleogene tectonic evolution of the Pacific Northwest: Journal of Geology, v. 88, p. 619-638.

Folk, R.L., 1974, Petrology of sedimentary rocks: Hemphill Publishing, Austin, Texas, 182 p.

Friend, P.F., Collinson, J.D., and Lewin, J., 1983, Towards the field classification of alluvial architecture or sequence. *in* Modern and ancient fluvial systems Special Publication 6 of the International Association of Sedimentologists: Blackwell Publishers, Oxford, p. 345-354.

Griggs, P.H., 1966, Palynological Interpretation of the Type Section, Chuckanut Formation, Northwestern Washington: Geological Society of America Special Paper 127.

Haeussler, P.J., Bradley, D.C., Wells, R.E., and Miller, M.L., 2003, Life and death of the Resurrection Plate; evidence for its existence and subduction *in* the northeastern Pacific *in* Paleocene-Eocene time: Geological Society of America Bulletin, v. 115, p. 867-880.

Hasiotis, S.T. 2003, Continental Trace Fossils: SEPM (Society for Sedimentary Geology) Short Course Notes No. 51, 132 p.

Haugerud, R.A., 1998, Preliminary report on significant thrusting and extension of the early Tertiary Chuckanut Formation, NW Washington, *in* Cook, F., and Erdmer, P., eds., Slave-Northern Cordillera Lithospheric Evolution (SNORCLE) and Cordilleran tectonics workshop: Lithoprobe Report: University of British Columbia, p. 203.

Heller, P.L., Tabor, R.W., and Suczek, C.A., 1987, Paleogeographic evolution of the United States Pacific Northwest during Paleogene time: Canadian Journal of Earth Sciences, v. 24, p. 1652-1667.

Hickin, E.J., 1993, Fluvial facies models; a review of Canadian research. *in* eds. Church M., Geomorphology in Canada: Progress in Physical Geography 17, no. 2, Edward Arnold Publishers, London, p. 205-222.

Hurst, P.D., 1991, Petroleum geology of the Bellingham Basin, Washington, and evaluation of the AHEL and Partners Birch Bay No. 1 well: Washington Geology, v. 19, p. 16-18.

Ingersoll, R.V., and Busby, C.J., 1995, Tectonics of Sedimentary Basins, *in* Ingersoll, R.V., and Busby, C.J., eds., Tectonics of Sedimentary Basins: Blackwell Science, Oxford. p. 1-51.

Jackson, R.G., II, 1976, Depositional model of point bars in the lower Wabash River: Journal of Sedimentary Petrology, v. 46, p. 579-594.

Johnson, S.Y., 1984, Stratigraphy, age, and paleogeography of the Eocene Chuckanut Formation, Northwest Washington: Canadian Journal of Earth Sciences, v. 21, p. 92-106.

Johnson, S.Y., Biddle, K.T., and Christie-Blick, N., 1985, Eocene strike-slip faulting and non-marine basin formation in Washington: SEPM (Society for Sedimentary Geology) Special Publication no. 37, Tulsa, OK, p. 283-302.

Journeay, J.M., and van Ulden, J., 1998, Neogene structural elements of northern Cascadia, British Columbia: Geological Survey of Canada, Paper 1998-A, p. 195-206.

Journeay, J.M., and Morrison, J., 1999, Field investigation of Cenozoic structures in the northern Cascadia Forearc: Geological Survey of Canada, Paper 1999-A, p. 239-250.

Kerr, S.A., 1942, The Tertiary sediments of Sumas Mountain [Unpublished Master's thesis]: University of British Columbia, Vancouver, B.C., Canada. 32 p.

Lasmanis, R., 1991, The geology of Washington: Rocks and Minerals, v.66, Washington State Department of Natural Resources p. 262-277.

Mackie, D.C., 2002, Structural Geology of the Gulf Islands, B.C. and its Relation to Groundwater Circulation Patterns. [Unpublished Masters thesis]: Simon Fraser University, Burnaby, British Columbia, Canada. 358 p.

Miall, A.D., 1978, Lithofacies types and vertical profile models in braided river deposits; a summary, Canadian Society of Petroleum Geologists memoir no. 5, p. 597-604.

—, 1980, Cyclicity and the facies model concept in fluvial deposits: Bulletin of Canadian Petroleum Geology, v. 28, p. 59-79.

Miall, A.D., 1985, Architectural-element analysis; a new method of facies analysis applied to fluvial deposits: Earth-Science Reviews, v. 22, p. 261-308.

—, 1988, Architectural elements and bounding surfaces in fluvial deposits; anatomy of the Kayenta Formation (Lower Jurassic), Southwest Colorado: Sedimentary Geology, v. 55, p. 233-262.

—, 1995, Collision-Related Foreland Basins, *in* Busby, C.J., and Ingersoll, R.V., eds., Tectonics of Sedimentary Basins: Oxford, Blackwell Science,. p. 393-424.

—, 1996, The Geology of Fluvial Deposits - Sedimentary Facies, Basin Analysis, and Petroleum Geology: Heidelberg, Springer-Verlag Inc., 582 p.

—, 2000, Principles of sedimentary basin analysis 3rd edition: Berlin, Springer, 616 p.

Miller, G.M., and Misch, P., 1963, Early Eocene angular unconformity at western front of northern Cascades, Whatcom County, Washington: Bulletin of the American Association of Petroleum Geologists, v. 47, p. 163-174.

Monger, J.W.H., 1990, Georgia Basin Project; scope and basin tectonic setting--: Cordilleran geology and exploration roundup: *in* Current Research, Part F; Geological Survey of Canada, Paper 90-1F, p. 18-19.

Monger, J.W.H., and Journeay, J.M., 1994, Guide to the Geology and Tectonic Evolution of the Southern Coast Mountains: Open file 2490, Geological Survey of Canada, 77 p.

Mustard, P.S., and Rouse, G.E., 1992, Tertiary Georgia Basin, British Columbia and Washington State; a view from the other side: Geological Survey of Canada Paper 1992-A, p. 13-23.

—, 1994, Stratigraphy and evolution of Tertiary Georgia Basin and subjacent Upper Cretaceous sedimentary rocks, southwestern British Columbia and northwestern Washington State, *in* Monger, J.W.H., ed., Geology and geological hazards of the Vancouver region, southwestern British Columbia: Geological Survey of Canada. Bulletin 481. p. 97-169.

Mustoe, G.E., and Gannaway, W.L., 1995, Palm fossils from northwest Washington: Washington Geology, v. 23, p. 21-26.

—, 1997, Paleogeography and paleontology of the early Tertiary Chuckanut Formation, Northwest Washington: Washington Geology, v. 25, p. 3-18.

Nilsen, T.H., and Sylvester, A.G., 1995, Strike-slip Basins. *in* Busby, C.J., and Ingersoll, R.V., eds., Tectonics of Sedimentary Basins: Oxford, Blackwell Science. p.423-457.

Ramos, A., Sopena, A., Collinson, J.D., and Lewin, J., 1983, Gravel bars in low-sinuosity streams (Permian and Triassic, central Spain): Oxford, Blackwell Science, p. 301-312.

Rouse, G.E., Mathews, W.H., and Blunden, R.H., 1975, The Lions Gate Member; a new late Cretaceous sedimentary subdivision in the Vancouver area of British Columbia: Canadian Journal of Earth Sciences, v. 12, p. 464-471.

Walker, R.G., and James, N.P., 1992, Facies, Facies Models and Modern Stratigraphic Concepts. *in* eds. Walker, R.G., and James, N.P. Facies models response to sea level change: Geological Association of Canada, GEOtext 1 p. 1-14.

Appendices

Appendix A - Maps and Photomosaics
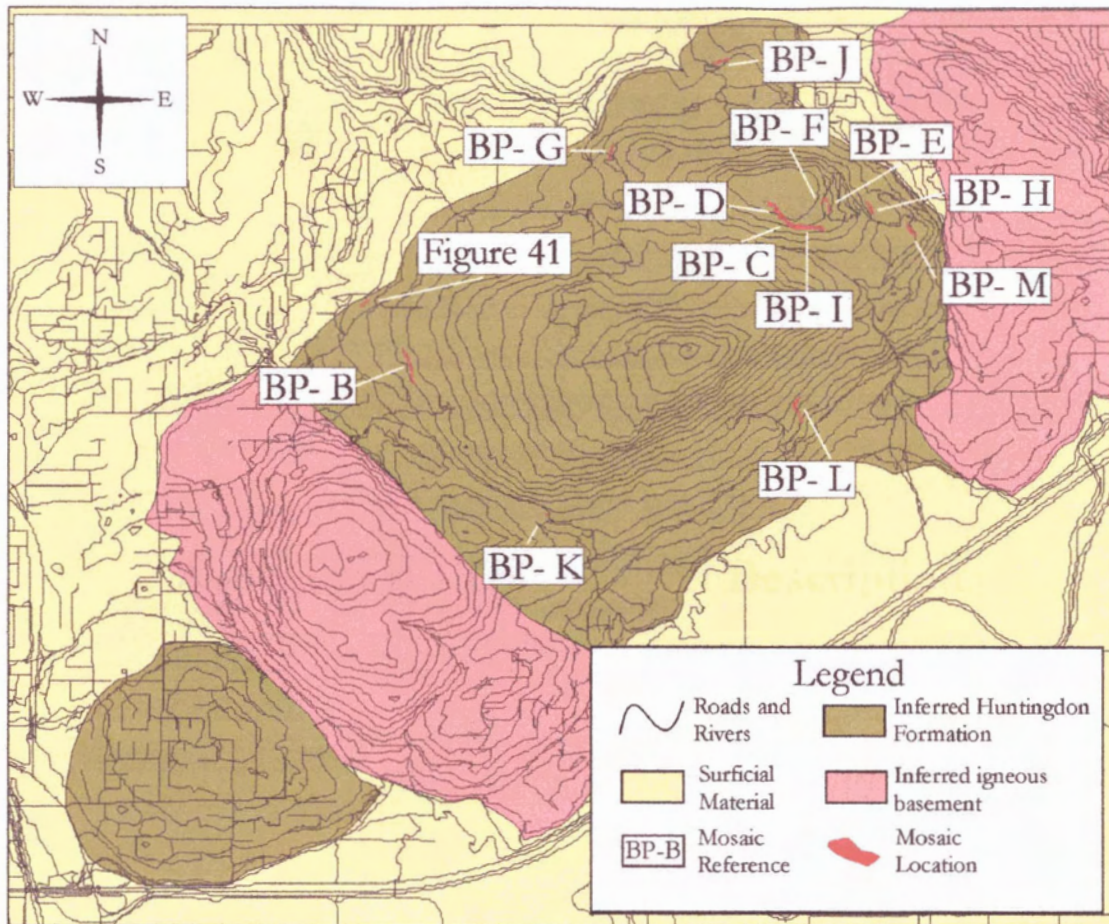
Figure 45 - Location Map for Photomosaics

Appendix B - Thin section Descriptions

Sample:BG-02-01
Station: BHG-02-001

Composition
Matrix %: 25   **Quartz %** 20   **Feldspar %** 10   **Rock Fragments %** 45
Quartz Types: Igneous and metamorphic
Feldspar Types: orthoclase
Rock Fragment Types: chert (~30% cryptocrystalline microcrystalline and megachert), volcanic rock fragments (5%), metamorphic rock fragments (5%), detrital mica (5%), organics (3%)

Accessory Minerals: apatite, sphene and zircons (3%), pyroxene and hornblende (<1%),
Compositional Maturity: immature

Texture
Grain Size: Medium- to coarse-grained sandstone   **Roundness:** subangular

Sorting: moderate   **Sphericity:** subspherical
Textural Maturity: submature

Cement/ Diagenesis

Quartz overgrowths: **Cement types:** mostly calcite (weathered, could be replacing porosity)
Grain contacts:
Alteration Types: **Authigenic Minerals:**

Representative Thin section Description:
Medium- to coarse-grained, submature sandstone, grains are subangular and subspherical. The most common grains are chert, then volcanic and metamorphic rock fragments, detrital mica, and organics.

Sample: BG-02-03
Station:

Composition
Matrix %:   Quartz %   Feldspar %   Rock Fragments %
Quartz Types
Feldspar Types
Rock Fragment Types

Accessory Minerals:
Compositional Maturity:

Texture
Grain Size: coarse- to very coarse-grained sandstone   Roundness:
Sorting:
Textural Maturity:

Cement/ Diagenesis
Quartz overgrowths: Cement types
Grain contacts:
Alteration
Types: Authigenic Minerals:

Representative Thin section Description:

                Virtually identical to BG-02-01 except coarser-grained
                sandstone

Sample: BG-02-029
Station:

Composition

Matrix %: 5   Quartz %: 10   Feldspar %: 0   Rock Fragments %: 85

Quartz Types: Metamorphic quartz

Feldspar Types: none

Rock Fragment Types: Chert (70%) including cryptocrystalline chert (50%), microcrystalline chert (10%), and megachert (10%). Detrital mica (<5%) mostly biotite/phlogopite, volcanic clasts (<3%)

Accessory Minerals: none

Compositional Maturity: immature

Texture

Grain Size: coarse- to fine-grained sand   Roundness: moderately rounded

Sorting: moderate to poorly sorted   Sphericity: subspherical

Textural Maturity: submature

Cement/ Diagenesis

Quartz overgrowths: none   Cement types: mostly (80%) calcite, some silica, trace clay

Grain contacts: matrix supported

Alteration Types: Authigenic Minerals:

Representative Thin section Description:

Coarse-grained sandstone to granule conglomerate moderately rounded moderate to poorly sorted grains. Contains abundant chert clasts, some quartz, detrital mica and volcanic clasts.

Sample: BG-02-32
Station: BHG-02-036

Composition

Matrix %: 25   **Quartz %:** 17   **Feldspar %:** 13   **Rock Fragments %:** 45

Quartz Types: mostly metamorphic quartz

Feldspar Types: orthoclase and plagioclase

Rock Fragment Types: mostly cryptocrystalline chert, some volcanic fragments

Accessory Minerals: detrital mica 3-5%, less than 3% high relief minerals, epidote and tourmaline

Compositional Maturity: submature

Texture

Grain Size: medium- to coarse- grained sand   **Roundness:** subangular to sub rounded

Sorting: moderate in thin section, poor in sample   **Sphericity:** subspherical

Textural Maturity: submature

Cement/ Diagenesis

Quartz overgrowths: **Cement types:** calcite, infilling porosity

Grain contacts:

Alteration Types: **Authigenic Minerals:**

Representative Thin section Description:

Medium- to coarse-grained, submature sandstone, grains are subangular to subrounded and subspherical. The most common grains are chert, then volcanic and metamorphic rock fragments, detrital mica, and organics. Cement is mostly calcite infilling porosity
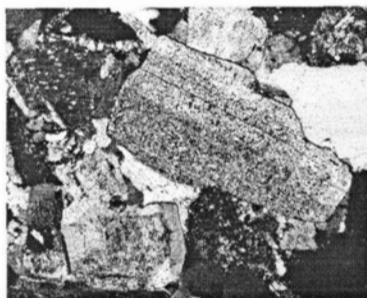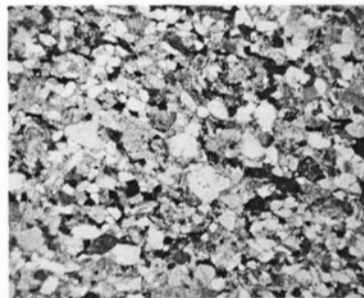
Field of view - 1.32 mm   FOV - 10.56 mm   FOV - 10.56 mm
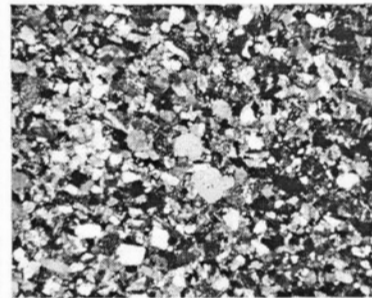
Sample: **BG-02-33**

Station: **BHG-02-036**

Composition

Matrix %: 25 **Quartz %:** 20 **Feldspar %:** 10 **Rock Fragments %:** 35

Quartz Types: irregular extinction strained quartz

Feldspar Types: 2/3 plagioclase, 1/3 orthoclase

Rock Fragment Types: mostly chert (3 types?), some volcanic fragments

Accessory Minerals: less than 5% mica, few high relief minerals

Compositional Maturity:

Texture

Grain Size: fine-grained sand   Roundness: subangular

Sorting: moderate   Sphericity: subspherical

Textural Maturity: submature

Cement/ Diagenesis

Quartz overgrowths: Cement types: mix of clay and calcite

Grain contacts:

Alteration Types: Authigenic Minerals:

Representative Thin section Description:

Submature, fine-grained sandstone. Grains are subangular and subspherical. the most common grains are lithic fragments, most of these are chert with some volcanic fragments. Quartz and feldspars are less common than lithic fragments. Cement is a mix of clay and calcite.

Sample: BG-02-34

Station: BHG-02-039

Composition

Matrix %:   **Quartz %: 40-50**   **Feldspar %:** 20   **Rock Fragments %:** 25

Quartz Types: metamorphic quartz

Feldspar Types: 3/4 plagioclase 1/4 orthoclase

Rock Fragment Types: mostly Chert (3 types) some volcanic fragments, some metamorphic fragments

Accessory Minerals:

Compositional Maturity: submature

Texture

Grain Size: coarse-grained sandstone   **Roundness:** subangular to subrounded

Sorting: moderate to poor   **Sphericity:** subspherical

Textural Maturity: submature

Cement/ Diagenesis

Quartz overgrowths: **Cement types:** silica, clay and calcite (replacing others)

Grain contacts:

Alteration Types: **Authigenic Minerals:**

Representative Thin section Description:

Submature, coarse-grained sandstone, grains are subangular to subrouned and subspherical. The most common grains are quartz then rock fragments and feldspar. Rock fragments are mostly chert with some volcanic and metamorphic grains. Cement is a mixture of silica, calcite and clay.
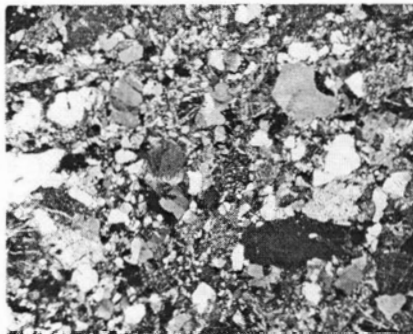
Field of View - 2.64 mm
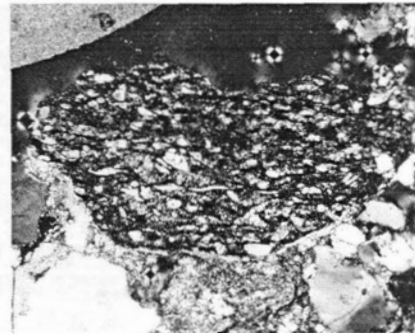
FOV - 2.64 mm

Sample: BG-02-36

Station

Composition

Matrix %: ~5   **Quartz %:** 30   **Feldspar %:** 5   **Rock Fragments %:** 60

Chert Types: Mega chert and meta /sutured quartz

Quartz Types: igneous quartz and stressed/ metamorphic quartz

Feldspar Types: mostly orthoclase

Rock Fragment Types: chert (megachert and metamorphic/sutured quartz) 40-50 %, detrital mica (mostly phlogopite or biotite, some muscovite) 15-20%

Accessory Minerals: some possible zircons 1%

Compositional Maturity: immature

Texture

Grain Size: medium-grained sandstone to conglomerate   **Roundness:** subangular- subrounded

Sorting: moderately sorted   **Sphericity:** subshperical

Textural Maturity: submature to immature

Cement/ Diagenesis

Quartz overgrowths: none

Grain contacts:

Alteration Types:

Cement types: silica (55%), calcite (35%), and clay/iron (10% concentrated in conglomeratic sections)

Authigenic Minerals: Sericite

Representative Thin section Description:

Coarse-grained sand to small pebble conglomerate and fine-grained rippled sandstone, contains subangular Grains of lithic fragments, quartz and feldspar. The majority of lithic fragments are chert (megachert or sutured quartz, 40-50%), but it also contains detrital micas (15-20%) which are deformed/bent around grains.
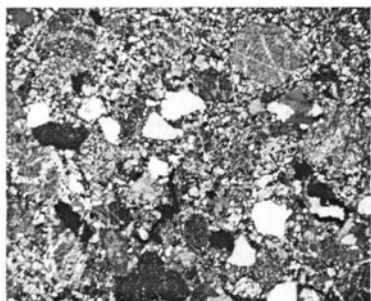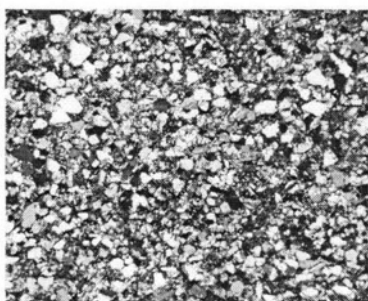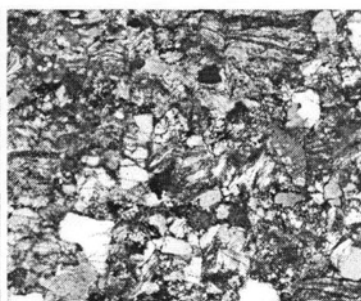
FOV - 1.32 mm   FOV - 2.64 mm   FOV - 10.56 mm

Appendix C - Measurements and Data

Fracture Measurements

Station	Formation	UTM East	UTM North	Fracture Type	Azimuth	Inclination
BHG-02-001	HUN	10553680	5431626	Shear	200	73
BHG-02-001	HUN	10553680	5431626	Shear	023	83
BHG-02-001	HUN	10553680	5431626	Shear	204	76
BHG-02-001	HUN	10553680	5431626	Shear	214	79
BHG-02-001	HUN	10553680	5431626	Shear	195	75
BHG-02-001	HUN	10553680	5431626	Shear	206	82
BHG-02-001	HUN	10553680	5431626	Shear	209	79
BHG-02-001	HUN	10553680	5431626	Shear	015	88
BHG-02-001	HUN	10553680	5431626	Shear	193	88
BHG-02-001	HUN	10553680	5431626	?	110	84
BHG-02-005	HUN	10554045	5432121	?	250	23
BHG-02-005	HUN	10554045	5432121	?	243	34
BHG-02-005	HUN	10554045	5432121	?	269	35
BHG-02-007	HUN	10556563	5433395	Shear	064	57
BHG-02-007	HUN	10556563	5433395	Shear	062	68
BHG-02-007	HUN	10556563	5433395	Slickenlines	17	070
BHG-02-007	HUN	10556563	5433395	Shear	071	57
BHG-02-007	HUN	10556563	5433395	Slickenlines	23	069
BHG-02-007	HUN	10556563	5433395	Shear	084	78
BHG-02-007	HUN	10556563	5433395	Slickenlines	33	099
BHG-02-007	HUN	10556563	5433395	?	195	44
BHG-02-007	HUN	10556563	5433395	?	230	30
BHG-02-007	HUN	10556563	5433395	?	217	35
BHG-02-007	HUN	10556563	5433395	?	225	33
BHG-02-007	HUN	10556563	5433395	?	205	36
BHG-02-007	HUN	10556515	5433352	?	278	39
BHG-02-007	HUN	10556515	5433352	?	287	36
BHG-02-007	HUN	10556515	5433352	?	202	66
BHG-02-007	HUN	10556515	5433352	?	220	56
BHG-02-007	HUN	10556515	5433352	?	190	39
BHG-02-007	HUN	10556445	5433383	?	145	59
BHG-02-007	HUN	10556445	5433383	?	146	55

Station	Formation	UTM East	UTM North	Fracture Type	Azimuth	Inclination
BHG-02-007	HUN	10556478	5433397	?	051	67
BHG-02-007	HUN	10556478	5433397	?	052	72
BHG-02-007	HUN	10556478	5433397	?	054	71
BHG-02-007	HUN	10556487	5433398	?	012	60
BHG-02-007	HUN	10556487	5433398	?	010	51
BHG-02-007	HUN	10556487	5433398	?	013	54
BHG-02-008	HUN	10555968	5433641	Ext	037	83
BHG-02-008	HUN	10555968	5433641	Ext	036	87
BHG-02-008	HUN	10555968	5433641	Ext	038	79
BHG-02-008	HUN	10555968	5433641	Ext	126	50
BHG-02-008	HUN	10555968	5433641	Ext	126	46
BHG-02-008	HUN	10555968	5433641	Ext	156	41
BHG-02-009	HUN	10556328	5433440	Ext	165	51.5
BHG-02-009	HUN	10556328	5433440	Ext	174	54
BHG-02-009	HUN	10556328	5433440	Ext	156	45
BHG-02-009	HUN	10556328	5433440	Ext	184	41
BHG-02-009	HUN	10556328	5433440	Ext	150	47
BHG-02-009	HUN	10556328	5433440	Ext	325	55
BHG-02-009	HUN	10556328	5433440	Ext	321	67
BHG-02-009	HUN	10556328	5433440	Ext	324	66
BHG-02-009	HUN	10556328	5433440	Ext	304	74
BHG-02-009	HUN	10556328	5433440	?	277	33
BHG-02-009	HUN	10556328	5433440	?	295	46
BHG-02-009	HUN	10556328	5433440	?	276	38
BHG-02-009	HUN	10556328	5433440	?	293	29
BHG-02-009	HUN	10556011	5433471	Shear	148	76
BHG-02-009	HUN	10556011	5433471	Shear	150	82
BHG-02-009	HUN	10556011	5433471	Shear	146	89
BHG-02-009	HUN	10556011	5433471	Shear	121	86
BHG-02-009	HUN	10555869	5433592	Shear	082	41
BHG-02-009	HUN	10555869	5433592	Shear	067	35
BHG-02-010	HUN	10556309	5433277	?	335	22
BHG-02-010	HUN	10556309	5433277	?	324	24

Station	Formation	UTM East	UTM North	Fracture Type	Azimuth	Inclination
BHG-02-010	HUN	10556309	5433277	?	055	78
BHG-02-010	HUN	10556309	5433277	?	052	86
BHG-02-010	HUN	10556309	5433277	?	054	82
BHG-02-010	HUN	10556309	5433277	?	140	52
BHG-02-010	HUN	10556309	5433277	?	143	49
BHG-02-011	?	10555998	5433357	Shear	326	79
BHG-02-011	?	10555998	5433357	Slickenlines	026	80
BHG-02-011	?	10555998	5433357	Shear	235	85
BHG-02-011	?	10555998	5433357	Shear	126	43
BHG-02-011	?	10555998	5433357	Shear	028	71
BHG-02-011	?	10555998	5433357	Shear	336	45
BHG-02-011	?	10555998	5433357	Shear	214	80
BHG-02-011	?	10555998	5433346	?	055	73
BHG-02-011	?	10555998	5433346	?	057	76
BHG-02-011	?	10555998	5433346	?	053	75.5
BHG-02-011	?	10555998	5433346	?	045	78
BHG-02-011	?	10555998	5433346	?	057	82
BHG-02-011	?	10555998	5433346	?	131	70
BHG-02-011	?	10555998	5433346	?	149	54
BHG-02-011	?	10555998	5433346	?	126	73
BHG-02-011	?	10555998	5433346	?	109	85
BHG-02-012	?	10556114	5433209	?	203	75
BHG-02-012	?	10556114	5433209	?	076	14
BHG-02-012	?	10556114	5433209	?	300	75
BHG-02-012	?	10556117	5433212	?	022	85
BHG-02-012	?	10556117	5433212	?	031	84
BHG-02-012	?	10556117	5433212	?	043	85
BHG-02-012	?	10556117	5433212	?	028	83
BHG-02-012	?	10556117	5433212	?	035	84
BHG-02-012	?	10556117	5433212	?	303	75
BHG-02-012	?	10556117	5433212	?	316	73.5
BHG-02-012	?	10556117	5433212	?	319	89
BHG-02-012	?	10556117	5433212	?	327	83

Station	Formation	UTM East	UTM North	Fracture Type	Azimuth	Inclination
BHG-02-012	?	10556571	5432970	?	203	84
BHG-02-012	?	10556571	5432970	?	229	76
BHG-02-012	?	10556571	5432970	?	235	86
BHG-02-013	?	10556262	5432990	?	035	80
BHG-02-013	?	10556262	5432990	?	041	82
BHG-02-013	?	10556262	5432990	?	031	87
BHG-02-013	?	10556262	5432990	?	032	89
BHG-02-013	?	10556262	5432990	?	040	75
BHG-02-013	?	10556262	5432990	?	283	87
BHG-02-013	?	10556262	5432990	?	287	84
BHG-02-013	?	10556262	5432990	?	280	70
BHG-02-013	?	10556262	5432990	?	284	66
BHG-02-013	?	10556314	5432898	?	013	87
BHG-02-013	?	10556314	5432898	?	024	86
BHG-02-013	?	10556314	5432898	?	022	85
BHG-02-013	?	10556314	5432898	?	035	85
BHG-02-013	?	10556314	5432898	?	040	85
BHG-02-013	?	10556261	5432734	?	207	82
BHG-02-013	?	10556261	5432734	?	222	69
BHG-02-013	?	10556261	5432734	?	222	75
BHG-02-013	?	10556261	5432734	?	202	80
BHG-02-014	?	10556171	5432656	?	052	86
BHG-02-014	?	10556171	5432656	?	053	87
BHG-02-014	?	10556171	5432656	?	054	82
BHG-02-014	?	10556419	5432560	?	064	70
BHG-02-014	?	10556419	5432560	?	067	62
BHG-02-014	?	10556419	5432560	?	038	79
BHG-02-014	?	10556419	5432560	?	043	75
BHG-02-014	?	10556419	5432560	?	020	70
BHG-02-014	?	10556463	5432576	?	029	67
BHG-02-014	?	10556463	5432576	?	025	87
BHG-02-014	?	10556463	5432576	?	230	71
BHG-02-014	?	10556463	5432576	?	215	72

Station	Formation	UTM East	UTM North	Fracture Type	Azimuth	Inclination
BHG-02-014	?	10556463	5432576	?	217	64
BHG-02-015	?	10555441	5432346	?	208	81.5
BHG-02-015	?	10555441	5432346	?	207	80
BHG-02-015	?	10555441	5432346	?	205	80
BHG-02-015	?	10555441	5432346	?	190	80
BHG-02-015	?	10555441	5432346	?	295	36
BHG-02-015	?	10555441	5432346	?	012	26
BHG-02-015	?	10555441	5432346	?	350	33
BHG-02-015	?	10555443	5432431	?	060	44
BHG-02-015	?	10555443	5432431	?	061	52
BHG-02-015	?	10555443	5432431	?	026	51
BHG-02-015	?	10555443	5432431	?	054	48
BHG-02-015	?	10555443	5432431	?	013	26
BHG-02-015	?	10555249	5432411	Ext	267	77
BHG-02-015	?	10555249	5432411	Ext	247	79
BHG-02-015	?	10555249	5432411	Ext	261	78
BHG-02-015	?	10555249	5432411	Ext	261	73
BHG-02-015	?	10555249	5432411	Ext	082	74
BHG-02-016	?	10554807	5432793	Shear	091	89
BHG-02-016	?	10554807	5432793	Shear	070	75
BHG-02-016	?	10554807	5432793	Shear	059	73
BHG-02-016	?	10554807	5432793	Shear	065	75
BHG-02-016	?	10554807	5432793	Shear	042	57
BHG-02-016	?	10554807	5432793	Shear	050	69
BHG-02-016	?	10554807	5432793	Shear	091	71
BHG-02-017	Hun	10555313	5435047	Ext	165	76
BHG-02-017	Hun	10555313	5435047	Ext	177	74
BHG-02-017	Hun	10555313	5435047	Ext	191	84
BHG-02-017	Hun	10555313	5435047	Ext	200	84
BHG-02-018	Hun	10555414	5434997	Ext	57	031
BHG-02-018	Hun	10555414	5434997	Ext	305	60
BHG-02-018	Hun	10555414	5434997	Ext	275	79
BHG-02-019	Hun	10555580	5434817	Ext	092	81

Station	Formation	UTM East	UTM North	Fracture Type	Azimuth	Inclination
BHG-02-019	Hun	10555580	5434817	Ext	116	88
BHG-02-019	Hun	10555580	5434817	Ext	275	86
BHG-02-019	Hun	10555580	5434817	Ext	123	74
BHG-02-019	Hun	10555580	5434817	Ext	106	74
BHG-02-019	Hun	10555580	5434817	Ext	030	88
BHG-02-019	Hun	10555580	5434817	Ext	037	87
BHG-02-019	Hun	10555580	5434817	Ext	015	87
BHG-02-024	Hun	10555989	5434081	?	216	074
BHG-02-026	Hun	10557424	5436764	Shear	350	81
BHG-02-026	Hun	10557424	5436764	Shear	335	70
BHG-02-026	Hun	10557424	5436764	Shear	334	70
BHG-02-026	Hun	10557424	5436764	Shear	334	66
BHG-02-026	Hun	10557424	5436764	?	165	68
BHG-02-026	Hun	10557424	5436764	?	139	81
BHG-02-026	Hun	10557424	5436764	?	154	74
BHG-02-026	Hun	10557424	5436764	?	150	74
BHG-02-026	Hun	10557529	5436580	Ext	345	70
BHG-02-026	Hun	10557529	5436580	Ext	300	88
BHG-02-026	Hun	10557529	5436580	Ext	295	89
BHG-02-026	Hun	10557529	5436580	Ext	305	80
BHG-02-026	Hun	10557529	5436580	Ext	200	89
BHG-02-026	Hun	10557529	5436580	Ext	205	85
BHG-02-026	Hun	10557529	5436580	Ext	105	86
BHG-02-026	Hun	10557529	5436580	Ext	325	90
BHG-02-026	Hun	10557529	5436580	Ext	325	84
BHG-02-026	Hun	10557529	5436580	Ext	120	80
BHG-02-026	Hun	10557529	5436580	Ext	159	68
BHG-02-026	Hun	10557529	5436580	Ext	261	5
BHG-02-026	Hun	10557529	5436580	Ext	245	19
BHG-02-026	Hun	10557529	5436580	Ext	240	3
BHG-02-026	Hun	10557529	5436580	Ext	280	2
BHG-02-026	Hun	10557529	5436580	Ext	222	6
BHG-02-026	Hun	10557529	5436580	Ext	235	1

Station	Formation	UTM East	UTM North	Fracture Type	Azimuth	Inclination
BHG-02-027	Hun	10556834	5435978	?	083	87
BHG-02-027	Hun	10556834	5435978	?	066	64
BHG-02-027	Hun	10556834	5435978	?	067	83
BHG-02-027	Hun	10556834	5435978	?	061	81
BHG-02-027	Hun	10556834	5435978	?	344	82
BHG-02-027	Hun	10556834	5435978	?	320	80
BHG-02-027	Hun	10556834	5435978	?	324	88
BHG-02-027	Hun	10556848	5435971	Ext	335	58
BHG-02-027	Hun	10556848	5435971	Ext	332	84
BHG-02-027	Hun	10556848	5435971	Ext	358	86
BHG-02-027	Hun	10556848	5435971	Ext	142	35
BHG-02-027	Hun	10556848	5435971	Ext	080	58
BHG-02-027	Hun	10556848	5435971	Ext	065	84
BHG-02-027	Hun	10556848	5435971	Ext	086	74
BHG-02-027	Hun	10556848	5435971	Ext	062	68
BHG-02-027	Hun	10556848	5435971	Ext	078	71
BHG-02-027	Hun	10556848	5435971	Ext	069	62
BHG-02-027	Hun	10556848	5435971	Ext	343	78
BHG-02-027	Hun	10556848	5435971	Ext	065	68
BHG-02-027	Hun	10556848	5435971	Ext	318	15
BHG-02-027	Hun	10556848	5435971	Ext	054	77
BHG-02-027	Hun	10556848	5435971	Ext	063	71
BHG-02-027	Hun	10556848	5435971	Ext	076	89
BHG-02-028	?	10559042	5434808	?	250	33
BHG-02-028	?	10559042	5434808	Ext	230	85
BHG-02-029	Hun	10556768	5434132	?	250	82
BHG-02-032	Hun	10557517	5433915	Shear	53	70
BHG-02-034	Hun	10555557	5434738	Ext	026	89
BHG-02-034	Hun	10555557	5434738	Ext	207	82
BHG-02-034	Hun	10555557	5434738	Ext	304	56
BHG-02-034	Hun	10555557	5434738	Ext	031	49
BHG-02-034	Hun	10555557	5434738	Ext	114	80
BHG-02-034	Hun	10555557	5434738	Ext	190	86

Station	Formation	UTM East	UTM North	Fracture Type	Azimuth	Inclination
BHG-02-034	Hun	10555557	5434738	Ext	191	85
BHG-02-034	Hun	10555557	5434738	Ext	195	84
BHG-02-034	Hun	10555557	5434738	Ext	025	85
BHG-02-034	Hun	10555557	5434738	Ext	208	81
BHG-02-034	Hun	10555557	5434738	Ext	122	84
BHG-02-034	Hun	10555557	5434738	Ext	119	82
BHG-02-034	Hun	10555557	5434738	Ext	195	79
BHG-02-034	Hun	10555557	5434738	Ext	204	81
BHG-02-034	Hun	10555557	5434738	Ext	199	82
BHG-02-034	Hun	10555557	5434738	Ext	014	89
BHG-02-034	Hun	10555557	5434738	Ext	010	88
BHG-02-034	Hun	10555557	5434738	Ext	029	83
BHG-02-034	Hun	10555557	5434738	Ext	122	83
BHG-02-034	Hun	10555557	5434738	Ext	261	23
BHG-02-034	Hun	10555557	5434738	Ext	205	79
BHG-02-034	Hun	10555557	5434738	Ext	211	71
BHG-02-034	Hun	10555557	5434738	Ext	092	74
BHG-02-034	Hun	10555557	5434738	Ext	279	84
BHG-02-034	Hun	10555557	5434738	Ext	175	86
BHG-02-034	Hun	10555557	5434738	Ext	175	82
BHG-02-034	Hun	10555557	5434738	Ext	198	61
BHG-02-034	Hun	10555557	5434738	Ext	161	66
BHG-02-034	Hun	10555557	5434738	Ext	029	89
BHG-02-034	Hun	10555557	5434738	Ext	025	90
BHG-02-034	Hun	10555557	5434738	Ext	030	86
BHG-02-034	Hun	10555557	5434738	Ext	312	89
BHG-02-034	Hun	10555557	5434738	Ext	340	66
BHG-02-035	Hun	10558231	5435691	Ext	110	85
BHG-02-035	Hun	10558231	5435691	Ext	119	89
BHG-02-035	Hun	10558231	5435691	Ext	320	75
BHG-02-035	Hun	10558231	5435691	Ext	314	72
BHG-02-035	Hun	10558231	5435691	Ext	328	79
BHG-02-035	Hun	10558231	5435691	Ext	044	75

Station	Formation	UTM East	UTM North	Fracture Type	Azimuth	Inclination
BHG-02-035	Hun	10558231	5435691	Ext	034	78
BHG-02-035	Hun	10558231	5435691	Ext	058	68
BHG-02-036	Hun	10557933	5435607	Ext	116	80
BHG-02-036	Hun	10557933	5435607	Ext	098	75
BHG-02-036	Hun	10557933	5435607	Ext	120	84
BHG-02-036	Hun	10557933	5435607	Ext	342	82
BHG-02-036	Hun	10557933	5435607	Ext	350	82
BHG-02-036	Hun	10557933	5435607	Ext	354	84
BHG-02-036	Hun	10557933	5435607	Ext	235	16
BHG-02-036	Hun	10557933	5435607	Ext	238	11
BHG-02-036	Hun	10557933	5435607	Ext	240	16
BHG-02-036	Hun	10557933	5435607	Ext	268	12
BHG-02-036	Hun	10557933	5435607	Ext	250	14
BHG-02-036	Hun	10557933	5435607	Ext	260	14
BHG-02-036	Hun	10557859	5435867	Ext	117	84
BHG-02-036	Hun	10557859	5435867	Ext	274	79
BHG-02-036	Hun	10557859	5435867	Ext	115	88
BHG-02-036	Hun	10557859	5435867	Ext	279	81
BHG-02-036	Hun	10557859	5435867	Ext	289	87
BHG-02-036	Hun	10557859	5435867	Ext	296	82
BHG-02-036	Hun	10557859	5435867	Ext	321	87
BHG-02-037	Hun	10558482	5435675	Ext	338	80
BHG-02-037	Hun	10558482	5435675	Ext	334	85
BHG-02-038	Hun	10558591	5435272	Shear	192	71
BHG-02-038	Hun	10558591	5435272	Shear	200	74
BHG-02-038	Hun	10558591	5435272	Shear	031	87
BHG-02-038	Hun	10558591	5435272	Shear	188	89
BHG-02-038	Hun	10558665	5435280	Shear	343	78
BHG-02-038	Hun	10558665	5435280	Shear	345	65
BHG-02-038	Hun	10558665	5435280	Shear	338	67
BHG-02-038	Hun	10558665	5435280	Slickenlines	005	170
BHG-02-038	Hun	10558612	5435263	Ext	341	77
BHG-02-038	Hun	10558612	5435263	Ext	324	64

Station	Formation	UTM East	UTM North	Fracture Type	Azimuth	Inclination
BHG-02-038	Hun	10558612	5435263	Ext	140	87
BHG-02-038	Hun	10558612	5435263	Ext	319	67
BHG-02-038	Hun	10558612	5435263	Ext	060	89
BHG-02-038	Hun	10558612	5435263	Ext	047	73
BHG-02-038	Hun	10558612	5435263	Ext	055	86
BHG-02-038	Hun	10558612	5435263	Ext	229	85
BHG-02-039	Hun	10558481	5435065	Shear	352	83
BHG-02-039	Hun	10558481	5435065	Shear	357	81
BHG-02-039	Hun	10558481	5435065	Shear	002	80
BHG-02-039	Hun	10558481	5435065	Shear	347	82
BHG-02-039	Hun	10558481	5435065	Shear	154	84
BHG-02-040	Hun	10558914	5434996	Ext	348	68
BHG-02-040	Hun	10558914	5434996	Ext	001	65
BHG-02-040	Hun	10558914	5434996	Ext	356	64
BHG-02-040	Hun	10558914	5434996	Ext	341	67
BHG-02-040	Hun	10558914	5434996	Ext	349	64
BHG-02-040	Hun	10558881	5434977	Shear	035	70
BHG-02-040	Hun	10558881	5434977	Slickenlines	022	62

Bedding Measurements

Station	Formation	UTM East	UTM North	Azimuth	Inclination
BHG-01-001	Hun	10553680	5431626	310	49
BHG-01-001	Hun	10553680	5431626	318	54
BHG-01-001	Hun	10553680	5431626	305	42
BHG-02-001	Hun	10553680	5431626	115	24
BHG-02-007	Hun	10556515	5433352	295	49
BHG-02-007	Hun	10556445	5433383	295	49
BHG-02-007	Hun	10556487	5433398	284	47
BHG-02-008	Hun	10555968	5433641	304	44
BHG-02-008	Hun	10555968	5433641	303	45
BHG-02-008	Hun	10555968	5433641	306	49
BHG-02-008	Hun	10555968	5433641	309	45
BHG-02-008	Hun	10555968	5433641	325	34
BHG-02-008	Hun	10555968	5433641	300	43
BHG-02-009	Hun	10556328	5433440	291	65
BHG-02-009	Hun	10556228	5433440	294	47
BHG-02-009	Hun	10556228	5433440	294	47
BHG-02-009	Hun	10556228	5433440	296	47
BHG-02-009	Hun	10556011	5433471	318	46
BHG-02-009	Hun	10556011	5433471	311	50
BHG-02-009	Hun	10555869	5433592	321	45
BHG-02-009	Hun	10555869	5433592	318	41
BHG-02-009	Hun	10555869	5433592	314	39
BHG-02-010	Hun	10556309	5433277	306	32
BHG-02-010	Hun	10556309	5433277	314	25
BHG-02-020	Hun	10555662	5434586	136	06
BHG-02-020	Hun	10555662	5434586	161	12
BHG-02-020	Hun	10555662	5434586	159	15

Station	Formation	UTM East	UTM North	Azimuth	Inclination
BHG-02-021	Hun	10556461	5433738	296	34
BHG-02-022	Hun	10556199	5433893	279	20
BHG-02-023	Hun	10556091	5433979	282	09
BHG-02-023	Hun	10556091	5433979	300	06
BHG-02-024	Hun	10556234	5433955	270	11
BHG-02-024	Hun	10556234	5433955	289	21
BHG-02-024	Hun	10556234	5433955	296	26
BHG-02-024	Hun	10555989	5434081	296	12
BHG-02-024	Hun	10555989	5434081	171	07
BHG-02-026	Hun	10557482	5436483	258	06
BHG-02-026	Hun	10557482	5436483	239	05
BHG-02-026	Hun	10557513	5436569	261	05
BHG-02-026	Hun	10557513	5436569	245	19
BHG-02-026	Hun	10557513	5436569	240	03
BHG-02-026	Hun	10557513	5436569	280	02
BHG-02-026	Hun	10557513	5436569	222	06
BHG-02-026	Hun	10557513	5436569	235	01
BHG-02-027	Hun	10556834	5435978	202	16
BHG-02-027	Hun	10556834	5435978	176	32
BHG-02-027	Hun	10556834	5435978	155	19
BHG-02-027	Hun	10556848	5435971	153	16
BHG-02-027	Hun	10556848	5435971	170	10
BHG-02-027	Hun	10556848	5435971	050	12
BHG-02-027	Hun	10556848	5435971	219	12
BHG-02-027	Hun	10556848	5435971	205	10
BHG-02-027	Hun	10556848	5435971	183	17
BHG-02-027	Hun	10556848	5435971	174	21
BHG-02-027	Hun	10556848	5435971	153	16

Station	Formation	UTM East	UTM North	Azimuth	Inclination
BHG-02-027	Hun	10556848	5435971	170	10
BHG-02-027	Hun	10556848	5435971	050	12
BHG-02-027	Hun	10556848	5435971	219	12
BHG-02-027	Hun	10556848	5435971	205	10
BHG-02-027	Hun	10556848	5435971	183	17
BHG-02-027	Hun	10556848	5435971	174	21
BHG-02-029	Hun	10556768	5434132	211	02
BHG-02-029	Hun	10556768	5434132	211	10
BHG-02-029	Hun	10556768	5434132	208	5
BHG-02-030	Hun	10555557	5434738	258	04
BHG-02-030	Hun	10555557	5434738	100	05
BHG-02-030	Hun	10555557	5434738	176	00
BHG-02-032	Hun	10557517	5433915	160	15
BHG-02-032	Hun	10557517	5433915	145	11
BHG-02-033	Hun	10558017	5436699	189	10
BHG-02-033	Hun	10558017	5436699	174	14
BHG-02-033	Hun	10558017	5436699	175	10
BHG-02-033	Hun	10558017	5436699	190	10
BHG-02-035	Hun	10558227	5435674	184	09
BHG-02-035	Hun	10558227	5435674	140	05
BHG-02-035	Hun	10558227	5435674	220	14
BHG-02-035	Hun	10558273	5435672	220	11
BHG-02-035	Hun	10558273	5435672	214	17
BHG-02-035	Hun	10558273	5435672	225	21
BHG-02-035	Hun	10558227	5435674	251	07
BHG-02-035	Hun	10558231	5435691	204	18
BHG-02-035	Hun	10558231	5435691	162	05
BHG-02-035	Hun	10558231	5435691	195	06

Station	Formation	UTM East	UTM North	Azimuth	Inclination
BHG-02-035	Hun	10558231	5435691	165	10
BHG-02-035	Hun	10558231	5435691	154	11
BHG-02-035	Hun	10558231	5435691	160	8
BHG-02-035	Hun	10558231	5435691	139	7
BHG-02-038	Hun	10558591	5435272	075	19
BHG-02-038	Hun	10558591	5435272	100	11
BHG-02-038	Hun	10558591	5435272	129	13
BHG-02-038	Hun	10558591	5435272	116	12
BHG-02-038	Hun	10558665	5435280	161	05
BHG-02-038	Hun	10558665	5435280	147	01
BHG-02-038	Hun	10558612	5435263	133	08
BHG-02-039	Hun	10558481	5435065	003	07
BHG-02-040	Hun	10558921	5434915	117	07
BHG-02-040	Hun	10558921	5434915	111	09
BHG-02-040	Hun	10558921	5434915	145	13
BHG-02-040	Hun	10558921	5434915	176	07
BHG-02-040	Hun	10558921	5434915	146	09
BHG-02-040	Hun	10558921	5434915	137	07
BHG-02-040	Hun	10558921	5434915	142	12
BHG-02-040	Hun	10558921	5434915	167	09
BHG-02-040	Hun	10558921	5434915	145	10
BHG-02-040	Hun	10558914	5434996	195	14
BHG-02-040	Hun	10558914	5434996	174	07
BHG-02-040	Hun	10558914	5434996	162	19
BHG-02-040	Hun	10558881	5434977	143	14

Paleocurrent Measurements

Planar Paleoflow indicators

Station	Lithology	UTM East	UTM North	Feature	Azimuth	Inclination
BHG-02-001	Hun	10553680	5431626	Cross-strata	178	28
BHG-02-004	Hun	10554456	5432712	Cross-strata	163	23
BHG-02-004	Hun	10554456	5432712	Cross-strata	159	29
BHG-02-004	Hun	10554456	5432712	Cross-strata	185	45
BHG-02-005	Hun	10554045	5432121	Cross-strata	149	31
BHG-02-010	Hun	10556309	5433277	Cross-strata	314	19
BHG-02-017	Hun	10555313	5435047	Cross-strata	155	21
BHG-02-017	Hun	10555313	5435047	Cross-strata	280	22
BHG-02-017	Hun	10555313	5435047	Cross-strata	157	18
BHG-02-018	Hun	10555414	5434997	Cross-strata	193	30
BHG-02-018	Hun	10555414	5434997	Cross-strata	168	32
BHG-02-019	Hun	10555612	5434733	Cross-strata	187	18
BHG-02-019	Hun	10555612	5434733	Cross-strata	137	18
BHG-02-019	Hun	10555612	5434733	Cross-strata	127	12
BHG-02-021	Hun	10556461	5433738	Cross-strata	198	24
BHG-02-021	Hun	10556461	5433738	Cross-strata	201	15
BHG-02-021	Hun	10556461	5433738	Cross-strata	190	21
BHG-02-022	Hun	10556199	5433893	Cross-strata	175	12
BHG-02-022	Hun	10556199	5433893	Cross-strata	075	10
BHG-02-022	Hun	10556199	5433893	Cross-strata	034	15
BHG-02-022	Hun	10556199	5433893	Cross-strata	206	10
BHG-02-022	Hun	10556199	5433893	Cross-strata	254	12
BHG-02-024	Hun	10555989	5434081	Cross-strata	194	20
BHG-02-024	Hun	10555989	5434081	Cross-strata	235	23
BHG-02-029	Hun	10556768	5434132	Cross-strata	129	18
BHG-02-027	Hun	10556848	5435971	Cross-strata	195	18
BHG-02-027	Hun	10556848	5435971	Cross-strata	189	25
BHG-02-027	Hun	10556848	5435971	Cross-strata	175	31
BHG-02-027	Hun	10556848	5435971	Cross-strata	196	21
BHG-02-027	Hun	10556848	5435971	Cross-strata	189	40

Station	Lithology	UTM East	UTM North	Feature	Azimuth	Inclination
BHG-02-039	Hun	10558482	5435063	Cross-strata	264	21
BHG-02-039	Hun	10558482	5435063	Cross-strata	272	25
BHG-02-039	Hun	10558482	5435063	Cross-strata	254	20
BHG-02-039	Hun	10558482	5435063	Cross-strata	243	16
BHG-02-039	Hun	10558482	5435063	Cross-strata	231	18
BHG-02-039	Hun	10558482	5435063	Cross-strata	241	17
BHG-02-039	Hun	10558482	5435063	Cross-strata	265	9
BHG-02-039	Hun	10558482	5435063	Cross-strata	264	17
BHG-02-039	Hun	10558482	5435063	Cross-strata	280	12
BHG-02-039	Hun	10558482	5435063	Cross-strata	265	23
BHG-02-030	Hun	10555557	5434738	Cross-strata	285	21
BHG-02-030	Hun	10555557	5434738	Cross-strata	283	14
BHG-02-027	Hun	10556848	5435971	Cross-strata	195	18
BHG-02-027	Hun	10556848	5435971	Cross-strata	189	25
BHG-02-027	Hun	10556848	5435971	Cross-strata	175	31
BHG-02-027	Hun	10556848	5435971	Cross-strata	196	21
BHG-02-027	Hun	10556848	5435971	Cross-strata	189	40
BHG-02-036	Hun	10557933	5435607	Cross-strata	200	25
BHG-02-036	Hun	10557933	5435607	Cross-strata	212	34
BHG-02-036	Hun	10557933	5435607	Cross-strata	203	23
BHG-02-036	Hun	10557933	5435607	Cross-strata	202	29
BHG-02-036	Hun	10557933	5435607	Cross-strata	203	24

Linear Paleoflow Indicators

Station	Formation	UTM East	UTM North	Feature	Plunge	Trend
BHG-02-009	Hun	10555869	5433592	Sole mark	44	025
BHG-02-009	Hun	10555869	5433592	Sole mark	36	019
BHG-02-009	Hun	10555869	5433592	Sole mark	36	050
BHG-02-009	Hun	10555869	5433592	Sole mark	40	041
BHG-02-009	Hun	10555869	5433592	Sole mark	49	016
BHG-02-009	Hun	10555869	5433592	Sole mark	45	020
BHG-02-009	Hun	10555869	5433592	Sole mark	37	030
BHG-02-009	Hun	10555869	5433592	Sole mark	41	044
BHG-02-009	Hun	10555869	5433592	Sole mark	39	031
BHG-02-009	Hun	10555869	5433592	Sole mark	31	049
BHG-02-017	Hun	10555313	5435047	AB plane	49	004
BHG-02-017	Hun	10555313	5435047	AB plane	35	019
BHG-02-017	Hun	10555313	5435047	AB plane	10	039
BHG-02-017	Hun	10555313	5435047	AB plane	20	025
BHG-02-017	Hun	10555313	5435047	AB plane	24	015
BHG-02-017	Hun	10555313	5435047	AB plane	30	064
BHG-02-017	Hun	10555313	5435047	AB plane	21	209
BHG-02-017	Hun	10555313	5435047	AB plane	27	357
BHG-02-017	Hun	10555313	5435047	AB plane	17	074
BHG-02-017	Hun	10555313	5435047	AB plane	74	206
BHG-02-017	Hun	10555313	5435047	AB plane	15	083
BHG-02-017	Hun	10555313	5435047	AB plane	13	334
BHG-02-017	Hun	10555313	5435047	AB plane	25	280
BHG-02-017	Hun	10555313	5435047	AB plane	43	251
BHG-02-017	Hun	10555313	5435047	AB plane	15	001
BHG-02-017	Hun	10555313	5435047	AB plane	23	014
BHG-02-017	Hun	10555313	5435047	AB plane	74	095
BHG-02-017	Hun	10555313	5435047	AB plane	10	333
BHG-02-017	Hun	10555313	5435047	AB plane	61	141
BHG-02-017	Hun	10555313	5435047	AB plane	08	080
BHG-02-017	Hun	10555313	5435047	AB plane	29	071
BHG-02-017	Hun	10555313	5435047	AB plane	29	081

Station	Formation	UTM East	UTM North	Feature	Plunge	Trend
BHG-02-017	Hun	10555313	5435047	AB plane	21	026
BHG-02-017	Hun	10555313	5435047	AB plane	74	251
BHG-02-017	Hun	10555313	5435047	AB plane	60	268
BHG-02-017	Hun	10555313	5435047	AB plane	76	004
BHG-02-017	Hun	10555313	5435047	AB plane	46	261
BHG-02-017	Hun	10555313	5435047	AB plane	62	021
BHG-02-017	Hun	10555313	5435047	AB plane	10	241
BHG-02-017	Hun	10555313	5435047	AB plane	62	070
BHG-02-017	Hun	10555313	5435047	AB plane	12	176
BHG-02-017	Hun	10555313	5435047	AB plane	55	037
BHG-02-017	Hun	10555313	5435047	AB plane	14	218
BHG-02-017	Hun	10555313	5435047	AB plane	06	169
BHG-02-017	Hun	10555313	5435047	AB plane	20	329
BHG-02-017	Hun	10555313	5435047	AB plane	35	209
BHG-02-017	Hun	10555313	5435047	AB plane	24	296
BHG-02-017	Hun	10555313	5435047	AB plane	25	280
BHG-02-017	Hun	10555313	5435047	AB plane	83	133
BHG-02-017	Hun	10555313	5435047	AB plane	24	350
BHG-02-017	Hun	10555313	5435047	AB plane	14	314
BHG-02-017	Hun	10555313	5435047	AB plane	19	179
BHG-02-017	Hun	10555313	5435047	AB plane	26	247
BHG-02-017	Hun	10555313	5435047	AB plane	44	299
BHG-02-021	Hun	10556461	5433738	AB plane	16	010
BHG-02-021	Hun	10556461	5433738	AB plane	02	350
BHG-02-021	Hun	10556461	5433738	AB plane	30	150
BHG-02-021	Hun	10556461	5433738	AB plane	05	345
BHG-02-021	Hun	10556461	5433738	AB plane	15	170
BHG-02-021	Hun	10556461	5433738	AB plane	15	008
BHG-02-021	Hun	10556461	5433738	AB plane	10	001
BHG-02-021	Hun	10556461	5433738	AB plane	07	281
BHG-02-021	Hun	10556461	5433738	AB plane	13	341
BHG-02-021	Hun	10556461	5433738	AB plane	16	080
BHG-02-021	Hun	10556461	5433738	AB plane	00	355

Station	Formation	UTM East	UTM North	Feature	Plunge	Trend
BHG-02-021	Hun	10556461	5433738	AB plane	10	355
BHG-02-021	Hun	10556461	5433738	AB plane	21	025
BHG-02-021	Hun	10556461	5433738	AB plane	32	225
BHG-02-021	Hun	10556461	5433738	AB plane	26	325
BHG-02-021	Hun	10556461	5433738	AB plane	14	335
BHG-02-021	Hun	10556461	5433738	AB plane	30	155
BHG-02-021	Hun	10556461	5433738	AB plane	20	251
BHG-02-021	Hun	10556461	5433738	AB plane	09	345
BHG-02-021	Hun	10556461	5433738	AB plane	13	351
BHG-02-021	Hun	10556461	5433738	AB plane	36	340
BHG-02-021	Hun	10556461	5433738	AB plane	21	315
BHG-02-021	Hun	10556461	5433738	AB plane	23	340
BHG-02-021	Hun	10556461	5433738	AB plane	30	254
BHG-02-021	Hun	10556461	5433738	AB plane	26	355
BHG-02-021	Hun	10556461	5433738	AB plane	09	114
BHG-02-021	Hun	10556461	5433738	AB plane	22	094
BHG-02-021	Hun	10556461	5433738	AB plane	90	041
BHG-02-021	Hun	10556461	5433738	AB plane	15	070
BHG-02-021	Hun	10556461	5433738	AB plane	21	054
BHG-02-021	Hun	10556461	5433738	AB plane	18	095
BHG-02-021	Hun	10556461	5433738	AB plane	15	166
BHG-02-021	Hun	10556461	5433738	AB plane	12	077
BHG-02-021	Hun	10556461	5433738	AB plane	19	211
BHG-02-021	Hun	10556461	5433738	AB plane	09	262
BHG-02-021	Hun	10556461	5433738	AB plane	39	322
BHG-02-021	Hun	10556461	5433738	AB plane	29	141
BHG-02-021	Hun	10556461	5433738	AB plane	43	141
BHG-02-021	Hun	10556461	5433738	AB plane	21	343
BHG-02-021	Hun	10556461	5433738	AB plane	23	059
BHG-02-021	Hun	10556461	5433738	AB plane	10	070
BHG-02-021	Hun	10556461	5433738	AB plane	26	045
BHG-02-021	Hun	10556461	5433738	AB plane	25	019
BHG-02-021	Hun	10556461	5433738	AB plane	25	082

Station	Formation	UTM East	UTM North	Feature	Plunge	Trend
BHG-02-021	Hun	10556461	5433738	AB plane	11	145
BHG-02-021	Hun	10556461	5433738	AB plane	36	017
BHG-02-021	Hun	10556461	5433738	AB plane	13	063
BHG-02-021	Hun	10556461	5433738	AB plane	15	319
BHG-02-021	Hun	10556461	5433738	AB plane	45	081
BHG-02-021	Hun	10556461	5433738	AB plane	25	112
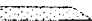
Minor Faults

Station	Lithology	UTM East	UTM North	Azimuth	Inclination
BHG-02-009	HUN	10556228	5433440	150	44
BHG-02-011	?	10555998	5433346	112	74
BHG-02-011	?	10555998	5433346	298	81
BHG-02-011	?	10555998	5433346	312	78
BHG-02-011	?	10555998	5433346	317	77
BHG-02-011	?	10555998	5433346	227	89
BHG-02-011	?	10555998	5433346	044	87
BHG-02-011	?	10555998	5433346	224	76
BHG-02-015	?	10555441	5432346	329	39
BHG-02-015	?	10555441	5432346	336	83
BHG-02-015	?	10555441	5432346	107	87
BHG-02-015	?	10555441	5432346	135	89
BHG-02-015	?	10555441	5432346	230	24
BHG-02-015	?	10555249	5432411	234	49
BHG-02-015	?	10555249	5432411	084	82
BHG-02-015	?	10555249	5432411	285	83
BHG-02-016	?	10555334	5433210	206	54
BHG-02-016	?	10555334	5433210	203	52
BHG-02-016	?	10555334	5433210	189	41
BHG-02-016	?	10554746	5432812	307	71
BHG-02-016	?	10554746	5432812	314	80
BHG-02-016	?	10554746	5432812	291	60
BHG-02-016	?	10554653	5433301	000	42
BHG-02-016	?	10554744	5433261	105	60
BHG-02-028	?	10559060	5434718	250	65
BHG-02-028	?	10559042	5434808	079	84
BHG-02-028	?	10559042	5434808	091	26

BHG-02-028	?	10559042	5434808	219	81
BHG-02-038	Hun	10558591	5435272	032	64
BHG-02-038	Hun	10558473	5435448	271	49
BHG-02-037	Hun	10558482	5435675	109	51
BHG-02-037	Hun	10558482	5435675	078	36
BHG-02-040	Hun	10558914	5434996	149	28
BHG-02-040	Hun	10558914	5434996	129	21
BHG-02-037	Hun	10558482	5435675	075	35
BHG-02-038	Hun	10558612	5435263	058	39

Appendix D - Stratigraphic Section

Legend for Stratigraphic Section

Conglomerate, sandstone matrix		Plant material / Woody debris
Pebbly Sandstone		Current ripple marks
Sandstone		Trough cross-stratification
Sandstone, thin-bedded		Planar tabular cross-stratification
Sandstone		Clast imbrication
silty mudstone		Ripup clasts
clayey mudstone		
Coal / Carbonaceous Mudstone		Concretion / Nodule horizon

Very fine-grained sandstone, with current ripple marks, minor interbedded mudstone

Interbedded slightly blocky siltstone, shale, mudstone and minor sandy layers, some carbonaceous detritus

Very fine-grained sandstone, current ripple marks

Blocky interbedded shale, mudstone and claystone, some carbonaceous detritus and fossil leaves, coal layers

Very fine-grained sandstone, abundant current ripple marks

Blocky shale and mudstone, minor very fine-grained sandstone interbeds, minor claystone interbeds, some fossil leaves

Medium-grained sandstone, minor coarse- to very coarse-grained lenses with pebbles, current ripple marks

Mudstone with shale interbeds, blocky, some fossil leaves

Coal layers with local interbedded thin silty or shale layers abundant fossilized tree material, some leaves

Mudstone with shale interbeds, blocky, some fossil leaves

Formation: Huntingdon

metres	weathered colour	fresh colour
	gry to tan	lt gry
	gry to tan	lt gry
	dk gry	dk gry
	gry	lt gry
	dk gry	dk gry
	gry	lt gry
	dk gry	dk gry
	gry to tan	lt gry
	dk gry	dk gry
	blk	blk
	dk gry	dk gry

photo   sample

cover mudst siltst vf f m c vc p c b
l u l u l u l u
sst   cgl

146

Medium-grained sandstone, some current ripple marks, minor cross-beds and covered material

Medium-grained sandstone, minor coarse- to very coarse-grained lenses with pebbles, current ripple marks

Coarse-grained sandstone

Coarse-grained sandstone, poorly exposed little visible structure

Shale some sandy sections, minor coal, beds, trace fossils (meniscate filled)

Formation

weathered colour

fresh colour

Huntingdon

metres

80
78
76
74
72
70
68
66
64
62
60
58
56
54
52
50
48
46
44
42
40

lt gry / lt gry
lt gry / lt gry
tan / lt gry
rd tan / lt gry
tan / gry

cover
mudst
siltst
vf f m c vc
sst
p c b
cgl

Formation / weathered colour / fresh colour

metres scale: 120, 118, 116, 114, 112, 110, 108, 106, 104, 102, 100, 98, 96, 94, 92, 90, 88, 86, 84, 82, 80

Huntingdon

Colours:
- lt gry / lt gry
- gry / gry
- dk gry / dk gry
- red / red
- gry red / gry red
- gry / gry
- dk gry / dk gry
- tan / lt gry
- lt gry / lt gry

Descriptions:

Sandstone and conglomerate, described on next page

Fine-grained sandstone, minor to some shale interbeds, common current ripple marks

Interbedded blocky shale and claystone, minor fine-grained sandstone interbeds

Very fine-grained sandstone trace to some interbedded shale and claystone, some current ripple marks

Blocky Mudstone

Silty, lower very fine-grained sandstone, little visible structure

Fine-grained sandstone, little visible structure

Medium-grained sandstone, some current ripple marks, minor cross-beds and covered material

Fine-grained sandstone, some current ripple marks and cross-beds

Grain scale (bottom axis): cover | mudst | siltst | vf l u / f l u / m l u / c l u / vc u (sst) | p c b (cgl)

148

Formation
weathered colour
fresh colour

Huntingdon

metres

160
158
156
154
152
150
148
146
144
142
140
138
136
134
132
130
128
126
124
122
120

gry | lt gry

dk gry | dk gry

dk gry | dk gry

dk gry | dk gry

gry | lt gry

dk gry | dk gry

lt gry | lt gry

Medium- to very coarse-grained sandstone with some pebble conglomerate interbeds, abundant trough cross-beds and erosional scours. Conglomerate contains multilithologic, subrounded clasts, averaging 1cm diameter, pebble lags occur above the base of some scours

Silty fine-grained sandstone, with claystone interbeds, some current ripple marks

Mudstone with claystone interbeds

Silty fine-grained sandstone, some current ripple marks

Coarse-grained sandstone trace planar tabular cross-beds

Mudstone with some interbedded claystone layers

Silty fine-grained sandstone, some current ripple marks

Interbedded medium-grained sandstone to conglomerate, abundant trough cross-beds and erosive scours, conglomerate consist of subrounded, multilithologic clasts, averaging 1 cm diameter

cover
mudst
siltst
l u l u l u l u l u
vf f m c vc
sst
p c b
cgl

149

Formation

weathered colour

fresh colour

Huntingdon

metres

200

198

196

194

192

190

188

186

184

182

180

178

176

174

172

170

168

166

164

162

160

red | dk gry

lt gry | lt gry

lt gry | lt gry

dk gry | dk gry

Very blocky mudstone, some sandy or silty layers, some concretionary horizons, some fractures have a 2 cm rim of reddish alteration and are more resistant to weathering

very fine-grained sandstone, some silt, slightly blocky, concretion horizons

Medium-grained sandstone, some trough cross-beds little visible structure

Blocky mudstone

cover
mudst
siltst
l u | l u | l u | l u | l u
vf | f | m | c | vc
sst
p | c | b
cgl

150

A stratigraphic column for the Huntingdon Formation, measured in metres from 200 to 240.

Column headers (rotated): Formation, weathered colour, fresh colour

Grain size scale (bottom): cover, mudst, siltst — sst (l u / vf, l u / f, l u / m, l u / c, l u / vc) — cgl (p, c, b)

Formation: Huntingdon

Colour columns (weathered / fresh), top to bottom:
- gry / gry
- dk gry / dk gry
- tan / lt gry
- tan / lt gry
- red / dk gry
- tan / lt gry
- red / dk gry
- red / dk gry

Descriptions (top to bottom):

Fine- to very fine-grained sandstone, some fissle shale interbeds, some concretionary horizons within sand layers, some current ripple marks

blocky mudstone

Very fine-grained sandstone, current ripple marks

Alternating layers/lenses of conglomerate and coarse- to very coarse-grained sandstone, abundant cross-beds and erosional scours, common pebble lags underlie sandstone layers, clasts are multilithologic, subrounded and average between 1 and 4 cm diameter

Very fine-grained sandstone, abundant current ripple marks

Medium-grained sandstone, some lenses of fine-grained sands, common cross-beds and current ripple marks, some concretionary horizons

Medium- to very coarse-grained sandstone, abundant cross-beds and erosional scours, common pebble lags, 10 cm thick lenses of pebble conglomerate, clasts are multilithologic, rounded to subrounded and average between 1 and 3 cm, diameter.

Blocky mudstone, some fractures have a 2 cm rim of reddish alteration and are more resistant to weathering

Medium-grained sandstone, abundant current ripple marks, some concretionary horizons, some fossil leaves

Blocky mudstone, some sandy or silty layers, some concretionary horizons, some fractures have a 2 cm rim of reddish alteration and are more resistant to weathering

151

Formation
weathered colour
fresh colour

280
278
276
274
272
270
268
266
264
262
260
258
256
254
252
250
248
246
244
242
240

metres

Huntingdon

tan | lt gry
tan | lt gry
dk gry | dk gry
tan | lt gry
tan | lt gry
tan | lt gry
gry | gry
dk gry | dk gry

Medium- to very coarse- grained sandstone and pebble conglomerate, some trough cross-beds and erosional scours, common pebble lags underlie sandstone layers, clasts are multilithologic, rounded to subrounded, averaging 2 cm diameter, some leaf fossils, minor cobbles

Pebble conglomerate, abundant cross-beds and erosional scours, some sandstone lenses with pebble lags, clasts are multilithologic, rounded to subrounded and average between 1 and 4 cm diameter, minor cobbles

Very fine-grained sandstone grading to blocky mudstone

Medium- to very coarse-grained sandstone and pebble conglomerate, abundant cross-beds and erosional scours, common pebble lags underlie sandstone layers, multilithologic clasts , rounded to subrounded average 2 cm diameter, minor cobbles

Pebble conglomerate, abundant cross-beds and erosional scours, clasts as above

Fine-grained sandstone

Blocky mudstone, some sand interbeds

Fine- to very fine-grained sandstone, some block shale interbeds, some concretionary layers, some current ripple marks

cover
mudst
siltst
l u | l u | l u | l u | l u
vf | f | m | c | vc
sst
p | c | b
cgl